DEVELOPMENT OF INDUCTIVELY COUPLED PLASMA SPECTROSCOPIC METHODS FOR THE DETERMINATION OF METALS IN BELUGA (*DELPHINAPTERUS LEUCAS)* AND PYGMY SPERM (*KOGIA BREVICEPS)* WHALE LIVER SAMPLES

A Thesis Submitted to
the Graduate School of Engineering and Sciences of
İzmir Institute of Technology
in Partial Fulfillment of the Requirements for the Degree of

MASTER OF SCIENCE

in Chemistry

by
Filiz PARLAYAN

July 2005
İZMİR

We approve the thesis of **Filiz PARLAYAN**

Date of signature

…….. **22 July 2005**
Assist. Prof. Ritchie EANES
Supervisor
Department of Chemistry
İzmir Institute of Technology

…….. **22 July 2005**
Assist. Prof. Durmuş ÖZDEMİR
Department of Chemistry
İzmir Institute of Technology

…….. **22 July 2005**
Assist. Prof. Figen KOREL
Department of Food Engineering
İzmir Institute of Technology

…….. **22 July 2005**
Assoc. Prof. Ahmet E. EROĞLU
Head of Department
İzmir Institute of Technology

……..
Assoc. Prof. Semahat ÖZDEMİR
Head of the Graduate School

ACKNOWLEDGEMENTS

Firstly, I wish to express my grateful thanks to Assist. Prof. Ritchie Eanes for his guidance, motivation, supports and encouragement throughout this project.

I would like to express my gratitude to Assist. Prof. Durmuş Özdemir who contributed his time, effort, assistance and expertise in data processing part of the project. Also I would like to thank to Assoc. Prof. Ahmet E. Eroğlu for his valuable critiques and assistance.

I wish to thank Ahmet Öğüt at Hıfzısıhha Institute for his helps in ICP-MS analysis and Steven Christopher at NIST for supplying the whale liver samples.

I wish to express my special thanks to our research specialists Oya Altungöz for her patient and tolerant work in ICP-OES analysis and Sinan Yılmaz for his valuable helps in microwave digestion of the samples.

I am grateful to all my friends in IYTE especially Arzu Erdem, Aslı Erdem, Betül Öztürk, Murat Erdoğan, Müşerref Yersel and Özge Tunusoğlu for their endless patience, support, encouragement, and motivation.

Finally, I would like to thank my family because without their support this project would never have been finished.

ABSTRACT

Inductively couple plasma optical emission spectrometry (ICP-OES) is widely used to monitor elements in biological samples from marine organisms for ecological evaluations. Matrix effects (particularly those related to acid and salt type and concentrations) can present a barrier to the applicability of this instrumental method. To have a better understanding of these effects and to choose a suitable internal standard to correct for the signal variations, a procedure based on Principal Component Analysis (PCA) of the data from an axial-mode ICP-OES instrument with sequential detection was performed.

Different from other published studies, it was found that ionic lines were more affected by matrix changes. Elements with high ionization energies and energy sums such as Cd and Zn showed a significant change for signal intensities and calculated concentrations due to the presence of acid, salt, and multielement matrix effects. It was observed that acid has a higher influence on the analyte signal as compared to the "salt-only" case. Furthermore, when several interfering elements were present in the sample, the matrix effect was either enhanced or reduced when compared with a solution containing only a single interfering element. Applicability of the proposed technique for the analysis of whale liver homogenate NIST certified material was investigated. The values of the corrected concentrations were in good agreement with the certified values, confirming the capabilities of the selected internal standards for compensation of matrix effects.

ÖZET

Deniz canlılarından alınan biyolojik örneklerdeki elementlerin analizi, denizlerdeki insan aktivitelerinin izlenmesi ve bu elementlerin deniz canlıları ve insanlar üzerindeki etkisinin araştırılması açısından önem taşımaktadır. İndüktif eşleşmiş plazma optik emisyon spektrometri (ICP-OES) tekniği element analizleri için oldukça sık kullanılmaktadır. Çoğunlukla, kullanılan asit ve tuzun çeşidi ve miktarından kaynaklanan matriks etkileri, bu tekniğin etkili bir şekilde kullanımını engelleyen en önemli problemlerden biridir. Bu çalışmada, matriks etkilerini daha iyi inceleyebilmek ve bu etkilerden kaynaklanan sinyal değişimlerini azaltmada kullanılacak uygun bir internal (iç) standart seçmek için Temel Bileşen Analizine dayanan bir prosedür uygulanmıştır. Kullanılan eksenel ICP-OES cihazı, siklonik püskürtme çemberi ve konsantrik cam püskürtücü içermekte ve dizisel dedeksiyon yapmaktadır.

Literatürdeki diğer çalışmalardan farklı olarak, iyonik dalga boylarının matriks değişimlerinden atomik dalga boylarına göre daha çok etkilendiği belirlenmiştir. Yüksek iyonlaşma enerjisi ve enerji toplamlarına sahip Cd ve Zn gibi elementlerin sinyallerinde ve hesaplanan derişimlerinde asit, tuz ve multielement değişimlerine bağlı olarak önemli değişiklikler görülmüştür. Asit miktarının değişimin, sadece tuz miktarı değişimine göre sinyaller üzerinde daha fazla etkiye sahip olduğu saptanmıştır. Ayrıca, örnekte birden fazla engelleyici element bulunmasının, tek engelleyici element içeren çözeltiye göre sinyaller üzerinde daha fazla azaltıcı ya da artırıcı bir etkiye sahip olduğu gözlenmiştir.

Önerilen tekniğin uygulanabilirliği, NIST den temin edilen bir balina karaciğer örneği, referans madde kullanılarak test edilmiştir. Düzeltilen derişimler referans madde ile karşılaştırıldığında, seçilen internal standartların matriks etkilerinin neden olduğu sinyal değişimlerini giderebildiği belirlenmiştir.

TABLE OF CONTENTS

LIST OF TABLES

Table **Page**

LIST OF FIGURES

Figure **Page**

CHAPTER 1

GENERAL CONCEPTS ABOUT PLASMA SPECTROMETRY

1.1. Introduction

Element analysis is an important area of scientific research because it allows monitoring the influence of the elements on human health and the environment. Plasma-spectrometry techniques, namely inductively coupled plasma optical emission spectrometry (ICP-OES) and inductively coupled plasma mass spectrometry (ICP-MS), are widely used in analytical laboratories for elemental analysis, mainly because of their ability to obtain low limits of detection (LOD), high sensitivity, precision and relatively high analytical throughput.

In these techniques, the analytical response depends directly on the number of analyte atoms present in the plasma and, thus on the analyte concentration in the sample. In ICP-OES, the radiation generated is finally measured using an appropriate detection system whereas in ICP-MS, analyte ions are extracted from the plasma and then directly recorded (Mora et al. 2003).

Although it may be said by some that there is no further need for development of ICP-OES and ICP-MS, since they have supposedly become mature techniques, work is still needed to improve the reliability and the accessibility of the instrument, to improve the analytical performance, to extract more information from the spectra, and to obtain reliable analytical results by performing more efficient data processing. The current developments are mainly related to sample introduction, signal collection, signal detection, data acquisition, and data processing (Mermet 2002).

1.2. Inductively Coupled Plasma

A plasma is an electrically conducting gaseous mixture containing a significant concentration of cations and electrons. In the frequently used argon plasma, argon ions and electrons are the principle conducting species, although cations from the sample will also be present in lesser amounts. Argon ions, once formed in a plasma are capable of absorbing sufficient power from an external source to keep the temperature at a level at which further ionization maintains the plasma indefinitely, temperatures as great as 10,000 K are encountered (Skoog et al. 1998).

The ICP is a highly efficient atomization source, which means that every molecule should be dissociated provided that operating conditions are optimized for this purpose. The ionization efficiency is also high, which justifies the use of ICP as an ionization source in inorganic mass spectrometry. Moreover, the ICP displays an excellent tolerance to high salt concentration: as a consequence, limits of detection in a solid prior to digestion are excellent (Mermet 2005).

The plasma core is the part to which the energy from the induction coil is coupled. This induction region (IR) is the hottest zone of the plasma. The core supplies energy to the remaining parts of the plasma, particularly to the sample in the aerosol, which is introduced via the center carrier gas. The first zone of the plasma, where the liquid sample is dried, melted and vaporized, is called the preheating zone (PHZ). In the initial radiation zone (IRZ) atoms are formed and excited emitting light. Ionic transitions predominate in the normal analytic zone (NAZ) which is found outside of the plasma core. Since no more energy is supplied in this zone, the temperature drops. Finally, the ions recombine with electrons to form atoms, and atoms react with each other to form molecules in the zone called the tail plume (Nölte 2003). Figure 1.1 shows the temperature profile of the plasma.

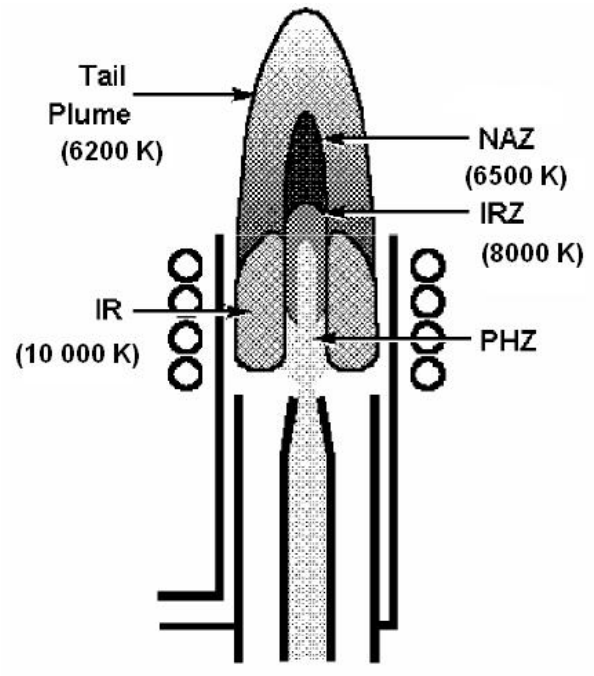

Figure 1.1. Temperature profile of the plasma
(Source: adapted from Skoog et al. 1998)

Axial viewing mode is generally used in most recent ICP systems. Often axial viewing improves the limits of detection by increasing the signal to background ratio thereby decreasing the relative standard deviation of the background noise.

However, it has been reported that axial viewing has an undesired higher sensitivity to matrix effects (Dubuisson 1997, Brenner et al. 1997, Dennaud et al. 2001, Stepan et al. 2001) and self-absorption phenomena. This can be explained from its probing of the atomization zone where most of the matrix effects occur because of different atomization kinetics, unlike the radial viewing. Self-absorption is also enhanced with axial viewing because this event may occur over a path of 20–25 mm along the plasma axis, while the path is reduced to the diameter of the central channel with radial viewing, i.e. 4–6 mm. These limitations can be decreased or minimized by using robust plasma conditions (Mermet 2002).

1.3. Robustness

The robustness term is used to describe plasma conditions where a change in the matrix or reagent concentration does not lead to a significant change in the analyte signal (Mermet 1998).

This term is related to the capability of the plasma to accept a matrix change without a change in the plasma conditions, i.e., the temperature and the electron number density. Sophisticated diagnostics were suggested to measure these characteristics based on Thomson and Rayleigh scattering (Mermet 1998). Because of their complexity, they can not be performed with commercially available ICP systems, therefore simple experiments are needed.

It is generally accepted that ionic lines are more sensitive to any change in the plasma conditions than atomic lines (Mermet 1998, Dennaud et al. 2001). So if the ratio of an ionic line intensity to an atomic line intensity is used, the behavior of the ionic line is normalized to that of the atomic line thus the ratio is then independent of the data acquisition conditions. Magnesium is commonly used as a test element for this purpose, particularly the Mg II 280 nm/Mg I 285 nm line intensity ratio, because the two wavelengths are relatively close, the intensities of the ionic and atomic lines are of the same magnitude, and transition probabilities values are known with an acceptable accuracy in order to compute theoretical ratios (Mermet 1991, Dennaud et al. 2001).

Based on the use of this Mg ratio, it has been verified that by using a high rf power (>1.2 kW), low carrier gas flow rate (< 0.8 ml/min) and large injector inner diameter (>2.3 mm) robust plasma conditions can be achieved (Romero et al. 1997a, Romero et al. 1997b, Mermet 1998). The aim is to obtain a high efficiency of the energy transfer between the surrounding plasma and the central channel. Under non-robust conditions, the plasma is said to be more sensitive to any small change in the forward power or in the amount of aerosol (Mermet 1998, Dennaud et al. 2001).

The Mg II/Mg I ratio could also be used to study ICP parameters such as residence time, aerosol transport rate, carrier gas flow rate, torch design, micronebulizers efficiency and effect of organic solvents, as well as other interferences (Dennaud et al. 2001, Fernandez et al. 1994, Grotti et al. 2000 and references therein). Since such ratio is independent of the detector, the absolute value of the ratio can also be used to compare different ICP systems and working conditions. This ratio was even

used to assign possible origins of the matrix effects, i.e. change of plasma conditions, or change in aerosol formation, transport and filtering (Fernandez et al. 1994, Carre et al. 1995, Novotny et al. 1996, Romero et al. 1998b). Preliminary investigations have indicated that the use of robust conditions corresponding to high Mg II/Mg I ratios could minimize, but not necessarily suppress matrix effects, particularly when ionic lines are of concern (Ivaldi and Tyson 1995, Dubuisson et al. 1997, Brenner et al. 1997, Todoli et al. 1998, Brenner et al. 1998).

The ideal case is observed when both no change in the Mg II/Mg I ratio and analyte signal are observed. However it is more common that changing the Mg II/Mg I ratio is still accompanied by a change in the analyte signal. This means that the plasma conditions were not changed, usually because of robust conditions, but the variation in the analyte signal can be explained by problems that arise at the aerosol transport and filtration level. This indicates also that these effects are not originating in the plasma. When both the Mg II/Mg I ratio and the analyte signal change, no conclusion can be given about the main origin of matrix effects since both the plasma and the spray chamber play a role in these effects (Dennaud et al. 2001).

The theoretical calculation of the Mg II 280 nm/Mg I 285 nm has been described in previous studies (Mermet 1991). Saha equation can be used as seen in Equation 1.1 to determine variables such as excitation energy, E_{exc}, ionization energy, E_{ion}, excitation temperature T_{exc}, ionization temperature T_e.

$$\frac{\boldsymbol{I_i}}{\boldsymbol{I_a}} = \left(\frac{4.83\times10^{21}}{\boldsymbol{n_e}}\right)\left(\frac{\boldsymbol{g_i}\cdot\boldsymbol{A_i}\cdot\lambda_a}{\boldsymbol{g_a}\cdot\boldsymbol{A_i}\cdot\lambda_i}\right)\boldsymbol{T_e}^{3/2}\exp\left(\frac{-\boldsymbol{E_{ion}}}{\boldsymbol{k}\cdot\boldsymbol{T_e}}\right)\exp\left[\frac{-(\boldsymbol{E_{exc,i}}-\boldsymbol{E_{exc,a}})}{\boldsymbol{k}\cdot\boldsymbol{T_{exc}}}\right] \qquad (1.1)$$

The statistical weights and transition probabilities are represented by g and A, respectively. When Local thermodynamic Equilibrium (LTE) is assumed, $T_e = T_{exc} = T$. The "a" and "i" subscripts refer to the atomic and ionic lines, respectively. By using the known gA values (Mermet 1991, Dennaud et al. 2001) of $5.32\text{x}10^8$ s^{-1} and $14.85\text{x}10^8$ s^{-1} for Mg II 280.270 and Mg I 285.213, respectively, it is possible to obtain a relation between T, the electron number density, n_e, and the I_i/I_a ratio (Table 1.1). It may be deduced that a value of at least 10 for I_i/I_a would correspond to an equilibrium in the plasma (robustness).

Table 1.1. Temperature T ($T_e = T_{exc} = T$) (K), electron number density (m^{-3}) and MgII/Mg I line intensity ratio computed assuming LTE
(Source: Dennaud et al. 2001)

T (K)	n_e (m^{-3})	I_i/I_a
6500	1.01×10^{20}	10.8
7000	2.83×10^{20}	11.4
7500	6.90×10^{20}	12.1
8000	1.51×10^{21}	12.7
8500	3.01×10^{21}	13.4
9000	5.57×10^{21}	14.1
9500	9.70×10^{21}	14.8
10000	1.60×10^{22}	15.4

Usually, there is no need to compensate for a different wavelength response curve as far as the same measurement conditions are used, e.g. the same high voltage in the case of a photomultiplier tube PMT, and the same amplifier gain. However, it may be necessary to use a correction factor in some cases. For instance, a 2400 line mm^{-1} grating may be used in the first order above 300 nm, and in the second order below 300 nm to achieve higher resolution in the UV region. Besides the use of an interference filter, the order selection can be performed by using a solar blind PMT with a wavelength cut-off near 300 nm. Consequently, the wavelength response may exhibit a significant slope near the two Mg wavelengths. Another case is the use of an echelle grating. The two Mg lines may be located in adjacent orders, or at different locations within the same order. As the diffraction efficiency is highly dependent on the location of the line within the order, it may also be necessary to compensate for a different wavelength response. A simple way to establish a correction factor is to assume that the continuum has a constant value in the range 280-285 nm. It is then sufficient to measure the background emission at 280.2 and 285.2 nm. If $B_{285}/B_{280} = \varepsilon$, the experimental Mg II/Mg I ratio has to be multiplied by ε. For instance, this multiplier value equals to 1.85 and 1.8, for the Perkin-Elmer Optima 3000 and Varian Vista ICP systems, respectively, and it should be verified for other systems (Dennaud et al. 2001).

It is reported that a ratio >8 in the radial viewing mode corresponds to robust conditions (Mermet 1991, Fernandez et al. 1994, Romero et al. 1997b, Dubuisson et al. 1998c) but lower Mg II/Mg I ratios are also considered to represent robust conditions with axial viewing (Dubuisson 1998b).When the radial mode is used, the Mg II/Mg I ratios are usually measured following an optimization of the observation height corresponding to the optimum of the ionic line emission. On the contrary, in axial

viewing mode, both atomic line and ionic line emission zones are probed (i.e., there is no optimal observation height), therefore an acceptable experimental Mg II/Mg I ratio can be lower for axial viewing than for radial viewing, even if the same ICP operating conditions are used (Dennaud et al. 2001).

1.4. Sample Introduction in Plasma Spectrometry

The main function of the sample introduction system is to introduce the maximum amount of analyte into the plasma in the most suitable form without changing its stability and without influencing the resulting emission signal (Mora et al. 2003, Nölte 2003). It has already been shown by several researchers that matrix effects also can be reduced or eliminated by a careful selection of the sample-introduction system (Maestre et al. 1999, Mermet 1998, Todoli and Mermet 1998b, Todoli and Mermet 1999, Todoli et al. 2002). In ICP-OES and ICP-MS, the success of the analysis strongly depends on the selection of an appropriate sample-introduction system (Maestre et al. 1999).

Generally, liquid samples are used in plasma spectrometry because of their homogeneity, ease of handling and the possibility of preparing calibration standards. The main parts of the sample introduction system can be summarized as (Mora et al. 2003):

i. a nebulizer, which converts the liquid sample into an aerosol;
ii. a spray chamber, which filters the aerosol and transports it to the plasma;
iii. a desolvation system to reduce the mass of solvent reaching the plasma; and,
iv. an injector tube to introduce the aerosol into the plasma base.

In Figure 1.2. a schematic diagram showing these parts is illustrated.

An ideal liquid sample-introduction system must fulfill the following requirements (Mora et al. 2003): high analyte-transport efficiency (amount of analyte reaching the plasma relative to the amount of analyte introduced into the sample introduction system); low solvent-transport efficiency, in order to avoid plasma deterioration and interferences caused by the solvent; good reproducibility; low memory effects, thus allowing high analytical throughput; robustness, i.e., stability of the system against changes in the sample matrix; ease of handling and low maintenance cost.

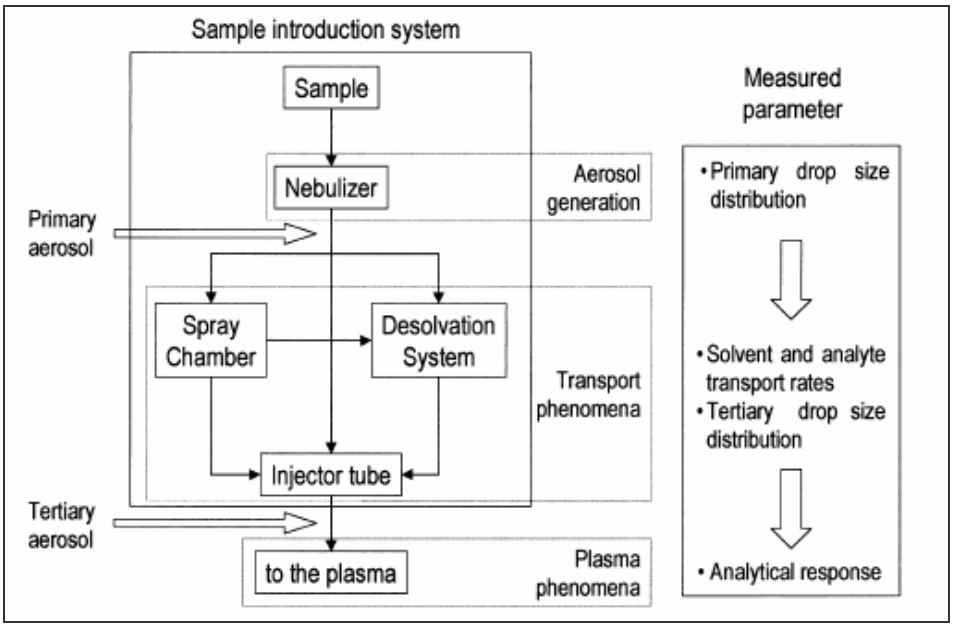

Figure 1.2. Diagram illustrating the sample introduction system
(Source: Mora et al. 2003)

1.4.1. Nebulizers

The characteristics of the aerosols depend on the amount of available energy and on the efficiency of the energy transfer. Therefore the classification of nebulizers is based on the type of energy employed. Thus aerosols can be produced;

i. by the kinetic energy of a high-velocity gas stream (pneumatic nebulizers) or of the liquid itself (hydraulic nebulizers);
ii. as the result of mechanical energy applied externally through a rotating (rotating nebulizers) or vibrating device (ultrasonic nebulizers); or,
iii. as a result of the mutual repulsion of charges accumulated on the surface (electrostatic nebulizers) (Mora et al. 2003).

1.4.1.1. Pneumatic Concentric Nebulizers

Pneumatic nebulizers can be classified in two groups according to the geometry of the interaction between the gas and liquid streams (Mora et al. 2003):

i. pneumatic concentric nebulizers (PCNs) (also known as Meinhard nebulizers) (the interaction takes place concentrically)

ii. cross-flow nebulizers (CFNs) (the liquid-gas interaction occurs perpendicularly)

In Figure 1.3. several types of the pneumatic nebulizer are shown .

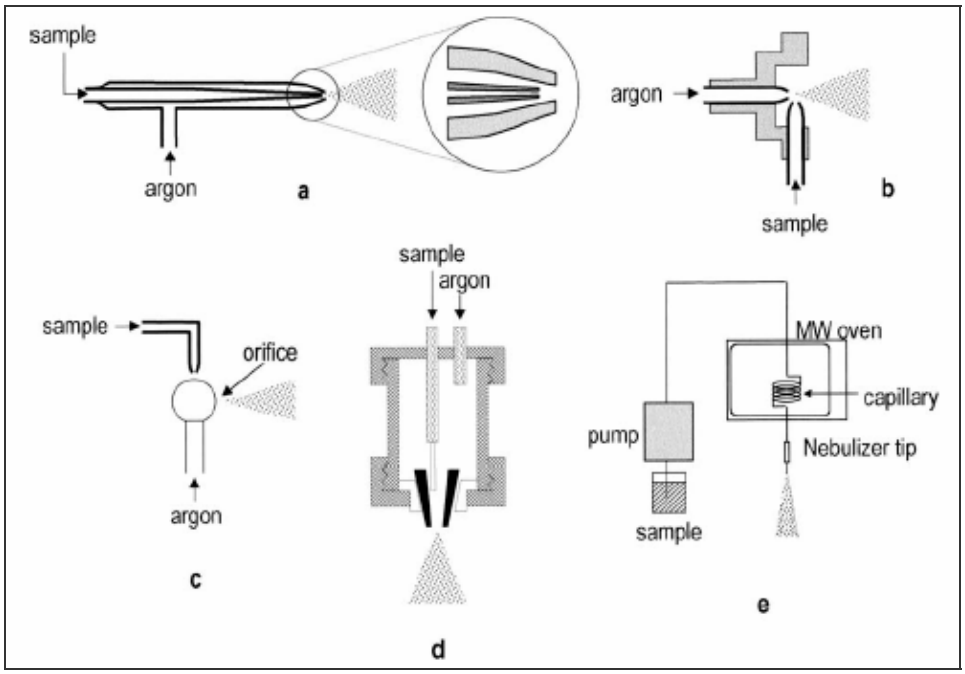

Figure 1.3. Types of pneumatic nebulizers. (a) concentric, (b) cross-flow, (c) Babington, (d) single-bore high-pressure, (e) microwave thermal
(Source: Mora et al. 2003)

PCNs (Figure 1.3a) are the most common ones because of their simplicity, robustness, ease of use and low cost. On the other hand, they have some disadvantages such as low transport efficiency (typically about 2% in ICP-OES) and tendency to get clogged when using high salt-content solutions (Mora et al. 2003).

Because of these drawbacks different nebulizer designs have been developed. Most of them are of the cross-flow type (based either on the Babington principle, such as the V-groove (VGN), the cone-spray, the Hildebrand grid nebulizers, etc.) or based on modifications of the conventional PCNs. The thermal nebulizer (TN) also known as thermospray has the disadvantage that it is not well suited to work with acidic or high salt-content solutions and slurries (Mora et al. 2003).

1.4.1.2. Ultrasonic Nebulizers (USN)

In USNs, the solution is pumped to the surface of a piezoelectric transducer. As a consequence of the interaction between the ultrasonic waves and the liquid film, a very fine aerosol is obtained. The sensitivity rises by a factor of about 10 when it is coupled to a desolvation system. Its main application is in trace analysis of samples which contain very small amounts of dissolved matter (Nölte 2003, Mora et al. 2003).

1.4.2. Aerosol-Transport Phenomena

The characteristics of the aerosols generated are very important since it influences both the signal and the noise. The parameters that must be considered for the quality of the aerosols are the aerosol droplet-size distribution (DSD) and the mean drop diameter, the aerosol yield, and the aerosol cone angle (Mora et al. 2003).

After the aerosol is generated (primary aerosol), before it reaches the plasma (tertiary aerosol), some modifications that change its original characteristics occur. All the processes that take place along the spray chamber or desolvation system are known as "aerosol-transport phenomena" (Mora et al. 2003). The final effects of these processes are: a reduction in the amount of aerosol reaching the plasma; a decrease in the turbulences associated with the aerosol-production process; a thermal and charge equilibrium; and a reduction in the aerosol mean-particle size. As a result, a more suitable aerosol for the plasma source is obtained (Mora et al. 2003 and references therein).

1.4.3. Spray Chambers

The main function of the spray chamber is to remove larger droplets, since these can destabilize the plasma. It is reported that, when less of 5% of the analyte nebulized is transported to the plasma, the spray chamber, rather than the nebulizer determines the characteristics of the aerosol injected into the plasma (Mora et al. 2003).

Spray chambers can be classified into three groups:

i. double-pass (DPSC), so-called Scott type or reverse-flow type;
ii. cyclonic (CSC), which includes several modifications such as vortex type, Sturman-Master or vertical rotary;
iii. single-pass or cylindrical type, also called direct spray chamber.

DPSC and CSC designs are the most frequently used spray chambers. Figure 1.4 shows these listed spray chambers.

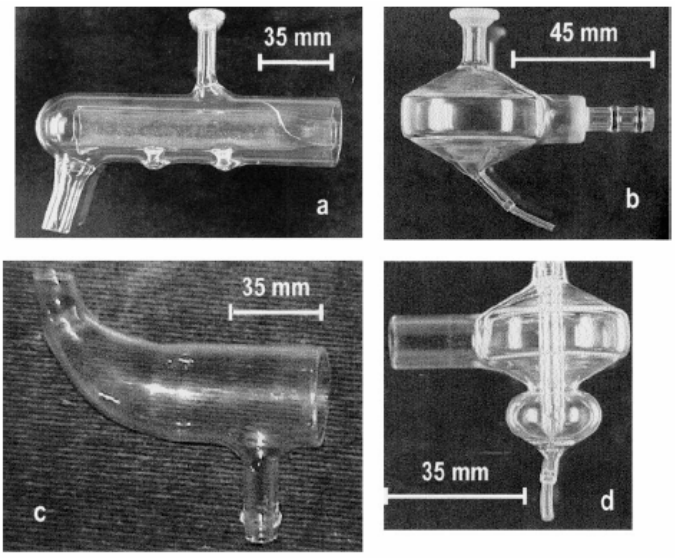

Figure 1.4. Common types of spray chambers. (a) double pass, (b) cyclonic, (c) single pass, (d) Genie (Source: Mora et al. 2003).

It has been reported that the DPSC produces finer tertiary aerosols than the CSC. As a result of the worse filtering action, the CSC affords higher analyte and solvent transport rates to the plasma than the DPSC. The wash-out times are lower for the CSC than for the DPSC. This can be due to the smaller inner volume of the CSC and the fact that the solution deposited on the spray-chamber walls can be easily removed in the CSC (Maestre et al. 1999, Mora et al. 2003).

Single-Pass Spray Chambers are used with systems that do not require a strong filtering action of the aerosol. With this chamber, a significant fraction of the aerosol reaches the plasma; therefore a desolvation system is highly recommended (Mora et al. 2003).

1.4.4. Desolvation Systems

To reduce the solvent load going into the plasma several desolvation systems have been proposed. The simplest device used to control this solvent load contains a thermostated spray chamber. In this design, the solvent vapor generated inside the spray chamber is removed from the aerosol stream. Most of desolvation systems include first a heating step, in which the solvent is totally or partially evaporated from the aerosol droplets and a second step in which solvent vapor is removed from the aerosol stream (Mora et al. 2003).

1.4.5. Micronebulizers

Micronebulizers (MNs) are the nebulizers specially designed to work efficiently at rates as low as 10 µl/min. Because the efficiency is improved both in terms of analyte and solvent transport, micronebulizers are also called high-efficiency nebulizers. As a result, they reduce or suppress waste, which is beneficial with hazardous wastes (Mermet 2002).

Several pneumatic concentric micronebulizers have been described:

i. the high-efficiency nebulizer (HEN);
ii. the MicroConcentric nebulizer (MCN);
iii. the MicroMist (MM);
iv. the direct-injection nebulizer (DIN); and,
v. the direct-injection high-efficiency nebulizer (DIHEN).

The HEN, MCN and MM are normally employed with a DPSC and are modified versions of the PCNs in which the liquid and gas cross-sectional areas and liquid capillary-wall thickness have been reduced. As a consequence, the liquid-gas interaction is improved, so that primary aerosols are finer than those generated by a conventional nebulizer. But since the HEN works at high pressures, a special gas-transport system is needed. Several low-volume spray chambers (LVSCs) have also been developed such as Cinnabar and Genie chambers. These spray chambers are reported to produce less severe matrix effects with inorganic species than the DPSC (Mora et al. 2003).

Because a spray chamber produces primary aerosol losses, sample introduction systems that do not include a spray chamber have been developed. In the DIN, the aerosol is generated at the plasma base and no analyte is lost downstream. The DIHEN minimizes cost and is easy to operate. It has been reported that both the DIN and DIHEN have shorter wash-out times, higher sensitivities and lower limits of detection than for any of the three remaining pneumatic concentric micronebulizers coupled to a spray chamber.

One of the drawbacks of the DIN and DIHEN is that they become easily blocked when working with high salt-content solutions. To overcome this, a new version of the DIHEN provided with a wider liquid sample capillary, called the large-bore direct injection high-efficiency nebulizer (LB-DIHEN), has been developed. The other limitations of the direct injection are severe solvent loading, and high velocity of the sample input into the plasma, which effect residence time of analyte in the plasma (Mermet 2002, Mermet 2005).

1.5. Detection

In principle, there are mainly two dispersive systems in ICP-OES; monochromators (so-called sequential systems) and polychromators (so-called simultaneous systems).

The main advantage of monochromators is the flexibility of wavelength selection. An optical mount often used is the Czerny-Turner. Monochromators are designed in such a way as to give better resolution than polychromators. Scanning monochromators can generate spectra in the neighborhood of the analytical line, which allows an accurate determination (Nölte 2003).

Polychromators are often based on the Paschen–Runge optical mounting, with the PMTs set up in the so-called Rowland circle. Even if all the analytical lines are measured simultaneously, the background correction measurement is typically carried out in a sequential manner. The main advantages of classical simultaneous spectrometers are short and long term stability and high analysis speed (Nölte 2003).

1.5.1. Photomultiplier Tube (PMT)

A PMT converts the photons into electrons by the photoelectric effect at a photocathode. The PMT presents some important advantages, such as a large wavelength range, including the UV region down to 120 nm, noise that is usually negligible at room temperature, thus not requiring any cooling device, and high amplifier gain. However, since the PMT is a single-channel detector, only little information is obtained from the emitted spectra compared to a photographic plate. In the case of a sequential system, it would be time consuming to work with several lines per element, and with a PMT-based polychromator; only one line can be selected per element because of the cost and the physical limitation of setting more than 30–40 PMTs. This then necessitates a detector that combines photon-current conversion of a photoelectric detector and the richness of information of a photographic plate which can be obtained by using a solid-state multichannel detector (Mermet 2002, Nölte 2003, Mermet 2005).

1.5.2. Solid State Detectors

Solid state detectors record wavelength bands and allow a sizeable gain of spectral information (array type) combined with simple signal processing capabilities. The smallest pictorial unit of a solid state detector is the pixel. The band of neighboring pixels which covers the complete detector widths described as an array, while a subarray covers only a part of the detector width. The charge capacity of a pixel is a measure of how many electrons can be collected in a pixel without being lost to surrounding pixels or electrodes. The charge capacity determines the dynamic range and linear range of the detector. If the charge capacity is exceeded, the charges spill over to adjacent pixels; this is called blooming and appears when the solid state detector is strongly overexposed (Nölte 2003).

Since multichannel detectors are based on charge transfer technology, they are categorized under the term charge-transfer device (CTD). CTDs consist of doped pure silicon. This light-sensitive material produces charges when struck by photons. Unlike the PMTs they have a relatively low dark current which gives a great advantage when

working in the lower wavelength range where there is very little background emission of the plasma. This low dark current is further reduced by external cooling to typically below 0^{o}C (Nölte 2003).

The two dimensional charge-coupled device (CCD) and charge-injection device (CID) detectors or a combination of linear CCD arrays are currently being used in ICP-OES systems and these permit fast acquisition of the entire UV-VIS spectrum (Mermet 2005).

In order to avoid blooming, the segmented charge-coupled device (SCD) detector is subdivided into relatively small photosensitive subarrays which are formed during manufacture. Each subarray has a grounding wire around it to efficiently prevent any potential spill over of charges to neighboring subarrays (Nölte 2003).

The advantages of multichannel detection can be divided into two groups. The first group is related to the richness of the acquired information, i.e., the entire UV-VIS spectrum (Mermet 2005):

i. full flexibility in analytical line selection,
ii. use of several lines of the same element to extend the dynamic range,
iii. use of a large number of lines of the same element to improve accuracy and to verify possible matrix effects or spectral interferences,
iv. qualitative analysis, and
v. fast diagnostics.

The second group is related to true simultaneous measurements (Mermet 2005);

i. speed of analysis,
ii. time correlation between lines of different elements to improve repeatability by internal standardization, and
iii. time correlation between line and adjacent background intensities to improve limits of detection and limits of quantitation.

On the other hand, these detectors have several limitations related to degradation in the resolution compared to PMT-based dispersive systems (possibly because of the pixilation), UV response, dynamic range and shot noise (Mermet 2002). Each individual pixel acts as an exit slit in solid state detectors. The major difference with a scanning monochromator is that each pixel will provide new information, while a scanning monochromator will provide for example only 20% new information for each step. The spectrum will be then cut into windows that correspond to the spectral bandpass of the pixel. Because the spectral bandpass of a pixel is larger than the physical line width, the

pixelation results in the difficulty of obtaining a fair measurement of the peak intensity and summation of pixels must be performed to the loss of the practical resolution. Because the absorption of photons in Si is from over a few nm for wavelengths below 200 nm, the efficiency of CTD detectors is usually poor in the UV therefore several techniques have to be used such as lumogen coating, open electrode technology and backside illumination (Mermet 2005). Dynamic range needs to be increased in order to facilitate the simultaneous measurement of lines with different intensities which can be obtained by reducing the readout noise down to a few electrons RMS. Another important limitation is the shot noise. For low signals such as background in the UV, the systems are usually shot noise limited, which necessitates long integration times to significantly decrease the relative standard deviation of the signal. This is particularly true when determining limits of detection. Moreover, time correlation between signals can only be observed if the non-correlated shot noise is not a limitation. It is said that multichannel detection with CCD and CID is highly beneficial to OES but these detectors at least for the time being are not ideal (Mermet 2002, Mermet 2005).

1.6. Method Development

For analysis with ICP-OES, a number of parameters are selected and optimized, such as analytical lines, excitation conditions, selection of the processing techniques (particularly the background correction), checking for and correcting for non-spectral interference (Nölte 2003).

Excellent analytical character of ICP-OES can be limited by spectral and non-spectral interferences. Non-spectral matrix effects are more important since these effects are not always obvious.

1.6.1. Spectral Interferences

These types of interferences originate from emissions of the structures of the spectral background and from sample components which emit light in the immediate neighborhood of the analytical line. If the cause of the spectral interference cannot be eliminated by selection of the appropriate line, then correction of these interferences

may be realized by improving the resolution, masking the interference by matrix matching, determining the impact of the interference by measuring an undisturbed wavelength of the interferent and subtracting its contribution from the interfering analyte line (inter-element correction) and/or applying a correction technique by multivariate regression (Nölte 2003).

1.6.2. Non-spectral Interferences

These interferences can occur because of changes in the sample transport, nebulizer properties, spray chamber aerodynamics and excitation conditions in the plasma. It was also reported that these interferences are caused by changes in the physical properties of the sample (particularly; viscosity, density, and surface tension), change in the rate of mass transfer into the plasma, temperature change at a constant RF power, or a change in the number of electrons in the plasma (Todoli and Mermet 1999, Todoli et al. 2002, Nölte 2003 and references therein). These types of interferences can be corrected by using matrix matching, use of an internal standard, calibration by analyte addition, addition of surfactants and ionization buffers (Nölte 2003).

1.7. Data Processing

Because of the availability of multichannel detection systems in recent years it is now possible to measure a larger number of lines per element, and consequently some general trends for operating conditions in the plasma, the sample introduction system and the excitation energy and the ionization state of the elements can be obtained. It has been emphasized by Mermet that in the selection of a set of lines the possibility of using compromised operating conditions and having lines that exhibit different behaviors for a change in matrix concentration or nature should be considered (Mermet 2002 and references therein).

Therefore, it is apparent that data processing should be adapted to take full benefit of the available information. The purpose is to obtain more accurate data by verifying the possible presence of spectral and chemical interferences, self-absorption, and drift. In addition, the increase in the amount of information should also be very

useful to obtain a better understanding of matrix effects (various contributions of sample introduction system, plasma conditions, torch design and observation mode in the matrix effects) (Mermet 2002).

The use of chemometrics should significantly improve data processing and several publications have already shown the advantages of these techniques (Griffiths et al. 2000, Moreda-Piñeiro et al. 2001, Grotti and Frache 2003b). Implementation of chemometrics in software and better knowledge of matrix effects should result in the introduction of an ideal software that should ask a limited number of questions such as: what is your matrix?, which elements do you want to determine?, what are the expected concentrations?, and what precision is required?. From the answers and based on a data base, the software should suggest several sets of analytical lines and appropriate operating conditions, i.e. power, nebulizer gas flow rate and integration time, at least for the most common matrices (Mermet 2002, Mermet 2005).

According to Mermet, the need for elemental analysis will remain forever as the determination of elements in various matrices will always be a request. Because there are not so many multi-element techniques, there is still room for OES if further improvements can be obtained. It is expected that most improvements will be related to more efficient data processing to take full benefit of the available emitted information. In addition, it is said that the same experiments should be performed on different ICP-OES instruments and in different conditions, probably through a collaborative study (Dennaud et al. 2000, Mermet 2005).

1.8. Aim of This Work

In the following chapters, studies of the elemental analysis of whale liver samples will be presented. The samples were obtained as part of the 2003 National Institute of Standards and Technology (NIST) / National Oceanic and Atmospheric Administration (NOAA) Interlaboratory Comparison Exercise for Trace Elements in Marine Mammals. Chapter 2 includes the initial analysis of the samples and focuses on the implications associated with the use of ICP-AES and ICP-MS. For Chapter 3, attempts to improve these analyses by using internal standards will be evaluated. The use of Principal Component Analysis (PCA) for choosing the appropriateness of several internal standards to compensate for various matrix effects will be demonstrated.

CHAPTER 2

WHALE LIVER ANALYSIS

2.1. Introduction

Metals enter the marine environment both naturally as well as from anthropogenic sources. On the other hand, discharges from various anthropogenic activities are the major cause of increased environmental concentrations of these elements (Hoekstra et al. 2003, Ikemoto et al. 2004). In the last decades, mass mortalities occurred in several marine mammal populations and toxic contaminants may have been a factor in a number of epizootics which have affected these animals (Harvell et. 1999, Law et al. 2003,). In order to evaluate the degree of contamination by trace elements, several investigations have been carried out on marine mammals (Mössner et al. 1997, Ponce et al. 1997, Becker 2000, Capelli et al. 2000, Bennett et al. 2001, Zhou et al. 2001, Anan et al. 2002a and 2002b, Méndez et al. 2002, Bustamante et al. 2003, Hoekstra et al. 2003, Law et al. 2003, Ikemoto et al. 2004, Kunito et al. 2004).

Marine mammals uptake the metals predominantly from food and due to their position at the top of the aquatic food chain and their long life-spans, such uptake can lead to the bioaccumulation of the elements in their tissues (Mössner et al. 1997, Ponce et al. 1997, Zhou et al. 2001).

Although metals are often classified as essential or nonessential, at sufficiently high concentrations, they may become toxic and cause multiple symptomatic effects that influence the health of both animals and humans (Zhou et al. 2001). The major toxic metals causing such effects are As, Cd, Cr, Sn, Ni and Hg. Elements that are essential but are potentially toxic include Fe, Se, Cu and Zn which are participating in the formation or function of enzymes involved in metabolism (Zhou et al. 2001, Bustamante et al. 2003, Ikemoto et al. 2004). Furthermore, there are some recent studies suggesting that several elements such as As, Cd, Co, Cr, Cu, Hg, Pb, Se, and V disrupt

estrogen receptor (ER)-, androgen receptor (AR)- or glucocorticoid receptor (GR)-mediated processes *in vivo* and *in vitro* in mammals at the environmentally relevant concentrations (Martin et al. 2002, Johnson et al. 2003, Kunito et al. 2004).

Therefore, it is important to investigate the contamination status of trace elements in tissues of marine mammals to reveal their possible adverse effects on these animals. Liver is routinely analyzed because it is the principle organ that can provide the best measurement for the largest number of elements. Also it is a major detoxification location for contaminants; therefore, it is a suitable organ for enzyme and metabolite analyses (Becker 2000, Pugh et al. 2003, Kunito et al. 2004).

Because the metal accumulation indicates the level of contamination of the sea, marine mammals could be considered as indicative organisms of marine pollution and can be used as an important tool for monitoring the long-term effects of the pollution of the marine environment on marine mammals and human health (Mössner et al. 1997, Zhou et al. 2001, Cardellicchio 2002). In addition, establishing a long term database on contaminants in marine mammals is needed to help in evaluating the role of contaminants in mortality events and to provide a basis for exploring, predicting and alleviating these events (Zhou et al. 2001, Ruelas-Inzunza and Páez-Osuna 2002).

Trace element determination in marine species is required to provide information about marine environmental quality, to evaluate their impact on human and animal health and nutrition, and to identify global, regional and point sources that release contaminants into the atmosphere and coastal ecosystem and find proper environmental solutions for these contaminants.

Accurate contaminant data is needed in order to estimate marine environmental quality more appropriately and to monitor the health status of certain marine species. Certified reference standards for this purpose are often unavailable and this limitation can lead to decisions based on subjective analytical results that can have significant economic and health consequences (NIST 2004).

The National Institute of Standards and Technology (NIST) administers periodic interlaboratory comparison exercises through several programs, including the National Marine Analytical Quality Assurance Program (NMAQAP), which is supported by the National Oceanic and Atmospheric Administration's National Marine Fisheries Service (NOAA/NMFS), through the Marine Mammal Health and Stranding Response Program. Through these interlaboratory studies, production of quality control and reference materials can be managed and a quality controlled resource of selected marine mammal

tissues can be maintained (Becker et al. 1997a and 1997b, Pugh et al. 2003, NIST 2004).

Scientists who are interested in marine studies have studied trace metal concentrations in marine mammal tissues (particularly in liver) using different analytical approaches including instrumental neutron activation analysis (INAA) (Becker et al. 1999) atomic absorption spectrometric techniques with flame (FAAS) for the determination of Cu, Fe, Mn, Cd, Zn (Cardellicchio et al. 2002, Méndez et al. 2002, Ruelas-Inzunza and Páez-Osuna 2002, Bustamante et al. 2003, Kunito et al. 2004); with graphite furnace (GFAAS) for Cd (Monaci et al. 1998, Ancora et al. 2002, Cardellicchio et al. 2002, Hoekstra et al. 2002, Ruelas-Inzunza and Páez-Osuna 2002), for Hg (Epstein 2000), and for As (Tilbury et al. 2002); with hydride generation (HGAAS) for the determination of As (Kunito et al. 2004) and with cold vapor atomic absorption spectrometry (CVAAS) for Hg (Epstein and Buehler 1998, Zhou et al. 2001, Kunito et al. 2002, Tilbury et al. 2002, Agusa et al. 2004, Ikemoto et al. 2004, Kunito et al. 2004). For Hg determination there are also other methods described such as advanced mercury analyzer (AMA) (Hoekstra et al. 2002, Bustamante et al. 2003) and flow injection mercury system (FIMS) (Monaci et al. 1998, Ancora et al. 2002).

Atomic absorption techniques have provided accurate determination of many trace elements in biological samples. Disadvantages of FAAS are that releasing agents or modifiers are necessary and it requires careful control of the flame stoichiometry to overcome chemical interferences (Tyler 1994). GFAAS has small sample consumption in the determination of trace levels but analysis time is longer than for other techniques. Although atomic absorption spectrometry offers sufficient performance, in most cases it is a single element technique and is therefore slow for multielement determinations.

The apparent method of choice for analyzing whale liver is inductively coupled plasma mass spectrometry (ICP-MS) (Chang and Jiang 1997, Epstein 2000, Christopher 2001, Anan et al. 2002a, Hoekstra et al. 2002, Kunito et al. 2002, Law et al. 2003, Agusa et al. 2004, Ikemoto et al. 2004, Kunito et al. 2004) for its multielement capability, high sensitivity, large dynamic range and short analysis times. In general, with ICP-MS, an upper total dissolved solids (TDS) limit of 0.1-0.2% (Ryan 1998) in the solution should not be exceeded to ensure continuous operation for an extended period. Above this limit, unacceptable levels of signal instability, deposition on cones and a decrease in the nebulization efficiency are encountered.

Inductively coupled plasma optical emission spectrometry (ICP-OES) is a useful alternative to ICP-MS in the analysis of marine mammal tissues (Monaci et al. 1998, Capelli et al. 2000, Zhou et al. 2001, Tilbury et al. 2002, Bustamante et al.2003, Yılmaz 2003) because of its ease of use and ability to handle higher levels of TDS (Johnson 1996). It also shares the same properties with ICP-MS such as multielement capability, and short analysis times but the sensitivity of ICP-OES is worse than that of either ICP-MS or GFAAS.

As a participant of an interlaboratory study administered by NIST, we were asked to perform measurements for 12 elements (As, Cd, Cu, Fe, Hg, Mn, Mo, Rb, Se, Sn, V and Zn) in two quality assurance materials; Beluga Whale Liver Homogenate, QC97LH2 and Pygmy Sperm Whale Liver Homogenate, QC03LH3.

Coming from an ocean environment, whale liver presents a challenging matrix in which precision, accuracy, and nonspectroscopic interferences such as EIEs can be examined so it would be instructive to use the whale liver matrix for comparison of ICP-MS and ICP-OES analyses. Both ICP-MS ad ICP-OES were performed and compared with regard to their relative analytical Figures of merit for the whale liver samples.

2.2. Experimental

2.2.1. Materials

2.2.1.1. Whale Liver Homogenates

The marine mammal samples used throughout this study were obtained as part of the 2003 National Institute of Standards and Technology (NIST) / National Oceanic and Atmospheric Administration (NOAA) Interlaboratory Comparison Exercise for Trace Elements in Marine Mammals and supplied by NIST Charleston Laboratory, South Carolina, USA.

Marine Mammal Whale Liver Homogenate III (labeled as QC97LH2) had been taken by NIST from Beluga Whale (*Delphinapterus leucas*) livers collected during a 1997 subsistence hunt at point Lay, Alaska, USA and was used as control material in the study. Intercomparison Exercise Whale Liver Homogenate III (labeled as QC03LH3) had been taken by NIST from Pygmy Sperm Whale (*Kogia breviceps*) and it had been previously issued as an unknown material in the 2001 NIST/NOAA Interlaboratory Comparison Exercise for Trace Elements in Marine Mammals. It was used again as the unknown sample for the current study.

These materials had been cryo-homogenized to reduce the possibility of changes in sample composition due to thawing and refreezing and their homogeneity verified by measurements performed at NIST. They were shipped in nitrogen containers and stored in Teflon jars (10 ml) at –80^{o}C until analyses were performed.

2.2.1.2. Reagents and Standard Solutions

Nitric acid (65%) and hydrogen peroxide (30%) were purchased from Riedel-de Haen (Germany) and were used for sample digestion and for the adjustment of acid content in the standards and samples. Doubly de-ionized water (18.2 MΩcm) obtained from a Milli-Q waters system (Millipore, USA) was used throughout the study.

Standard solutions and synthetic samples were prepared from the ICP Multielement standard solution IV (1000 mg/L) that contains Ag, Al, B, Ba, Bi, Ca, Cd, Co, Cr, Cu, Fe, Ga, In, K, Li, Mg, Mn, Na, Ni, Pb, Sr, Tl, Zn as purchased from Merck (Darmstadt, Germany).

One mg/L multielement stock solution (containing Cd, Cu, Fe, Mn, and Zn) which was used for spiking for the recovery studies was prepared by taking 1 ml of 1000 mg/L multielement standard solution IV and then diluting it to 1000 ml. The final concentration of this spike was then 33.33 mg/L in the sample.

A 100 mg/L stock solution of Hg was prepared by mixing 0.1360 g $HgCl_2$ solid with 5 ml of 65% HNO_3 and then diluting to 100 ml. A 200 mg/L stock solution of As was used which was prepared previously from As_2O_3 to prepare the 10 mg/L stock solution of As and other As standard solutions (As_2O_3 has been prepared by adding 5 ml NaOH and 2.5 ml H_2SO_4, then diluting to 250 ml). The stock solution of As (10 mg/L) was prepared by taking 2500 µl from the 200 mg/L As solution and then diluting it to a

final volume of 50 ml. This 10 mg/L As stock solution was used to prepare the As standard solutions.

After taking appropriate amounts from the stock solutions, 8 ml of HNO_3 and 1 ml of 30% H_2O_2 were added to standard solutions and diluted to a final volume of 25 ml to attempt matching the acid matrices to the samples (H_2O_2 was added to help dissolve organic matter). Before measurements, 500 µl of Rh internal standard solution (10 mg/L from Merck, Darmstadt, Germany) were added to both samples and standards.

2.2.2. Microwave Digestion of Whale Liver Homogenates

In order to minimize contamination, all the receiving vessels and implements used in this study were previously washed in a 10% nitric acid solution prior to the experiments, and the Teflon vessels used in the microwave digestions were boiled in a 10% nitric acid solution. A plastic knife was used to transfer the samples into the Teflon vessels before weighing to avoid metal contamination.

For the microwave digestion of control samples, 7 aliquots of approximately 0.4 g of each homogenized sample were digested in Teflon containers with 8 ml of 65% HNO_3 and 1 ml of 30% H_2O_2 using a microwave digestion instrument (MILESTONE Microwave Laboratory Systems ETHOS PLUS labstation with HPR-1000/10S high pressure segmented rotor). In six of these seven vessels, one ml of H_2O was added before digestion. Into the other one ml of 1000 mg/L ICP multielement standard solution IV was added as a spike. The microwave oven was operated at 150 ^oC for 10 min, at 200 ^oC for 10 min, then at 200 ^oC again for 20 min at a power of 500 W. At the end of the temperature program the turntable was rotated continuously for 20 min for ventilation. After allowing the digest to cool to room temperature, each sample was transferred to acid-washed polyethylene vials (and also volumetric flasks) and was brought to a final volume of 25 ml with ultra pure water. Also, 3 blanks were digested at the same time with the liver homogenates by adding 8 ml of 65% HNO_3, 1 ml of 30% H_2O_2 and 1 ml of H_2O to the vessels. For unknown samples, applying the same procedure, 6 aliquots of the unknown homogenized sample were digested.

2.2.3. Trace Metal Analysis

2.2.3.1. Instrumentation and Operating Conditions

Metal analyses were performed by both inductively coupled plasma optical emission spectrometry (ICP-OES) and inductively coupled plasma mass spectrometry (ICP-MS) for As, Hg, Cd, Cu, Fe, Mn, and Zn. For ICP-MS analyses, a Hewlett Packard 4500 Series ICP-MS with a Shield Torch System was used. Instrument operating conditions are listed in Table 2.1.

Table 2.1. ICP-MS instrument operating conditions

ICP-MS Hewlett Packard 4500 Series	
Plasma Gas Flow Rate	15.1 L/min
Auxiliary Gas Flow Rate	1.00 L/min
Carrier Gas Flow Rate	1.00 L/min
Plasma Power	1450 Watt (RF Power)
Sampling Depth	8 mm
Torch –H	-1.1 mm
Torch –V	0.7 mm
Peristaltic Pump	0.1 rps
S/C Temperature	2^{o}C
Pump Uptake Speed	0.50 rps
Uptake Time	20 sec
Stabilization Time	5 sec

^{75}As, ^{202}Hg, ^{114}Cd, ^{63}Cu, ^{55}Mn, ^{57}Fe, ^{66}Zn, and ^{103}Rh isotopes were analyzed. A Varian Liberty Series II inductively coupled plasma optical emission spectrometer (Varian Inc., Australia) employing the axial viewing mode, an air path monochromator, a cyclonic spray chamber, and a concentric glass nebulizer was used. Instrument properties and typical operation conditions are listed in Table 2.2.

Table 2.2. ICP-OES instrumentation and operating conditions

ICP-OES Varian Liberty Series II		
Spectrometer	Optical configuration	0.75 meter Czerny-Turner
	Grating	90 x 100 mm holographic
	Grating density	1800 grooves/mm
	Plasma viewing mode	Axial
	Injector id	2.5 mm
	Detector	Photomultiplier
Sample introduction	Nebulizer	Concentric glass
	Spray chamber	Cyclonic (Sturman-Masters)
	Torch	One-piece quartz type
	Plasma gas flow rate	15.0 L/min
	Auxiliary gas flow rate	1.5 L/min
	Pump rate	15 rpm
RF Generator	Operating frequency	40.68 MHz
	Type	Crystal controlled with solid state driver and water cooled power tube
	RF power	1.2 kW
	Interface	Nickel cooled cone interface

The Mg II 280 /Mg I 285 ratio used for monitoring the plasma robustness and excitation conditions as cited by Mermet (1991). The value that was found was 8.74, therefore, it can be concluded that the samples were analyzed under robust plasma conditions and the analysis was not affected by the instrument and plasma conditions.

Elements and their selected wavelengths measured in this study by ICP-OES were As I 228.812 nm, Cd II 226.502 nm, Cu I 324.754 nm, Fe II 259.940 nm, Hg I 253.652nm, Mn II 257.610 nm, Zn I 213.856 nm, and Rh II 249.077 nm.

For the control samples, four replicates were run. A Q-test was applied when deciding to discard results. However, in some cases, the Q-test did not allow the discarding of data. Therefore, there are four results reported for some control replicates. Likewise, all numbers are reported as if four digits were significant except in cases where rounding may alter the results. In such cases a guard digit was retained.

2.3. Results and Discussion

The results for the analyses of the control whale liver sample (CWLS) and laboratory exercise test whale liver sample (LETWLS) obtained by both ICP-OES and ICP-MS techniques are represented in the following tables. The control and test samples contained other elements in addition to those analyzed. It should be noted that the

control sample contained Mo, Rb, Se, Sn, V at concentrations of approximately 0.685, 1.31, 24.30, 0.044, and 0.295 µg/g, respectively. The complex nature of the matrix, the problems associated with the handling and preparation of the sample material, and the possible interferences related to the analysis of these materials must be noted. Where appropriate, explanation is given.

Table 2.3. Values for the Control Material Beluga Whale Liver Homogenate obtained at Hıfzısıhha Institute by using ICP-MS

Element (isotope)	**Normal Calibration (ug/g, wet mass)**	**NIST certified value (ug/g, wet mass)**	**Difference from certified value %**	**Recoveries %**	**RSD %**
Cd - 114	1.87 ± 0.29	2.35 ± 0.06	20,4	147.3	15,5
Cu - 63	13.61 ± 0.6	13.16 ± 0.4	3,4	127.9	4,4
Mn - 55	2.10 ± 0.13	2.37 ± 0.08	11,4	92.12	6,2
Hg - 202	47.08 ± 1.76	40.31 ± 2.51	16,8	_	3,7
Zn - 66	37.46 ± 5.67	26.31 ± 0.66	42.4	169.2	15,1
As - 75	0.760 ±0.107	0.391 ± 0.027	94.4	_	14,1
Fe - 57	442 ± 12	668 ± 15	33.8	80.94	2,7

Table 2.4. Values for the Control Material Beluga Whale Liver Homogenate obtained at İYTE by using ICP-OES

Element (wavelength,nm)	**Normal Calibration (ug/g, wet mass)**	**NIST Certified value (ug/g, wet mass)**	**Difference from certified value %**	**Recoveries %**	**RSD %**
Cd II – 226.502	2.05 ± 0.19	2.35 ± 0.06	12.8	91.10	9.3
Cu I – 324.754	14.54 ± 0.76	13.16 ± 0.4	10.5	103.2	5.2
Mn II – 257.610	2.41 ± 0.20	2.37 ± 0.08	1.7	82.68	8.3
Hg I – 253.652	44.19 ± 1.51	40.31 ± 2.51	9.6	_	3.4
Zn I – 213.856	33.44 ± 1.78	26.31 ± 0.66	27.1	66.79	5.3
As I – 228.812	73.83 ± 5.12	0.391 ± 0.027	18782	_	6.9
Fe II – 259.940	780 ± 4	668 ± 15	16.8	109.4	0.5

2.3.1. Recovery Values

Recoveries were calculated for the elements Cd, Cu, Fe, Mn and Zn. The recovery values between 85 – 115 % can be considered acceptable for an analysis. In the ICP-OES analysis for control (CWLS) and test (LETWLS) material, these values for Cd (91.10% and 90.31%), Cu (103.2% and 106.7%), and Fe (109.4 and 109.1) fall in this range whereas Mn (82.7 and 83.01) and Zn (66.79 and 65.30) were outside of this range. On the other hand, for the ICP-MS analyses these recovery values were somewhat larger for Cd, Cu, Mn and Zn. Cd had a recovery value of 147.3% for control material and 132.9% for test material which are very high as compared with the ICP-OES values. Similarly, Zn had recovery values of 169.2% and 156.1% for control and test material, respectively. These large values can be explained by the isobaric interferences (^{114}Sn on ^{114}Cd and $^{34}S^{16}O^{16}O$ or $^{32}S^{34}S$ on ^{66}Zn) which affect the analysis of these elements. For Cu and Mn, the differences are not so high.

2.3.2. Control Whale Liver Sample (CWLS)

When the measured concentrations for the control sample (Beluga Whale liver homogenate) are compared with the certified values, the results for Cd, Cu, and Mn whether measured by ICP-MS or ICP-OES were considered acceptable within experimental error although some problems in accuracy exist. As can be seen from Table 2.3, ICP-MS analysis gave (accuracy) values between 3.4% and 20.4% relative to the certified values whereas ICP-OES analysis (Table 2.4) gave values between 1.7% and 12.8% relative to the same certified values. For the same control whale liver sample, ICP-MS gave the more accurate results for Cu while ICP-OES gave more accurate results for Mn.

Precision expressed as the percent relative standard deviation (%RSD) for the measurement of Cd, Cu, and Mn by ICP-MS were 15.5%, 4.4%, and 6.2%, respectively. For the same elements, the precision by ICP-OES analysis was 9.3%, 5.2%, and 8.3%, respectively. Overall for these three elements, the greatest precision and accuracy were obtained for measurements of Cu by both methods. The other elements analyzed (Zn, As, Hg, and Fe) overall gave less precise and accurate results.

Moreover, according to a t-test applied to the calculated concentrations, for the ICP-MS analysis, the determined value for the concentration of Cu is in good agreement with the certified value while for the ICP-AES analyses of Cd, Mn, and Hg, their determined values were found to be acceptable within the reported error of the certified value. Each individual element analyzed in the control material and possible sources of errors were described below.

2.3.2.1. Cadmium

A lack of accuracy for Cd by ICP-MS can be due to an isobaric interference from ^{114}Sn which was present in the control sample at a concentration of 0.044 μg/g. It is possible to apply a mathematical correction by measuring the intensity of ^{118}Sn and using the following equation:

$$^{114}\mathrm{Cd} = \mathrm{mass114} - (0.0268 \times {}^{118}\mathrm{Sn}) \qquad (2.1)$$

where the number 0.0268 represents the ratio of natural abundances of two isotopes of Sn (^{114}Sn/^{118}Sn = 0.65% / 24.23%). Such an isobaric interference should give a positive error. Based on the precision for our measurements for Cd by ICP-MS (15% RSD), it is still possible that Sn is an interferent. Unfortunately, we could not perform this correction because of the unavailability of Sn in our ICP multielement standard solution.

Line selection in ICP-OES is very important to avoid spectral interferences. When choosing the appropriate emission line for Cd analysis by ICP-OES, the most intense line for Cd at 228.802 nm was not chosen due to a spectral overlap of As at the same wavelength. To avoid a known spectral overlap with As, the 226.502 nm line for Cd was chosen. The lack of accuracy for ICP-OES analysis of Cd has been attributed to the rather large concentration of Fe in the control whale liver sample (WEB_1). In the presence of 100 ppm Fe, an analysis for Cd can give a positive error of approximately 0.03 ppm. Considering the precision of the analysis (9.3% RSD), it may be possible that Fe was a small interference.

2.3.2.2. Copper

For all the elements analyzed by ICP-MS and ICP-OES, the best accuracy and precision was obtained for copper. However, it should be noted that for ICP-OES analyses large deviation (10.5%) from the certified value of copper can be caused by the possible positive errors due to presence of Fe and V in this sample. In an analysis for Cu, the presence of 100 ppm Fe can give a positive error of approximately 0.003 ppm and 100 ppm V can give an error of 0.02 ppm (WEB_1).

2.3.2.3. Manganese

For Mn, the lack of accuracy in the ICP-MS analysis is most likely due to an isobaric interference at $^{40}Ar^{15}N^{+}$ at m/z 55. The nitric acid matrix (25%) would be a major source of nitrogen for formation of this isobar. ICP-OES results for Mn were successful without the need for any correction. As can be inferred from Table 2, the measured value was less than 2% of the certified value.

2.3.2.4. Mercury

In the analysis of Hg with ICP-MS, the lack of accuracy may be due to its high ionization energy (10.44 eV) causing poor ionization efficiency (approx. 30%) and severe memory effects (Paul et al. 2003). Although several washings were done between the sample runs, this memory effect could not be overcome and a value higher than the certified value was found. It is well known that after a sample containing Hg is nebulized into a spray chamber, significant levels of Hg can still be detected for several minutes after analysis. Hg either adsorbs onto the spray chamber walls or is retained as vapor in the dead volume of the spray chamber (Nixon et al. 1999). It was thought that the use of a complexing agent might be useful to reduce memory effects by preventing interactions between the analyte and the surface area of the introduction system. A number of different solutions have been used by several researchers with ICP-MS analysis to eliminate the mercury memory effect using gold and dichromate in

hydrochloric acid (Nixon et al. 1999), sulfur containing complexing agents like D-penicillamine, Dimercaprol, or Meso-2,3-dimercaptosuccinic acid (DMSA) (Harrington et al. 2004, Chen et al. 2000), and 4% (v/v) aqueous methanol (Paul et al. 2003). Unfortunately these corrections could not be performed because of the unavailability of the ICP-MS instrument on our campus.

Also, for the ICP-OES analysis of Hg, as in the case of arsenic, the most prominent lines of Hg fall below 200 nm (194.163 nm and 184.950 nm having highest intensities) requiring use of a vacuum-UV equipped instrument. So to be able to measure Hg signals, a less intense Hg atom line at 253.652 nm was chosen. The accuracy obtained by ICP-OES was better than for ICP-MS whereas the precision by both instruments for Hg was found to be identical.

2.3.2.5. Zinc

As can be seen from Table 1 and Table 2, zinc was one of the elements having less precise and accurate results obtained by both techniques. In the ICP-MS analysis this can be explained by the possible interferences of $^{34}S^{16}O^{16}O$ or $^{32}S^{34}S$ on the ^{66}Zn signal. The precision obtained in our ICP-OES analysis can be considered to be better than for our ICP-MS analyses although the difference between the certified value and measured value is high.

2.3.2.6. Arsenic

Arsenic was the element having the least precise and accurate results in its analysis by both techniques. Although the ICP-MS results seem much better than for ICP-OES, this large difference between the control material and certified value for As can be explained by the possible occurrence of Cl in the liver matrix which can cause the polyatomic interference of $^{40}Ar^{35}Cl$ on the ^{75}As signal. Since As is monoisotopic, it is not possible to choose another isotope to overcome this interference. A mathematical correction is generally used to solve this problem (Van Den Broeck et al. 1997). The idea of this correction is that the ratio of the signal for $^{40}Ar^{35}Cl$ to that of $^{40}Ar^{37}Cl$ will be equal to the ratio of the abundance of the two isotopes ^{35}Cl and ^{37}Cl, which is

75.77/24.23. To calculate the signal for $^{40}Ar^{35}Cl$ present at m/z 75 (^{75}As), the signal for $^{40}Ar^{37}Cl$ at m/z 77 (^{77}Se) can be measured. Since Se exists in the whale liver matrix, then correction will be based on the ^{82}Se signal. The correction equation is therefore;

$$^{75}As = {}^{75}As - 3.127 \times \left[{}^{77}Se - \left(0.815 \times {}^{82}Se\right)\right] \quad (2.2)$$

Unfortunately, because of the lack of Se element in our ICP multielement standard, this correction could not be performed appropriately.

For our ICP-OES analysis of As, the large errors may possibly can be attributed to the detection limits of the ICP-OES and the selected wavelength. Since the most prominent and most intense lines of As are located below 200 nm which are 188.979 nm and 193.696 nm, the proper reading of As signals was not possible. The arsenic line that was used in this study was 228.812 nm (possible As line above 200 nm with the highest intensity) can explain this erroneous result. Moreover, at 228.802 nm Cd has a more intense line than As which can cause a serious spectral interference. This can be corrected by choosing another spectral order.

2.3.2.7. Iron

In the ICP-MS determination of Fe, because of the possible polyatomic interference of $^{40}Ar^{16}O$ on ^{56}Fe signal due to water used in sample preparation, our calculations were based on the ^{57}Fe isotope. But still, there is another interference of $^{40}Ar^{16}O^{1}H$ caused from OH coming from the water environment and thus interfering with the ^{57}Fe signal. Although the precision seems quite good for ICP-MS, this interference may be a reason for this lack of accuracy. On the other hand, the accuracy and precision obtained by ICP-OES appear better than for ICP-MS. The large gap within the range of concentrations used for the calibration of iron can be another reason for the lack of accuracy in the analysis of Fe. Dilution of the sample, of course, is the simplest solution to this problem.

2.3.3. Internal Standardization

Rh internal calibration was also done to improve the analyses but unfortunately the results were not satisfactory so they were not included here. There might be an incomplete mixing of Rh with the samples causing inaccurate data collection. In the ICP-OES analysis, there is strong spectral interference on the Rh II 249.077 nm signal caused by the more intense Fe atom line at 249.064 nm. Possibly due to high Fe concentration in the liver matrix, the successful use of Rh as an internal standard was prevented; therefore, the Rh internal standard calibration curves could not be obtained.

2.3.4. Laboratory Exercise Test Whale Liver Sample (LETWLS)

Results from the analysis of the test whale liver sample are shown in Tables 3 and 4, for ICP-MS and ICP-OES, respectively. It should be noted of course that similar errors which affected the precision and analysis for the control whale liver sample (CWLS) will be present for the sample (LETWLS). The two matrices are from whale liver, but from two different species which live in two different regions of the world.

Table 2.5. Values for the Sample Material Pygmy Sperm Whale Liver Homogenate obtained at Hıfzısıhha Institute by using ICP-MS

Element (isotope)	Normal Calibration (ug/g, wet mass)	Recoveries %	Calibration equations
Cd - 114	6.06 ± 0.16	132.9	y = 344153x + 5181.1 R^2 = 0.9961
Cu - 63	2.51 ± 0.1	122.4	y = 1054444.19x + 14051.43 R^2 = 0.9986
Mn - 55	1.24 ± 0.11	85.11	y = 4224337.44x + 8787.23 R^2 = 1.00
Hg - 202	2.21 ± 0.28	–	y = 157523x - 238.12 R^2 = 0.9998
Zn - 66	23.38 ± 2.18	156.1	y = 12268x + 12900 R^2 = 0.9764
As - 75	0.702 ± 0.050	–	y = 149855x - 218.1 R^2 = 1.00
Fe - 57	512 ± 14	70.03	y = 97479x – 1786.8 R^2 = 0.9978

Table 2.6. Values for the Sample Material Pygmy Sperm Whale Liver Homogenate obtained at İYTE by using ICP-OES

Element (wavelength, nm)	Normal Calibration (ug/g, wet mass)	Recoveries %	Calibration equations
Cd II – 226.502	5.89 ± 0.07	90.31	y = 49052x + 330,45 R^2 = 0.9999
Cu I – 324.754	2.45 ± 0.10	106.7	y = 19794x - 73,591 R^2 = 0.9996
Mn II – 257.610	1.26 ± 0.06	83.01	y = 63573x + 78,803 R^2 = 0.9996
Hg I – 253.652	2.87 ± 0.51	–	y = 4539.3x + 2007.9 R^2 = 1.00
Zn I – 213.856	22.04 ± 1.54	65.30	y = 51107x - 1788,8 R^2 = 0.9994
As I – 228.812	186 ± 2.7	–	y = 1480.4x + 134.52 R^2 = 0.9948
Fe II – 259.940	800 ± 5.9	109.1	y = 10920x + 12003 R^2 = 0.9982

Without the ability to apply corrections, it can only be assumed that the results for Cu will be the most accurate and precise based on matrix effects, sample preparation, and analysis errors due to sample introduction and interferences. However, it is believed that general comparisons can still be made with respect to the elements Cd, Cu, Mn, Hg, and Zn.

As the results show, regardless of whether analysis was performed by ICP-MS or ICP-OES, the concentrations of metals in the control (CWLS) and test (LETWLS) material differ from each other. If we assume similarity for both whale liver matrices, then the measured concentrations of Cd, Cu, Mn and Hg in the test whale liver sample (LETWLS) are expected to be reasonably correct. Moreover the results for both the ICP-MS and ICP-OES analyses of these elements is very similar (range 6 - 43%), further supporting the validity of the measurements for Cd, Cu, Mn and Hg.

After receiving the certified values from NIST for the pygmy whale, a t-test was applied to the calculated concentrations. According to these results it was found that only our submitted results for the ICP-MS analysis of Cd and Zn values were in good agreement with the certified values. After a second evaluation of our ICP-AES results (not submitted to NIST), it was seen that our results for the ICP-AES analyses of Cd, Cu, Zn and Hg had actually been acceptable within the reported errors of the certified values for each of these elements.

The concentration of Zn was relatively the same for both whale liver types. In contrast, the concentrations of Cd, Cu, Mn and Hg were quite different from one whale liver matrix to the other. These differences can most likely be explained by the different geographical location in which whale species are found and different feeding habits that these species have. The Beluga whale lives seasonally in ice-free Arctic seas, mainly in circumpolar areas and feeds on plankton, fish, mollusks and other bottom-living invertebrates whereas the Pygmy Sperm whale is widely distributed in tropical, sub-tropical, and temperate seas and eats small fish, cuttlefish, deep-sea shrimps and squid (WEB_1). Such differences in matrices further stress the need for preparation and availability of appropriate standards by such organizations as NIST.

It should be noted that an alternative analysis such as the standard addition method could improve these analyses. However, generally for ICP analyses, standard addition is not preferred because this method is time consuming and not appropriate for multielement analysis.

2.3.5. Evaluation of Our Measurements for the NOAA Exercise

For many elements such as Cd, Fe, Hg, Mn, and Zn, ICP-OES showed better results when compared with ICP-MS. These can most probably be mainly attributed to the isotopic interferences that affected the ICP-MS analysis. Several problems were encountered especially in the analysis of As and to some extent for Hg. The general accepted methods for the determination of As and Hg are those techniques containing hydride generation and cold vapor methods, respectively.

2.4. Conclusions

It is important to monitor the elements in biological samples to assess the impact of human activities on the marine environment and to investigate the adverse effects of these elements on marine organisms and humans. There are numerous techniques for the determination of trace elements in biological samples but the inductively coupled plasma (ICP) coupled with mass spectrometry (MS) or optical emission spectrometry (OES) are widely used ones.

As a participant of an interlaboratory comparison exercise administered by NIST, we analyzed some of the trace elements (As, Cd, Cu, Fe, Hg, Mn and Zn) in Beluga and Pygmy Sperm whale liver homogenates, using ICP-MS and ICP-OES techniques. For many elements such as Cd, Cu, and Mn the results were considered as acceptable within experimental errors by both techniques. The other elements analyzed (Zn, As, Hg, and Fe) gave less precise and accurate results.

Although the accuracy and precision obtained by both instrumental methods can be considered as acceptable, these analyses can be improved. Further investigations in Chapter 3 will be concentrating on the improvement of the ICP-OES analysis of trace elements in complex biological matrices such as liver samples. Proper wavelength selection, consideration of both atom and ion line, exploring the acid and salt effect and its influence on our analysis, as well as choosing the right internal standard and robust plasma conditions will be the main points of focus.

CHAPTER 3

CORRECTING FOR MATRIX EFFECTS IN ICP-OES USING INTERNAL STANDARDS AS SELECTED BY PRINCIPAL COMPONENT ANALYSIS

3.1. Introduction

3.1.1. Matrix Effects

In inductively coupled plasma optical emission spectrometry (ICP-OES) maintaining accuracy and precision is generally limited by the non-spectral interferences (so-called matrix effects) that are caused by the major elements in the samples (e.g. easily ionizable elements (EIEs) such as Na, K, Li) or reagents used for sample digestion and solution storage (e.g. mineral acids such as HNO_3, H_2SO_4, HCl).

Since the first studies on ICP-OES, matrix effects have been widely investigated by several researchers to find possible explanations about their origins and their influences on analyte signal. There are two recent reviews by Todoli and his coworkers that focus on elemental matrix effects (Todoli et al. 2002) and on acid interferences (Todoli and Mermet 1999).

In the literature it was reported that matrix effects cause either suppression or enhancement of the analyte signal (Brenner et al. 1997, Dubuisson et al. 1998c, Grotti et al. 2000, Stepan et al. 2001, Iglesias et al. 2004). Furthermore there is a general agreement that matrix effects are generally caused by two major factors (Iglesias et al. 2004, Kola and Perämäki 2004);

i. changes in the energy transfer between the plasma and sample (during the processes of atomization, excitation and ionization) and

ii. changes in the efficiency of sample aerosol formation, transport and filtration.

In addition, in the study by Iglesias et al. (2004), it was proposed that the magnitude of matrix effects depends also on the optical transition of the elements (being a resonant or non-resonant line).

On the other hand, in the case of elemental matrix effects, there is no satisfactory study explaining the causes and mechanism of these interferences due to the complexity of the processes related to these effects. As explained by Lehn et al. (2003) this could be because of the differences in the behaviors of the elements and although a hypothesis can be used to explain the effects for the most of the elements, there is usually at least one element that does not follow the observed trend. In addition it is also difficult to compare the results obtained by the studies performed under different conditions and with different instruments (Todoli et al. 2002).

The studies which attempt to find possible mechanisms in order to understand the causes of EIE effects and to investigate the characterization of these effects, mainly focused on the plasma properties, such as electron temperature (T_e), electron number density (n_e), gas-kinetic temperature (T_g), analyte atom and ion number densities which affect the electrical and thermal conductivity, viscosity and processes occurring in the plasma, such as atomization, excitation and ionization equilibria, volatilization, collision processes, ambipolar diffusion, lateral diffusion, Penning ionization by metasTable argon, and charge transfers involving argon species (Mermet 1991, Galley et al. 1993, Galley and Hieftje 1994, Wu and Hieftje 1994, Sesi and Hieftje 1996, Romero et al. 1997a, Romero et al. 1997b, Hobbs and Olesik 1997, Grotti et al. 2000, Todoli et al. 2002, Lehn et al. 2003 and references therein). In addition, there has been other research related to aerosol drop size distribution, analyte and solvent transport rates (Romero et al. 1997b; O'Hanlon et al. 1997; Dubuisson et al. 1998a; Dubuisson et al. 1998c; Mermet 1998, Todoli et al. 2002).

The acid effects (i.e. changes that occur in the behavior of the system induced by the acid) are generally classified in two groups. The first group includes the changes related to operating conditions resulting from changes in the physical properties of the solution occurring in the sample introduction system (i.e. the reduction in the nebulizer aspiration rate when free aspiration is used, primary and tertiary aerosol drop size distributions, the modification of mass of the solution transported to the plasma, and the element concentration as a function of the drop size, change in the aerosol

characteristics due to a variation of the surface tension and volatility, decreased solution uptake as a result of increased viscosity). The second group includes the effects caused by the processes that occur in the plasma (such as changes in atomization and excitation conditions) (Todoli and Mermet 1999, Todoli and Mermet 2000, Brenner and Zander 2000, Grotti and Frache 2003b, Lehn et al. 2003 and references therein).

It was reported that the acid effect observed depends on the type and concentration of the acid present in the sample (Botto 1985; Stewart and Olesik 1998a). In general, at low acid concentrations (< 1% v/v) an increase in the analyte intensity and at high acid concentrations a decrease in the net line intensity with respect to water is observed (Dubuison 1998a, Todoli and Mermet 1999).

3.1.2. Variables Affecting the Matrix Effects

The liquid sample introduction system has a major effect on the matrix interferences. This can be easily understood by taking into account that the introduction system influences the total mass of the analyte and solvent transported towards the plasma and the aerosols characteristics. The solvent injected into the plasma modifies its thermal characteristics, whereas the aerosol drop size changes the plasma location at which the drop vaporization is complete (Todoli et al. 2002).

The other most important variables which have an influence on the matrix effects are the plasma observation height, the nebulizer gas flow rate (also injector i.d.), and the rf power (Todoli et al. 2002).

In the Initial Radiation Zone (IRZ), elemental matrix effects are known to be strongest while in the Normal Heating Zone (NAZ) few effects exist. It was reported that studying matrix effects (acid and elemental effects) at a given observation height may result in signal variations that do not correspond to the actual situation (Todoli and Mermet 1999, Todoli et al. 2002).

It has been reported that by applying a high power (>1.2kW), a low carrier gas rate (< 0.8 ml/min) and high injector i.d. (>2 mm), robust plasma conditions (i.e. operating conditions that could allow changes in the nature or concentration of the matrix components without a significant change in the analyte signals) are achieved (Mermet 1991). It is thought that under robust plasma conditions any observed effect is mainly due to the aerosol generation and transport system, i.e. to the sample

introduction system and matrix effects can be reduced by using operating conditions that lead to an efficient energy transfer between the plasma and the sample (Fernandez et al. 1994, Carre et al. 1995, Dubuisson et al. 1998a, Mermet 1998, Stewart and Olesik 1998a, Stewart and Olesik 1998b, van Veen, and Loos-Vollebregt, 1999).

A decrease in the gas flow rate leads to a decrease in the solvent and matrix plasma load and also an increase in the aerosol residence time, thus increasing the efficiency of the energy transfer to the analyte. Increasing the residence time is also achieved by employing injector diameters higher than 2 mm. An increase in the rf power leads to increases in the total amount of energy available to excite the analyte. Moreover, the role of the electrons in the analyte excitation should also be considered. For a plasma operated at low rf power and high nebulizer gas flow rate, the electron density is low. Under these conditions, the additional electrons supplied by the interferent could modify the extent of analyte excitation. According to Todoli these extra electrons hardly affected the global electron number density under robust conditions (Todoli et al. 2002).

In addition, under robust plasma conditions, electron number density (n_e) and excitation temperature (T_{exc}) both for water and acids are identical. Under non-robust plasma conditions, reductions in T_{exc} and/or n_e and dependence of the signal reduction on the excitation energy (E_{exc}) or energy sum (E_{sum}) of the ionic line appeared (Todoli and Mermet 1999).

Generally the Mg II 280.270 nm to Mg I 285.213 nm line intensity ratio is used as a measure of the plasma robustness. Mermet (1991) suggested that for radial viewing this ratio should be larger than 8 to have robust conditions. In the case of axial viewing, Dubuisson et al. (1998b) reported that robust conditions can be represented by a Mg II / Mg I ratio of less than 8. This difference is explained by the fact that in the radial mode, the observation height is adjusted to obtain optimum of the ionic line emission. In contrast, when the axial viewing mode is used, both atomic and ionic line emission zones are probed by the collimating system (Dennaud et al. 2001).

The observation mode also has an effect on how matrix effects may be controlled. Several studies have been published which compare the axial (end-on) observation mode with the radial (end-on) mode in terms of matrix effects (Ivaldi and Tyson 1995, Dubuisson et al. 1997, Brenner et al. 1997, Dubuisson et al. 1998a, Masson 1999, Masson et al. 2000, Dennaud et al. 2001a, Garavaglia et al. 2002, Sun et al. 2003). It was observed by these researchers that the axial viewing mode is more

sensitive to matrix effects than radial viewing. This is best understood if one considers that the axial mode (as opposed to the radial) allows viewing of a larger portion of the plasma and therefore larger regions of temperature and plasma energy gradients. The atomization, excitation and ionization events associated with the matrix depend greatly on these gradients.

Although robust operating conditions and proper choice of observation height are said to decrease the effects caused by matrices that contain the acid and salt, these interferences can not be totally eliminated (Brenner et al. 1999, van Veen and de Loos-Vollebregt 1999, Dennaud et al. 2001 and references therein). Different strategies have been suggested to compensate for matrix effects.

3.1.3. Methods for Overcoming Matrix Effects

When ICP-OES was still in its infancy as an analytical method, Botto (1985) mentioned that methods for correcting the matrix effects should fulfill the following conditions:

i. single set of reference solutions for any aqueous sample matrix should be used
ii. it must be applicable to both single and multielement analysis
iii. it should be simple and applicable to a mixture of matrices and to different compounds
iv. it should not require periodic calibration

Unfortunately, there is no single method that meets all of these requirements because of the complexity of the effects caused by acid and salt matrices.

Matrix matching is a frequently applied procedure to overcome matrix effects (Todoli and Mermet 1999, Todoli et al. 2002, Iglesias et al. 2004). But, this method is not always feasible because it is neither possible to know the exact composition of sample matrices nor to control the various processes of sample preparation as is the case for environmental and biological samples. It is also possible to use the method of standard additions, but this technique is generally time consuming and increases the cost of the analysis; therefore, it is not recommended for routine analysis. Another method to reduce matrix effects which are caused by EIEs is the usage of an ionization buffer. This is typically an element that is added to solutions and standards at high

concentrations and its influence predominates over the influence of other elements such as Na or Li. Generally, Cesium (Cs) is chosen as a buffer because of its low ionization energy (3.894 eV) and poor sensitivity of detection by ICP-OES (Dennaud et al. 2001a).

In some case modification of the sample introduction system especially to reduce the effects caused by the acids have been attempted (Todoli and Mermet 2002). These modifications include elimination of the spray chamber (Direct Injection Nebulizer – DIN), use of desolvation systems and chemical modifiers (Mermet 2002 and references therein).

Besides this traditional techniques, because of the complexity of matrix effects and because more than one variable must be considered, the use of chemometric approaches to study and reduce these interferences has gained great interest and various multivariate calibration techniques such as multiple linear regression (MLR), principle components regression (PCR) and partial least squares (PLS) have been proposed for this purpose (Villaneuva et al. 2000, Griffiths et al. 2000, Grotti et al. 2000, Moreda-Piñeiro et al. 2001 and references therein).

Lopez-Molinero et al. (1994) tried to find the correlation of the spectral data of emission lines in ICP-OES using Principle Component Analysis (PCA). They concluded that through theoretical studies of multielemental data (using the energy level of the upper and lower state for each transition line, the statistical weights of the upper and lower states and the transition probability), it is possible to define groupings of spectral lines that possess similar experimental characteristics and these groupings make it easier to classify the behavior of the spectral lines.

Brenner et al. (1995) also applied a principal component analysis procedure to classify rare earth elements according to their empirical behavior in the presence of nitric acid considering several theoretical parameters (e.g. ionization energy, excitation energy, oxide bond strength). These researchers concluded that small differences between the strength of the oxide bonds and excitation energy could strongly modify the response of the lines in the presence of nitric acid.

Villaneuva et al. (2000) applied the MLR technique to correct for matrix effects induced by Ca and Mg and they concluded that by using MLR it was possible to correct for the total matrix effect (i.e. combination of effects from the interfering species and spectral interferences both affecting the analytical signal).

Griffiths et al. (2000) compared the application of traditional correction techniques (such as univariate calibration, inter-element correction, matrix matching)

and multivariate techniques like PCR, PLS1, PLS2 and MLR to the complex matrices. They concluded that by using matrix matching and PLS1 they could obtain good results but they also reported that in the case of incorrect matching of standards and samples, matrix matching failed and with elements present at low concentrations the PLS1 method was not efficient.

One requirement of multivariate methods is that the factor space defined by the multi-element standards used for model calibration must include all possible constituents (analytes and interferents) and concentrations of the real sample matrices. Therefore, it is necessary to obtain data for the multivariate calibration model using an appropriate experimental design (Griffiths et al. 2000).

3.1.4. Internal Standardization

Internal standardization is a well-established calibration method to improve long term stability by correcting for instrumental drift, the accuracy and precision of the analyses, and to compensate for matrix effects. By calculating the ratio of the analyte and selected internal standard emission intensities, the signal changes caused by matrix effects as well as errors due to the flicker noise and drift are expected to be reduced. In order to achieve efficient correction the selected internal standard line should behave exactly the same way as the analyte line for interference effects and instrumental noise (Grotti and Frache 2003b, Kola and Peramaki, 2004).

Several researchers (Romero et al. 1997a; Dubuisson et al. 1998c; Chausseau et al. 2000b; Stepan et al. 2001; Grotti and Frache 2003b) reported that there are four issues to address in order to obtain an efficient internal standardization for ICP-OES analyses;

i. operation under optimal conditions to minimize the plasma-related matrix effects
ii. true simultaneous measurement of the analytical and reference signals
iii. consideration of additive effects rather than multiplicative ones
iv. optimal selection of the reference lines

3.1.4.1. Operation under Optimal Conditions

It is well known that both the operating conditions and the viewing mode (radial/axial) greatly affect the correction efficiency of internal standardization. Under robust plasma conditions since matrix effects are mainly assigned to the aerosol transport and filtering processes, then it is thought that the behavior of each element is similar, which simplifies the use of internal standardization to achieve high accuracy (Romero et al. 1997a, Dubuisson et al. 1998c, Kola and Perämäki 2004).

The studies by Mermet and his coworkers (Romero et al. 1997a, Dubuisson et al. 1998c) showed that the changes in the aerosol production and transport under robust conditions permit the efficient use of a single internal standard but when there is a change in the energy transfer several internal standards are required because of the different sensitivities of individual lines for matrix effects. On the other hand, non-robust conditions were not recommended for internal standardization because of possible uncorrelated behavior among the line intensities of various elements under these conditions.

In another study, the so-called Myers-Tracy Signal Compensation Method (MTSCM) was used. These researchers measured the emission intensity for the internal standard (i.e. Mn) and several analytical lines of different ionization and excitation energies simultaneously. They concluded also that the internal standardization was efficient when robust operating conditions were used (Todoli and Mermet 1999, Todoli et al. 2002).

Lastly, it has been also concluded by several investigators that the efficiency of internal standardization was decreased when the axial viewing mode was used compared to the radial mode (Romero et al. 1997a, Dubuisson et al. 1998c, Brenner and Zander 2000, Todoli et al. 2002).

3.1.4.2. True Simultaneous Measurement of the Analytical and Reference Signals

It has been reported that any element can be used as an internal standard to compensate for matrix effects, provided that true simultaneous measurements of the

analytes and the internal standard intensities are performed and this is called real-time internal standardization (Sedcole et al. 1986, Mermet and Ivaldi 1993, Ivaldi and Tyson 1996, Romero et al. 1997a and references therein). Until the 1990s, studies with ICP-OES had been performed using instruments equipped with photomultiplier tubes (PMT) and either simultaneous polychromators (which are line number limited) or sequential monochromators (which are time limited). After the introduction of the detectors such as charge injection device (CID) and charge coupled device (CCD) which are based on multichannel detection, then more efficient and true time correlation between the signals could be obtained (Stepan et al. 2001).

3.1.4.3. Considering Additive Effects

Stepan et al. have reported on the use of a correction scheme to correct for so called 'multiplicative' and 'additive' effects (Stepan et al. 2001). Accordingly corrections based on normal internal standardization calibration make a correction based on a multiplicative correction factor from a calibration curve. In contrast, Stepan demonstrated the simple use of the relationship between signal response as a function of energy sum (i.e. the response for each separate element). If such a plot is made for two solutions of different sodium concentration, a 'quasi-constant shift' is observed (Stepan et al. 2001). Stepan then chose to use the proportionality factor for an arbitrary internal standard (nickel in this case) for choosing a proportionality correction based on 'additive' effects (Stepan et al. 2001). He reported that corrections based on these 'additive' effects produced better corrections for bias due to sodium matrix interference for cases where the standards and samples are matrix mismatched (Stepan et al. 2001).

3.1.4.4. Optimal Selection of the Internal Standards

It has been reported by several authors (Ivaldi and Tyson 1995, Brenner et al. 1997, Dubuisson et al. 1998c) that the high-energy ion lines are more susceptible to interference than the low-energy ion and atomic lines. Suppression of high-energy potential lines has been attributed to energy withdrawal from the plasma-energy required to atomize the high concentrations of Ca and Na. This process is accompanied

by a decrease in excitation temperatures. However, the situation with Na is less pronounced and other processes have been invoked to explain variations of line intensity with increasing Na concentrations e.g. changes in the quality of the tertiary droplet sizes (Brenner and Zander 2000).

It was also shown that the use of internal standardization was efficient for ionic lines since the behavior of atomic lines is more complex and ionic lines show a similar depressive effect to matrix interferences. For example Chausseau et al. (2000) explained that ionic and atomic lines have different excitation pathways and therefore, the sensitivity to operating conditions will modify the behaviors according to the nature of the lines.

It was observed by Chan et al. (2000) that alkali elements produce matrix effects less severe than alkaline earth elements and they proposed that for a given periodic group of elements, the lower the second ionization potential of the interferent, the stronger the matrix effects. Therefore the changes in plasma characteristics are said to be attributed to the interactions between the doubly charged matrix ions and argon species. Thus, since the former has a higher energy the energy of the doubly charged species would be transferred to argon. As a result the argon–analyte equilibrium is distributed giving rise to a redistribution of the argon and analyte energies (Todoli et al. 2002 and references therein).

It was also reported by Brenner et al. (1998) that the magnitude of the correction by internal standardization depends on the similarity of the energies of the analyte and internal standard emission lines. The choice of the element to be used as an internal standard is of crucial importance.

In general, internal standardization is performed with either an added or a contained element. Several elements like scandium (Sc 424.7 nm, Sc II 361.384 nm), yttrium (Y 371.030 nm), cobalt (Co 238.892 nm), cadmium (Cd II 226.502 nm) and nickel (Ni II 231.604 nm) have been used as internal standards (Mermet and Ivaldi 1993, Ivaldi and Tyson 1996, Brenner et al. 1997, Dubuisson et al. 1998c, Grotti and Frache 2003b and references therein). Mermet and Ivaldi concluded that a single spectral line fully compensates for intensity variations when the energy potentials of the analyte lines are similar to that of the internal standard (Mermet and Ivaldi 1993). Other researchers used the major constituents of the samples as internal standards such as the H-ß 486.133 nm emission line (Botto 1985) and the Argon 794.8 nm line (Hoenig et al. 1998). Botto (1985) normalized H-ß emission intensities with respect to a reference

solution and illustrated the effect of matrix by plotting the normalized H-ß signals versus the C_i/H-ß ratio, C_i being the apparent concentration of a given element; it was concluded that based on these curves, matrix effects could be efficiently corrected. Hoenig et al. (1998) reported that accuracy and precision were improved using argon as an internal standard.

As indicated by several studies, individual lines may show different sensitivity for matrix effects and the use of a single internal standard is not usually enough to correct for matrix effects; therefore, the use of several internal standards was also recommended (Romero et al. 1997a, Todoli and Mermet 1999).

Several procedures have been suggested based on the use of several internal standards, such as the generalized internal reference method (GIRM), the parameter-related internal standard method (PRISM), interactive matrix matching (IMM), common analyte internal standardization (CASI), and the generalized regression neural network (GRNN) (Al-Ammar and Barnes 1998, Villaneuva et al. 2000, Grotti et al. 2003a and references therein).

In the PRISM method, Ramsey and Thomson applied a PCA method and observed that by taking only two emission lines with two single plasma parameters, the responses of 24 elements under 10 sets of operating conditions could be predicted (Todoli and Mermet 1999, Todoli et al. 2002).

For the CASI method which was developed by Al-Ammar and Barnes, two lines of the analyte were used to compensate for non-spectroscopic interferences. One of the lines was used as an internal standard. The method requires that the relative intensity changes shown by both lines be as different as possible, since in this way the lines' ratio is a function of the sample composition. Although this method is simple and does not require complicated mathematical corrections, finding two appropriate analytical spectral lines is sometimes problematic (Al-Ammar and Barnes 1998).

A systematic procedure which includes the classification of the emission lines by PCA was proposed by Grotti and coworkers to choose the suitable internal standard and they applied this procedure to compensate for the matrix effects due to large amounts of iron, aluminum, calcium, sodium and potassium (Grotti et al. 2003) and acid effects (Grotti and Frache 2003) separately. They obtained a score plot showing the groups of the emission lines of analytes and potential internal standards indicating their empirical behavior with respect to the considered matrix. They concluded that the closer the analyte and the reference lines are in the score plot, the higher is their similarity to

the matrix effect and the interference on a given analytical line can be eliminated by using a reference line which shows similarity to the element of interest according to the score plot. They claimed that although their procedure is a general and simple method, it should be verified for its efficiency for different instrumental systems or for other types of matrix effects.

In a recent study by Kola and Perämäki (2004), a model was developed for the behavior of the emission lines when the operating conditions are changing (robust, semirobust, and nonrobust conditions) by using multiple linear regression (MLR) in a radially viewed sequential instrument. They suggested that this MLR-generated model can be used to select internal standards to correct for matrix effects and drift and also can be used to evaluate the efficiency of internal standardization quantitatively. However, they also concluded that by using a simultaneous detection ICP-OES system which would give a larger group of emission lines, more accurate results for obtained models could be realized.

3.1.5. Principal Component Analysis (PCA)

Principal Component Analysis (PCA) is a multivariate statistical technique which can be applied to a set of variables to reduce their dimensionality. The main idea of PCA is to determine the underlying information from multivariate raw data. In other words, it can be used to replace a large set of inter-correlated variables with a smaller set of independent (i.e. uncorrelated) variables. These new variables (or principal components) are linear combinations of the original variables describing each specimen (Cave 1998 and references therein, Miller and Miller 2000) so it helps to examine the matrix effects caused by sodium and acid at the same time.

Approximation of the original matrix $\boldsymbol{X}$ by a product of two small matrices (the score and loading matrices) is performed according to the following illustration (Otto 1998);

$$\boldsymbol{X} = \boldsymbol{T}\boldsymbol{L}^{\boldsymbol{T}} \tag{3.1}$$

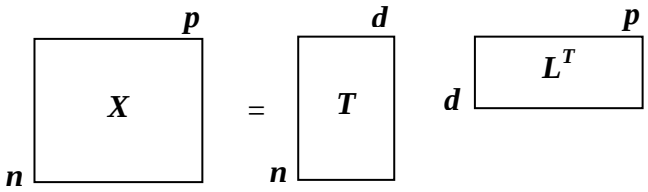

Here $\boldsymbol{X}$ represents the original data matrix which consists of $\boldsymbol{n}$ rows (objects) and $\boldsymbol{p}$ columns (features); $\boldsymbol{T}$ is the scores matrix with $\boldsymbol{n}$ rows and $\boldsymbol{d}$ columns (number of principal components); $\boldsymbol{L}$ is the loading matrix with $\boldsymbol{d}$ columns and $\boldsymbol{p}$ rows; and superscript "T" represents the transpose of a matrix. The columns in $\boldsymbol{T}$ are the score vectors and the rows in $\boldsymbol{L}$ are called loading vectors. The principal components can be considered as projections of the original data matrix X, on the scores, T.

If we rearrange the equation 3.1, then the equation becomes

$$\boldsymbol{T} = \boldsymbol{XL} \tag{3.2}$$

The new coordinates are linear combinations of the original variables;

$$\begin{aligned} \boldsymbol{t}_1 &= \boldsymbol{x}_{11}\boldsymbol{l}_1 + \boldsymbol{x}_{12}\boldsymbol{l}_2 + \boldsymbol{x}_{13}\boldsymbol{l}_3 + ... + \boldsymbol{x}_{1n}\boldsymbol{l}_n \\ \boldsymbol{t}_2 &= \boldsymbol{x}_{21}\boldsymbol{l}_1 + \boldsymbol{x}_{22}\boldsymbol{l}_2 + \boldsymbol{x}_{23}\boldsymbol{l}_3 + ... + \boldsymbol{x}_{2n}\boldsymbol{l}_n \end{aligned} \tag{3.3}$$

where $t_1, t_2, \ldots, t_n$ describes the principal components. The coefficients x_{11}, x_{12}, etc. are chosen so that the new variables, unlike the original variables, are not correlated with each other.

The principal components are determined according to the maximum variance criterion. Each subsequent principal component describes a maximum of variance that is not modeled by the former components. Therefore, the first principal component accounts for most of the variation in the data set, and the second principal component accounts for the next largest variation. Hence in the second component there is more information than in the third, etc. Finally as many principal components are computed as are needed to explain a preset percentage of the variance.

Visualization of the data can be obtained by plotting the principal components against each other. Since the first principal component and second principal component

account for most of the variation in the data set and contain more information, generally plotting the first two principal components is sufficient (Miller and Miller 2000).

3.1.6. The Aim of the Study

When exploring the matrix interferences researchers in the area of ICP-OES analyses often consider either one concomitant element or acid as separate variables of research study. Owing to the complexity of the processes involved in the presence of both acid and salt matrices, a small number of studies (Dennaud et al. 2001, Todoloi et al. 2002 and references therein) have been reported that explore and compensate for their combined effects on ICP-OES analyses. To the best of our knowledge a study that investigates the use of internal standardization to correct for these combined effects does not exist.

Although a more appropriate way of applying internal standardization is by using simultaneous detection, many analysts worldwide have been using sequential instruments in their research or routine analyses laboratories. When solid state detectors are used, the resolution is degraded as compared to PMT-based systems (Mermet 2002). Additionally, in order to eliminate the contribution of shot and detector noise to obtain an efficient internal standardization, the cooling of the multichannel detector to minimize the readout noise is required (Chausseau et al. 2000). It is reasonable to assume that many researchers worldwide will not wish to invest in a CCD instrument immediately and sequential instruments may indeed become more economical. After the work and publications of other authors were reviewed, it was decided to optimize the use of a sequential ICP for assessment of internal standardization for analysis of sample matrices containing various concentrations of both acid and salt. Also our goal was to select the appropriate internal standard by using PCA. Then these selected internal standards would be used for the determination of a number of elements present in certified whale liver homogenates supplied from NIST.

3.2. Experimental

3.2.1. Instrumentation and Operating Conditions

The Inductively Coupled Plasma Optical Emission Spectrometer (ICP-OES) (Varian Inc., Australia) includes axial viewing mode, an air path monochromator, cyclonic action spray chamber, and a concentric glass nebulizer. Instrument properties and selected operation conditions are listed in Table 3.1.

Table 3.1. Instrumentation and Operating conditions

Varian Liberty Series II		
Spectrometer	Optical configuration	0.75 meter Czerny-Turner
	Grating	90 x 100 mm holographic
	Grating density	1800 grooves/mm
	Plasma viewing mode	Axial
	Injector id	2.5 mm
	Detector	Photomultiplier
Sample introduction	Nebulizer	Concentric glass
	Spray chamber	Cyclonic (Sturman-Masters)
	Torch	One-piece quartz type
	Plasma gas flow rate	15.0 L/min
	Auxiliary gas flow rate	1.5 L/min
RF Generator	Operating frequency	40.68 MHz
	Type	Crystal controlled with solid state driver and water cooled power tube
	RF power	1.2 kW
	Interface	Nickel cooled cone interface

The Mg II 280.270 nm / Mg I 285.213 nm ratio was used for monitoring the plasma robustness and excitation conditions. Mermet (1991) suggested that for radial viewing this ratio should be larger than 8 to have robust conditions. Dubuisson et al. (1998b) reported that for axial viewing, as opposed to radial viewing, a Mg II / Mg I ratio less than 8 represents robust conditions. The values measured were 8.99 ± 0.58 throughout our studies here so it can be concluded that the samples were analyzed under robust plasma conditions and the analyses were not affected by the instrument and plasma conditions.

3.2.2. Reagents and Standard Solutions

Nitric acid (65%) and hydrogen peroxide (30%) were purchased from Riedel-de Haen (Germany) and were used for sample digestion and for the adjustment of acid content in the standards and samples. Sodium chloride (extra pure) used for the salt content of samples and standards was also purchased from Riedel-de Haen (Germany). Doubly de-ionized water (18.2 MΩcm) obtained from a Milli-Q waters system (Millipore, Bedford, USA) was used throughout the studies.

Standard solutions and synthetic samples were prepared using an ICP Multielement standard solution IV that contains the following elements at a concentration of 1000 mg/L:Ag, Al, B, Ba, Bi, Ca, Cd, Co, Cr, Cu, Fe, Ga, In, K, Li, Mg, Mn, Na, Ni, Pb, Sr, Tl, Zn and ICP Multielement standard solution XVI that contains Sb, As, Be, Ca, Cd, Co, Cr, Cu, Fe, Pb, Li, Mg, Mn, Mo, Ni, Se, Sr, Tl, Ti, V, Zn all at a concentration of 100 mg/L. Single element stock standards of Cd, Mn, Zn, Co, and Ni (at a concentration of 1000 mg/L) and Rh internal standard solution (at a concentration of 10 mg/L) were also used for the validation studies. All standard solutions were purchased from Merck (Darmstadt, Germany).

3.2.3. Sample Preparation

3.2.3.1. Microwave Digestion of the Sample Materials for Preliminary Studies

The marine mammal samples which were supplied by NIST from a previous interlaboratory comparison study were also used for these experiments. These samples were Beluga Whale (*Delphinapterus leucas*) liver homogenate as a control whale liver sample (CWLS) and Pygmy Sperm Whale (*Kogia breviceps*) liver homogenate as a laboratory exercise test whale liver sample (LETWLS).

For microwave digestion, 0.4 g of each homogenized sample was precisely weighed (± 0.1 mg) in Teflon containers with 8 ml of 65% HNO_3 and 1 ml of 30% H_2O_2. Microwave digestion was accomplished with a MILESTONE Microwave Laboratory

Systems ETHOS PLUS labstation with a HPR-1000/10S high pressure segmented rotor. To one of these vessels 1 ml of ICP multielement standard solution was added as a spike. For the unspiked samples, 1 ml of H_2O was added before digestion. The microwave oven was operated at 150 ^oC for 10 min, at 200 ^oC for 10 min, then at 200 ^oC again for 20 min at a power of 500W. At the end of the temperature program the turntable was rotated continuously for 20 min during ventilation. After allowing the digest to cool to room temperature, each sample was transferred to acid-washed polyethylene vials for trial studies and to volumetric flasks for the final studies. Each was brought to a final volume of 30 ml with ultra pure water. Also, blanks were digested at the same time with the liver homogenates by adding 8 ml of 65% HNO_3, 1 ml of 30% H_2O_2 and 1 ml of H_2O to the vessels.

3.2.3.2. Initial Acid Effect Studies

After taking appropriate amounts from the stock solutions, 8 ml of HNO_3 and 1 ml of H_2O_2 were added to sample solutions and diluted to a final volume of 25 ml. For the standard solutions with the volume of 50 ml, 12 ml of HNO_3 and 2 ml of H_2O_2 were used in order to match the acid matrices to the samples.

Before the measurements, the proper amount of Rh internal standard solution was added to give a final concentration of 0.1 mg/L for both standards and samples.

In order to investigate the nitric acid effect on the ICP-OES analysis, a number of standard solutions with a volume of 50 ml containing Cd, Mn, and Zn were also prepared from multielement standard solution IV. A series of acid matrix standards were prepared with the following final concentrations of nitric acid: 25%, 10%, and 5%. To each of the 50 ml solutions, 2 ml of 30% H_2O_2 was added.

3.2.3.3. Combined Acid and Salt Effect Studies

A set of synthetic sample solutions containing varying multielement (0.05 mg/L, 0.5 mg/L, 1 mg/L), acid (0%, 12%, 25%) and sodium (0%, 0.1%, 0.3%) concentrations were prepared according to a 3^3 full factorial design. For the preparation of 12% HNO_3, 9 ml of 65% HNO_3 stock solution and for the 25% HNO_3, 19 ml of 65 % HNO_3 stock

solution were added to the synthetic samples. For the salt content, 0.05g and 0.15g of NaCl were added and diluted to 50 ml to obtain 0.1% and 0.3% salt concentrations, respectively. For the multielement studies of these synthetic samples, the ICP multielement solution XVI was used. Standard solutions were prepared using only this multielement standard solution XVI without any addition of acid and salt. The factorial design plan containing coded values and real values is shown in Table 3.2.

Table 3.2 Experimental design plan

Real values				Coded values		
Sample no	**Acid % (v/v)**	**NaCl % (w/v)**	**ME (mg/L)**	**Acid**	**NaCl**	**ME**
1	0	0	0.05	-1	-1	-1
2	0	0	0.5	-1	-1	0
3	0	0	1.0	-1	-1	1
4	0	0.1	0.05	-1	0	-1
5	0	0.1	0.5	-1	0	0
6	0	0.1	1.0	-1	0	1
7	0	0.3	0.05	-1	1	-1
8	0	0.3	0.5	-1	1	0
9	0	0.3	1.0	-1	1	1
10	12	0	0.05	0	-1	-1
11	12	0	0.5	0	-1	0
12	12	0	1.0	0	-1	1
13	12	0.1	0.05	0	0	-1
14	12	0.1	0.5	0	0	0
15	12	0.1	1.0	0	0	1
16	12	0.3	0.05	0	1	-1
17	12	0.3	0.5	0	1	0
18	12	0.3	1.0	0	1	1
19	25	0	0.05	1	-1	-1
20	25	0	0.5	1	-1	0
21	25	0	1.0	1	-1	1
22	25	0.1	0.05	1	0	-1
23	25	0.1	0.5	1	0	0
24	25	0.1	1.0	1	0	1
25	25	0.3	0.05	1	1	-1
26	25	0.3	0.5	1	1	0
27	25	0.3	1.0	1	1	1

In this factorial design the number 3 corresponds to levels (lowest, middle and highest concentrations which are represented as -1, 0, and +1 respectively) and the superscript 3 corresponds to the factors that were chosen (acid, salt and multielement concentrations).

Wavelengths were chosen as a compromise between signal intensity and spectral interferences. Atom lines used for this study were Ca 422.673 nm, Co 345.350 nm, Li

610.362 nm, Li 670.784 nm, Ni 341.476 nm, Rh 343.489 nm, Mn 279.482 nm, Cu 324.754 nm, Fe 275.574 nm, Cd 228.802 nm, Zn 213.856 nm and ion lines used were Ca 317.933 nm, Co 237.862 nm, Ni 231.604 nm, Rh 251.752 nm, Mn 257.610 nm, Cu 224.700 nm, Fe 259.940 nm, Cd 214.438 nm. In addition to these elements, Argon emission lines at 706.722 nm, 750.387 nm, 751.465 nm, and 772.421 nm were measured to check the stability of the plasma during analysis.

Analytical errors (E) were calculated using the following formulae as suggested by Grotti et al. (2003a);

$$E = \frac{(C_1 - C_n)}{C_1} \times 100 \tag{3.4}$$

$$E = \frac{(C_2 - C_n)}{C_2} \times 100 \tag{3.5}$$

$$E = \frac{(C_3 - C_n)}{C_3} \times 100 \tag{3.6}$$

where C_1, C_2, C_3 correspond to the concentrations of solutions that do not contain any acid and salt and C_n corresponds the considered analyte concentration.

As can be seen from Table 3.2, the first three samples contain only elements which were analyzed in three different concentrations without the presence of acid or salt. They can be considered as reference solutions for the corresponding multielement concentrations that have varying amounts of acid and salt. Samples 1-3 were used as blank correction for all other samples according to the appropriate concentration levels. Equation 3.4 was used for the calculation of errors for the solutions containing a 0.05 mg/L multielement spike, equation 3.5 was used for the calculation of errors for the solutions containing a 0.5 mg/L multielement spike and equation 3.6 was used for the solutions containing a 1.0 mg/L multielement spike but having different amounts of acid and salt. Use of these equations for the experimental data will be made more clear in the discussion part.

These analytical errors were then used as the data matrix for the principal component analysis were processed using MATLAB® 6.5 (The MathWorks, Inc.). Using the results from the principal component analysis, score plots and loading plots showing the behaviors of the emission lines of the elements and relationships between the matrices were plotted using Microsoft Excel.

3.2.3.4. Validation of Acid and Salt Effect Studies

The use of selected reference (Co, Ni, Rh) and analyte (Cd, Mn, Zn) lines were tested with a validation study. Another set of synthetic sample solutions containing various multielement (0.05 mg/L, 0.5 mg/L, 1 mg/L), acid (0%, 12%, 25%) and sodium (0%, 0.1%, 0.3%) concentrations were prepared according to the previous factorial design. It should be noted that for this study instead of multielement stock solutions, single element standards of Cd, Mn, Zn, Co, Ni and Rh were used and appropriate amounts of these stocks were mixed in order to have a multielement solution of only these elements. For the preparation of 12% HNO_3, 4.62 ml of 5% HNO_3 stock solution and for the 25% HNO_3, 9.42 ml of 65 % HNO_3 stock solution were added to the synthetic samples. For the salt content, 0.025 g and 0.15 g of NaCl were added and diluted to 25 ml to obtain 0.1% and 0.3% salt concentrations, respectively. Standard solutions were prepared using only the element standards without any addition of acid and salt. In this way the effect of add acid and salt will be readily apparent.

The wavelengths used for two separate trials for the analysis were listed in Table 3.3. It should be noted that these wavelengths were chosen with a compromise between signal intensity and spectral interferences.

Table 3.3. The wavelengths used in the validation studies

Element	Wavelengths (nm)			
	For the first trial		For the second trial	
	Atom lines	Ion lines	Atom lines	Ion lines
Cd	326.106	214.438	326.106	214.438
	228.802	226.502	228.802	226.502
Mn	279.827	257.610	279.827	257.610
	403.076	259.373	403.076	259.373
Zn	213.856	206.200	213.856	206.200
	334.502	202.551	334.502	202.551
Co	345.350	228.616	345.350	228.616
	340.512	258.033	340.512	237.862
Ni	352.454	231.604	352.454	231.604
	351.505	221.647	341.476	221.647
Rh	343.489	249.077	343.489	249.077
	369.236		369.236	
Ar	751.465	-	751.465	-
	706.722		750.387	
H	656.272	-	656.272	-
	H_β486.133			

It should be noted that the concentrations which were calculated by using argon and hydrogen as the internal standards were not included in the results and discussion section. Only the concentrations obtained for Cd I 228 and Cd II 214 lines were included in Appendix A.

3.2.3.5. Modified Analysis of Whale Liver Samples Using Internal Standardization

The Beluga Whale (*Delphinapterus leucas*) liver homogenate (CWLS - certified material which was supplied by NIST) which was also used in the preliminary trials was digested again for this study using the same digestion procedure.

Differently, in this procedure, aliquots of approximately 0.4 g and 0.3 g of homogenized liver samples were digested in Teflon containers with 8 ml of 65% HNO_3 and 1 ml of 30% H_2O_2 using the microwave digestion to see the effect of changing the amount of whale liver being digested. In order to perform internal standardization, to some of these vessels 0.1 mg/L of Co, Ni and Rh was added as a spike. After allowing the digest to cool to room temperature, each sample was transferred to acid-washed polyethylene vials and brought to a final volume of 25 ml with ultrapure water. Also, blanks were digested at the same time with the liver homogenates by adding 8 ml of 65% HNO_3, and 1 ml of 30% H_2O_2 to the vessels.

Appropriate amount of HNO_3 and NaCl were added into the standards for normal calibration and internal standardization for matrix matching.

The signals of the measured emission lines were listed in Table 3.4. Because of its low intensity and possible interference of Fe line in the whale liver samples, the Rh line at 251.752 nm could not be measured properly. It should be pointed out that concentrations calculated by using argon and hydrogen as the internal standards were only listed for Cd I 228 and Cd II 214 lines in Appendix A.

Table 3.4. The wavelengths used for the analysis of whale liver samples

Element	Wavelengths (nm)	
	Atom lines	Ion lines
Cd	326.106	214.438
	228.802	226.502
Mn	279.827	257.610
	403.076	259.373
Zn	213.856	206.200
		202.551
Co	345.350	228.616
	340.512	237.862
Ni	352.454	231.604
	341.476	221.647
Rh	369.236	249.077
		251.752
Ar	751.465	-
H	656.272	-

3.3. Results and Discussion

Elements and their selected wavelengths measured throughout this study are shown in Table 3.5. In this table excitation potentials for atomic lines and sum of excitation and first ionization potentials for ionic lines are also listed.

Table 3.5. Spectral Line Characteristics (Sources: Romero et al. 1997a, Grotti et al. 2003, Dennaud et al. 2001, Stepan et al. 2001, Brenner and Zander 2000)

Element	λ, nm	EP, eV	IP, eV	Energy Sum, eV
Ca I	422.673	2.93	6.11	9.04
Ca II	317.933	7.04	6.11	13.15
Cd I	228.802	5.41	8.99	14.40
Cd I	326.106	3.68*	8.99	12.67 -12.77
Cd II	226.502	5.47	8.99	14.46
Cd II	214.438	5.78	8.99	14.77
Co I	345.350	3.47*	7.86	11.33 – 11.43
Co I	340.512	4.07	7.86	11.93
Co II	228.616	5.84	7.86	13.70
Co II	258.033	4.65*	7.86	12.51 – 12.61
Co II	237.862	5.62	7.86	13.48
Cu I	324.754	3.82	7.73	11.55
Cu II	224.700	8.23	7.73	15.96
Fe I	275.574	4.35*	7.87	12.22 – 12.32
Fe II	259.940	5.22	7.87	13.09
Li I	610.362	3.87	5.39	9.26
Li I	670.784	1.85	5.39	7.24
Mn I	279.482	4.43	7.44	11.87
Mn I	403.076	3.08	7.44	10.52
Mn II	259.373	4.77	7.44	12.21
Mn II	257.610	4.81	7.44	12.25
Ni I	341.476	3.66	7.64	11.30
Ni I	352.454	3.54	7.64	11.18
Ni I	351.505	3.41*	7.64	11.05 – 11.15
Ni II	231.604	6.39	7.64	14.03
Ni II	221.647	6.03	7.64	13.67
Rh I	343.489	3.60	7.45	11.05
Rh I	369.236	3.25*	7.45	10.7 – 10.8
Rh II	251.752	4.76*	7.45	12.21 – 12.31
Rh II	249.077	7.07	7.45	14.52
Zn I	213.856	5.80	9.39	15.19
Zn I	334.502	7.78	9.39	17.19
Zn II	206.200	6.01	9.39	15.4
Zn II	202.551	6.12	9.39	15.51

"*" represents the estimated energy values which were calculated by using the equation $E = hc/\lambda$.

3.3.1. Initial Acid Effect Studies

In Tables 3.6 and 3.7, values obtained by the second analysis of whale liver homogenates are represented. As an internal standard the Rh atomic line at 343.489 nm was used and the acid content of both samples and standards were matched to have a value of 25% nitric acid.

Table 3.6. Values for the Control Material (Beluga Whale Liver Homogenate)

Element (nm)	**Normal calibration** (μg/g, wet mass)	**Internal Standard calibration** (μg/g, wet mass)	**NIST certified value** (μg/g, wet mass)	**% difference from the certified value**	
				Norm calibration	**Int Std calibration**
Cd I 228	1.99 ± 0.06	2.23 ± 0.12	2.35 ± 0.06	-15.3	- 5.3
Cu I 324	12.67 ± 0.23	12.63 ± 0.84	13.16 ± 0.4	- 3.7	- 4.0
Fe II 259	693 ± 0.2	688 ± 33	668 ± 15	3.8	3.0
Mn II 257	1.34 ± 0.04	2.14 ± 0.03	2.37 ± 0.08	- 43.4	- 9.9
Zn I 213	27.45 ± 0.68	27.95 ± 1.98	26.31 ± 0.66	4.3	6.2

Table 3.7. Values for the Test Material (Pygmy Sperm Whale Liver Homogenate)

Element (nm)	**Normal calibration** (μg/g, wet mass)	**Internal Standard calibration** (μg/g, wet mass)	**NIST certified value** (μg/g, wet mass)	**% difference from the certified value**	
				Norm calibration	**Int Std calibration**
Cd I 228	5.64 ± 0.02	5.77± 0.38	5.94 ± 0.38	- 5.1	- 2.8
Cu I 324	2.83 ± 0.04	2.56 ± 0.17	2.74 ± 0.19	3.1	- 6.6
Fe II 259	712 ± 7.6	677 ± 41	694 ± 45	2.6	- 2.4
Mn II 257	0.39 ± 0.004	1.17 ± 0.04	1.43 ± 0.10	- 73.0	-18.1
Zn I 213	25.81 ± 1.48	25.25 ± 2.65	21.15 ± 1.65	22.0	-9.4

As can be seen from the tables, an improvement both for control and test material are obtained when using Rh 343 line as the internal standard. Among the elements studied, Cd, Mn and Zn values seemed to be very different from the certified value, thus requiring correction.

According to an applied t-test, for the Beluga whale liver sample, calculated concentrations for Cu, Fe and Zn were acceptable after only using a simple normal calibration (i.e. no internal standard). After applying internal standardization with Rh, values for all selected elements except Mn were not different from the certified value at the 95% confidence level. Therefore, it can be concluded that through correction by internal standardization, the computed values for all elements were within the

uncertainty range of the NIST certified values and successful correction by internal standardization was achieved.

For the Pygmy whale liver sample, values obtained with the normal calibration for Cd, Cu and Fe were considered to be acceptable after application of the t-test. The calculated concentrations using internal standardization were good as well (i.e., they too were not very different from the certified value) for all elements. However, according to the t-test comparison of these results to those of the NIST certified values showed that the most significant improvements were only achieved for Cd, Cu and Fe when applying correction by internal standardization.

Furthermore, in order to investigate the effect of the nitric acid content on the analysis of Cd, Mn and Zn as well as the ability to apply internal standardization under various concentrations of acid content, another study was performed measuring the responses of these elements at three different acid levels (5%, 10%, and 25%). Figures 3.1, 3.2, and 3.3 show the calibration curves which were obtained by normal calibration for Cd, Zn, and Mn, respectively.

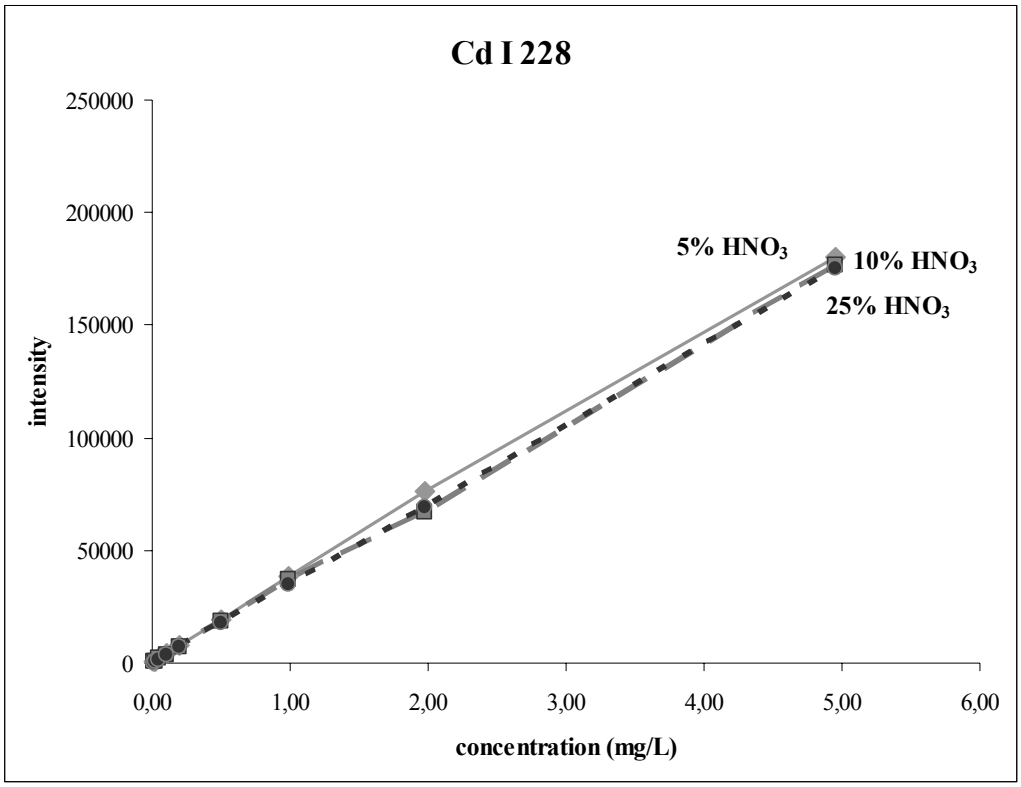

Figure 3.1. Normal calibration graph showing the acid effect for the Cd I 228 line

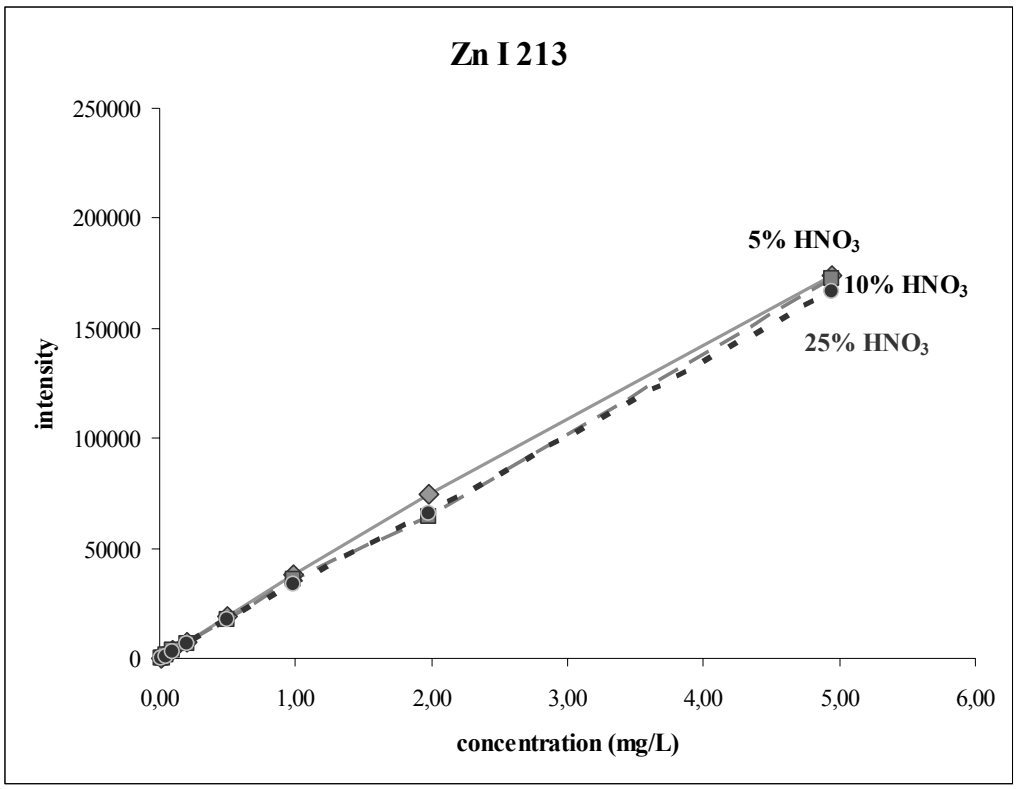

Figure 3.2. Normal calibration graph showing the acid effect for the Zn I 213 line

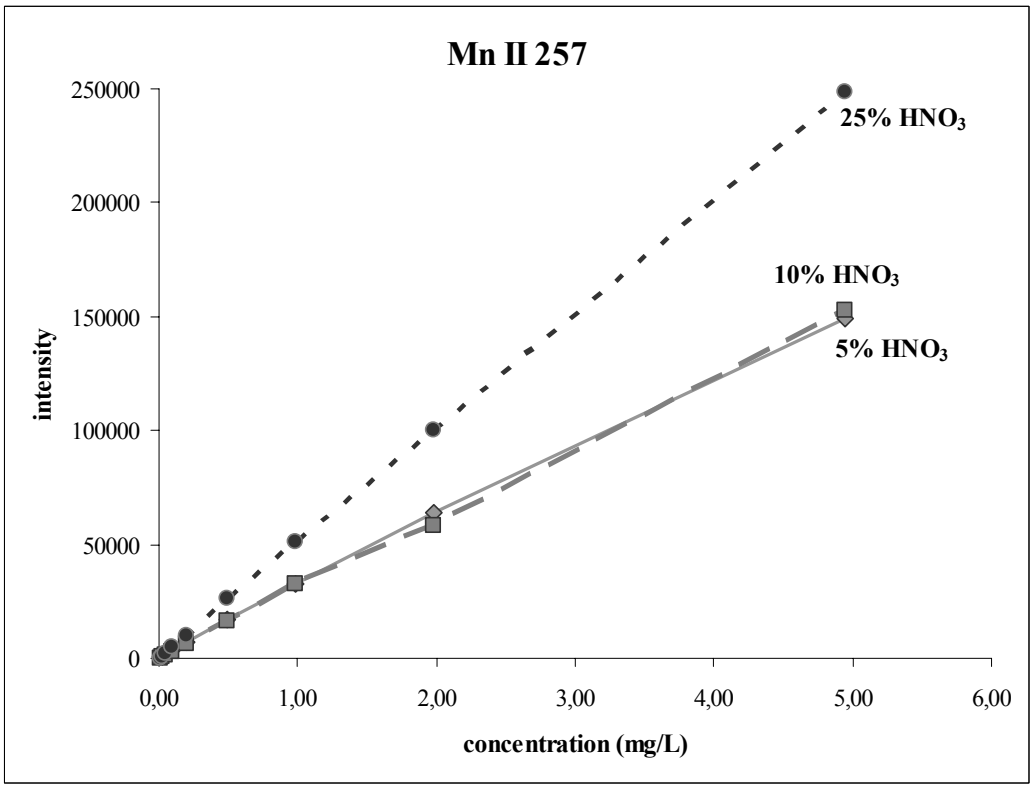

Figure 3.3. Normal calibration graph showing the acid effect for the Mn II 257 line

As can be seen there was a similar depressive effect for Cd and Zn lines confirming the trend observed by Todoli et al. (2002). Conversely, an enhancement was observed in the normal calibration curve for the sample containing Mn at 25% HNO_3 case whereas the effect is almost similar for 5% and 10% HNO_3 contents. This can be due to the atom and ion line differences chosen for the analysis because it has been reported by other researchers that the atomic lines are more sensitive to the changes in the matrix than ionic lines (Mermet 2002). It is worth noting that even when Rh was used as an internal standard the effect of acid matrix could not be corrected.

In order to test the reproducibility of this effect of acid on the determined concentrations of Cd, Mn, and Zn with respect to both atom and ion lines in the presence of nitric acid, new calibration graphs were drawn by using the results from similar studies performed in our lab. As can be seen in Figures 3.4 - 3.6, the same behavior was observed for both for the ion and atom lines. In contrast to the other results (Figs. 3.1 - 3.3), there is an increase in signal intensities when acid is present (Figs. 3.4 -3.6). However, it is interesting to note that after acid is added, the trend appears similar in most cases, i.e. simply the presence of acid appears to suppress signal intensity as a function of acid concentration. Further studies are needed to understand the trends between acid concentration and the point at which either an increase or decrease in signal intensity occurs.

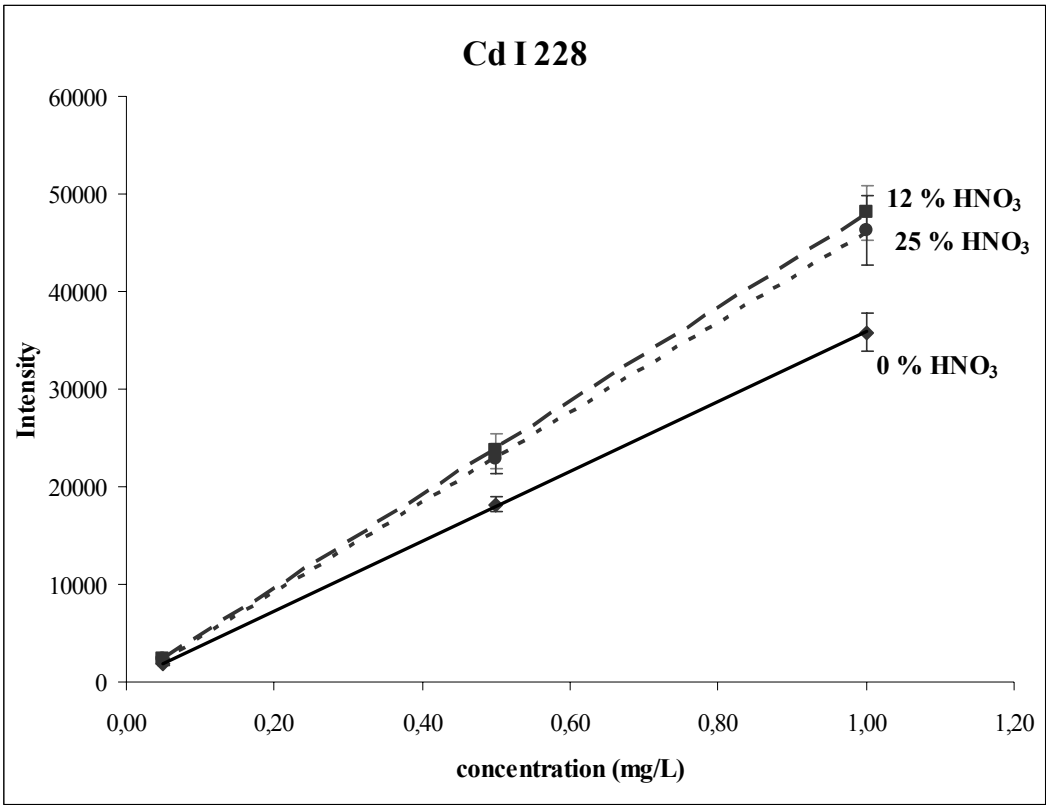

Figure 3.4. Normal calibration graph showing the acid effect for the Cd I 228 line

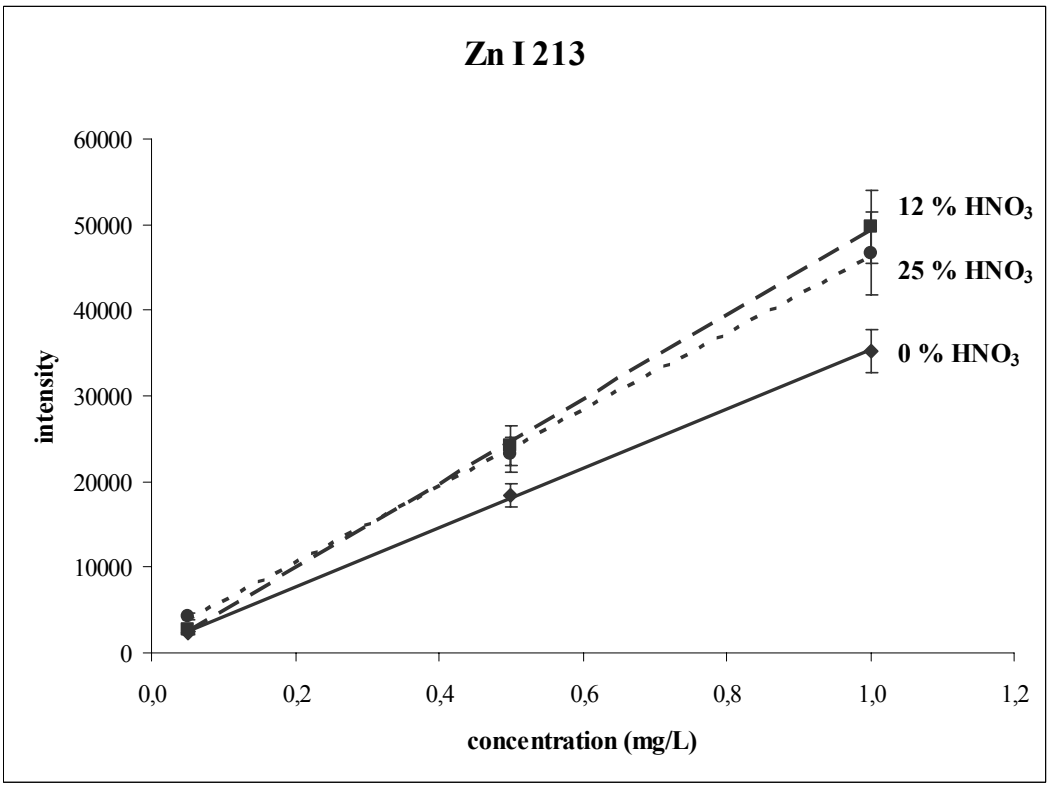

Figure 3.5. Normal calibration graph showing the acid effect for the Zn I 213 line

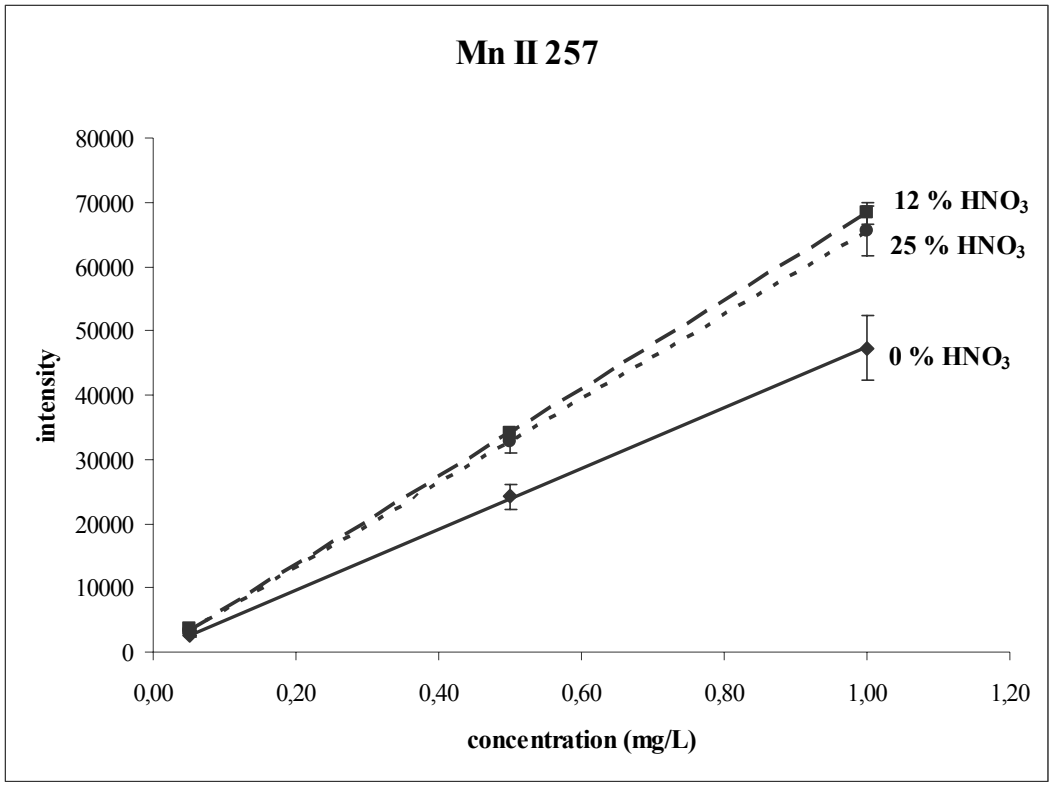

Figure 3.6. Normal calibration graph showing the acid effect for the Mn II 257 line

Obviously there are other factors other than acid which are affecting the responses of these lines such as salt content of the samples and changing multielement concentration. Therefore, the combined effect of these factors should be studied.

3.3.2. Combined Acid and Salt Effect Studies

To choose an optimal internal standard, the effect of the expected variation in matrix concentration on both the analytes and the potential internal standards should be studied with a trial experiment prior to an actual analysis. Therefore, in order to have a better understanding of the effects of these different acid and salt content on the signal changes of the elements that are being analyzed and to choose a suitable internal standard to correct for the signal variations caused by these matrix interferences, a systematic procedure which was adapted from the study by Grotti et al. (2003a) was performed.

Firstly, a set of synthetic sample solutions containing varying multielement (0.05 mg/L, 0.5 mg/L, 1 mg/L), acid (0%, 12%, 25%) and sodium (0%, 0.1%, 0.3%)

concentrations were prepared according to a 3^3 full factorial design. Then these solutions were measured with ICP-OES. The values obtained are shown in the Tables 3.6 and 3.7 for the three concentration levels which are 0.05, 0.5 and 1 mg/L.

As can be seen in Table 3.8, the atom lines of Ni, Mn and Rh appear to be less affected by acid and salt matrix changes. There was an increase in the concentration values for the Co line after the addition of matrix components but it also does not seem to have a serious influence. Differently, a depression was observed for the Cu atom line. The other elements Ca, Li, Fe, Cd and Zn were the most affected elements in the presence of acid and salt (NaCl) matrices. For these elements addition of NaCl caused an erroneous enhancement in the measured concentrations. In the presence of acid matrix there was a depression in the signals but again after the addition of salt content, an increase was observed for the signals. It has been reported previously that the higher the potentials, the lower the extent of the interference (Todoli et al. 2002) so since Ca, Li and Fe have lower excitation potentials (Ca 2.93 eV, Li 1.85 and 3.87 eV and Fe approx. 4.35 eV), these enhancements on the analyte signals may be expected for these lines. But in contrast although Cd and Zn have moderate excitation potentials (5.41 and 5.80 eV respectively), enhancements were also very high. On the other hand, Cd and Zn have very high 1^{st} ionization potentials (Cd 8.99 eV and Zn 9.39 eV). So it can be concluded that as also cited by Mermet (2002) there is no simple relationship between the excitation energy and magnitude of the matrix effect regardless of the ionization energy.

Table 3.8. Calculated concentrations for selected atom lines (in mg/L)

Sample	Acid %	Salt %	Ca 422.673	Co 345.350	Li 610.362	Li 670.784	Ni 341.476	Rh 343.489	Mn 279.482	Cu 324.754	Fe 275.574	Cd 228.802	Zn 213.856
1	0	0	0.05	0.05	0.05	0.04	0.04	0.05	0.05	0.05	0.06	0.05	0.07
2	0	0	0.55	0.52	0.50	0.46	0.51	0.55	0.50	0.51	0.54	0.51	0.55
3	**0**	**0**	**1.04**	**1.01**	**1.01**	**0.99**	**1.00**	**1.04**	**1.00**	**0.99**	**1.03**	**1.02**	**1.04**
4	0	0.1	0.38	0.07	0.07	0.11	0.07	0.07	0.06	0.06	0.11	0.06	0.12
5	0	0.1	0.83	0.58	0.71	1.10	0.56	0.62	0.56	0.51	0.67	0.64	0.67
6	**0**	**0.1**	**1.62**	**1.21**	**1.48**	**2.24**	**1.12**	**1.14**	**1.15**	**1.03**	**1.43**	**1.31**	**1.37**
7	0	0.3	0.17	0.07	0.04	0.12	0.03	0.07	0.07	0.06	0.10	0.06	0.12
8	0	0.3	0.83	0.62	0.73	1.13	0.54	0.63	0.49	0.44	0.76	0.64	0.74
9	**0**	**0.3**	**1.66**	**1.20**	**1.50**	**2.30**	**1.10**	**1.19**	**1.05**	**0.85**	**1.46**	**1.27**	**1.38**
10	12	0	0.08	0.08	0.06	0.06	0.05	0.09	0.06	0.05	0.11	0.07	0.08
11	12	0	0.50	0.55	0.58	0.64	0.53	0.59	0.52	0.49	0.83	0.68	0.73
12	**12**	**0**	**1.00**	**1.15**	**1.17**	**1.32**	**1.07**	**1.06**	**1.05**	**0.92**	**1.64**	**1.37**	**1.49**
13	12	0.1	0.15	0.08	0.06	0.10	0.06	0.08	0.05	0.05	0.10	0.06	0.08
14	12	0.1	0.71	0.54	0.65	0.98	0.53	0.61	0.52	0.44	0.75	0.63	0.69
15	**12**	**0.1**	**1.30**	**1.15**	**1.30**	**1.96**	**1.05**	**1.16**	**1.01**	**0.88**	**1.46**	**1.27**	**1.37**
16	12	0.3	0.15	0.10	0.06	0.11	0.06	0.08	0.06	0.05	0.08	0.06	0.10
17	12	0.3	0.74	0.61	0.65	1.05	0.53	0.61	0.50	0.44	0.72	0.62	0.66
18	**12**	**0.3**	**1.44**	**1.16**	**1.32**	**2.07**	**1.03**	**1.13**	**1.01**	**0.86**	**1.39**	**1.22**	**1.34**
19	25	0	0.08	0.10	0.05	0.05	0.05	0.07	0.06	0.05	0.10	0.07	0.13
20	25	0	0.42	0.59	0.49	0.56	0.53	0.56	0.51	0.46	0.79	0.65	0.69
21	**25**	**0**	**0.89**	**1.15**	**1.05**	**1.19**	**1.09**	**1.05**	**1.02**	**0.92**	**1.60**	**1.34**	**1.41**
22	25	0.1	0.08	0.10	0.06	0.09	0.05	0.07	0.03	0.05	0.09	0.06	0.07
23	25	0.1	0.61	0.60	0.60	0.92	0.52	0.61	0.50	0.44	0.73	0.61	0.66
24	**25**	**0.1**	**1.20**	**1.15**	**1.20**	**1.81**	**1.05**	**1.13**	**0.98**	**0.87**	**1.42**	**1.22**	**1.30**
25	25	0.3	0.11	0.07	0.06	0.10	0.05	0.08	0.05	0.04	0.12	0.06	0.07
26	25	0.3	0.69	0.57	0.62	0.98	0.52	0.59	0.49	0.42	0.70	0.60	0.65
27	**25**	**0.3**	**1.32**	**1.16**	**1.23**	**1.93**	**1.05**	**1.13**	**0.97**	**0.85**	**1.38**	**1.20**	**1.28**

Table 3.9. Calculated concentrations for selected ion lines (in mg/L)

Sample	Acid %	Salt %	Ca 317.933	Co 237.862	Ni 231.604	Rh 251.752	Mn 257.610	Cu 224.700	Fe 259.940	Cd 214.438	Zn 202.551
1	0	0	0.06	0.05	0.05	0.11	0.05	0.06	0.05	0.05	0.07
2	0	0	0.59	0.53	0.53	0.61	0.52	0.52	0.53	0.53	0.56
3	**0**	**0**	**1.09**	**1.04**	**1.04**	**1.16**	**1.03**	**1.02**	**1.03**	**1.06**	**1.08**
4	0	0.1	0.29	0.06	0.06	0.07	0.06	0.06	0.09	0.07	0.13
5	0	0.1	0.71	0.61	0.61	0.66	0.62	0.64	0.62	0.86	0.92
6	**0**	**0.1**	**1.52**	**1.30**	**1.35**	**1.12**	**1.32**	**1.31**	**1.33**	**1.85**	**2.06**
7	0	0.3	0.17	0.08	0.08	0.10	0.07	0.07	0.08	0.11	0.22
8	0	0.3	0.87	0.69	0.77	0.39	0.66	0.66	0.66	1.07	1.47
9	**0**	**0.3**	**1.77**	**1.44**	**1.58**	**1.20**	**1.32**	**1.35**	**1.30**	**2.23**	**2.88**
10	12	0	0.16	0.08	0.08	0.12	0.08	0.08	0.10	0.12	0.17
11	12	0	0.90	0.73	0.80	0.50	0.75	0.79	0.74	1.22	1.55
12	**12**	**0**	**1.73**	**1.47**	**1.61**	**1.02**	**1.51**	**1.51**	**1.48**	**2.42**	**3.16**
13	12	0.1	0.17	0.07	0.07	0.13	0.07	0.07	0.07	0.11	0.17
14	12	0.1	0.83	0.67	0.74	0.29	0.66	0.69	0.66	1.10	1.49
15	**12**	**0.1**	**1.52**	**1.34**	**1.46**	**0.92**	**1.33**	**1.37**	**1.32**	**2.27**	**2.89**
16	12	0.3	0.16	0.06	0.07	0.05	0.07	0.08	0.07	0.11	0.21
17	12	0.3	0.76	0.64	0.70	0.31	0.64	0.66	0.63	1.09	1.39
18	**12**	**0.3**	**1.51**	**1.28**	**1.40**	**1.14**	**1.27**	**1.32**	**1.27**	**2.16**	**2.85**
19	25	0	0.17	0.07	0.09	0.05	0.07	0.08	0.08	0.12	0.27
20	25	0	0.87	0.70	0.76	0.32	0.73	0.72	0.71	1.16	1.48
21	**25**	**0**	**1.67**	**1.46**	**1.57**	**1.15**	**1.47**	**1.47**	**1.45**	**2.40**	**2.99**
22	25	0.1	0.10	0.06	0.07	0.10	0.07	0.07	0.07	0.11	0.15
23	25	0.1	0.76	0.66	0.72	0.32	0.65	0.67	0.65	1.08	1.43
24	**25**	**0.1**	**1.51**	**1.30**	**1.42**	**1.13**	**1.28**	**1.33**	**1.28**	**2.15**	**2.79**
25	25	0.3	0.12	0.07	0.08	0.04	0.06	0.07	0.09	0.10	0.15
26	25	0.3	0.74	0.63	0.70	0.32	0.62	0.64	0.62	1.05	1.37
27	**25**	**0.3**	**1.46**	**1.24**	**1.36**	**1.08**	**1.25**	**1.27**	**1.25**	**2.06**	**2.70**

It is apparent from Table 3.9 that the ion lines were strongly influenced by the matrix changes and enhancement occurred for all the lines. Among these elements the magnitude of error produced by the presence of salt and acid on the Ca, Cd and Zn lines was more significant for ionic lines.

By using these concentration values, analytical errors which were used in the Principal Component Analysis were calculated by using the following formulae;

$$E_1 = \frac{(C_1 - C_1)}{C_1} \times 100 \tag{3.7}$$

$$E_2 = \frac{(C_2 - C_2)}{C_2} \times 100 \tag{3.8}$$

$$E_3 = \frac{(C_3 - C_3)}{C_3} \times 100 \tag{3.9}$$

$$E_4 = \frac{(C_1 - C_4)}{C_1} \times 100 \tag{3.10}$$

$$E_5 = \frac{(C_2 - C_5)}{C_2} \times 100 \tag{3.11}$$

$$E_6 = \frac{(C_3 - C_6)}{C_3} \times 100 \tag{3.12}$$

$$E_7 = \frac{(C_1 - C_7)}{C_1} \times 100 \tag{3.13}$$

. . .

$$E_{27} = \frac{(C_3 - C_{27})}{C_3} \times 100 \tag{3.14}$$

Computed errors and corresponding samples are shown in Tables 3.10 and 3.11 for the atom and ion lines, respectively. Since the first three samples did not contain any added interferents (i.e. salt and acid) and they contain only the analytes of interest, they were considered as the blanks for the corresponding concentration level. The errors for the first three samples (E1, E2, and E3) were considered as the ideal response (no matrix effects) and therefore considered as zero error as a necessary point of reference. It should also be noted that (-) and (+) signs indicate the difference from the

corresponding concentration level and not the true value. Three dimensional graphs of these matrix induced errors can be seen in Appendix B.

Table 3.10. Matrix-induced errors calculated for atom lines for generating the multielement score plot

Error	Acid %	Salt %	Ca 422	Co 345	Li 610	Li 670	Ni 341	Rh 343	Mn 279.4	Cu 324	Fe 275	Cd 228.8	Zn 213
E1	0	0	0	0	0	0	0	0	0	0	0	0	0
E2	0	0	0	0	0	0	0	0	0	0	0	0	0
E3	0	0	0	0	0	0	0	0	0	0	0	0	0
E4	0	0.1	-644	-47	-37	-165	-77	-37	-9	-4	-79	-15	-85
E5	0	0.1	-52	-10	-40	-137	-10	-13	-13	0	-25	-25	-22
E6	0	0.1	-56	-20	-47	-127	-11	-10	-15	-4	-39	-28	-32
E7	0	0.3	-236	-35	15	-188	12	-47	-33	-6	-70	-24	-81
E8	0	0.3	-51	-19	-45	-144	-6	-14	1	14	-42	-24	-36
E9	0	0.3	-60	-19	-48	-133	-9	-14	-5	14	-41	-25	-33
E10	12	0	60	75	18	53	36	83	13	3	74	31	22
E11	12	0	8	-4	-15	-37	-3	-7	-5	5	-55	-33	-33
E12	12	0	4	-14	-16	-33	-7	-1	-6	7	-59	-35	-43
E13	12	0.1	-186	-72	-26	-150	-49	-49	4	18	-62	-23	-19
E14	12	0.1	-29	-4	-30	-112	-3	-11	-4	13	-39	-22	-27
E15	12	0.1	-25	-14	-29	-99	-5	-11	-1	11	-42	-25	-31
E16	12	0.3	-204	-98	-30	-160	-39	-63	-18	10	-39	-22	-44
E17	12	0.3	-35	-16	-30	-127	-3	-10	0	14	-34	-20	-22
E18	12	0.3	-39	-15	-31	-110	-2	-9	-1	13	-35	-20	-29
E19	25	0	-48	-109	-2	-26	-31	-46	-14	10	-66	-26	-87
E20	25	0	23	-12	3	-20	-4	-2	-3	9	-47	-27	-27
E21	25	0	15	-14	-4	-20	-8	0	-3	7	-55	-31	-35
E22	25	0.1	-57	-106	-14	-125	-29	-33	45	11	-41	-20	0
E23	25	0.1	-11	-14	-19	-98	-2	-10	1	14	-35	-19	-21
E24	25	0.1	-15	-14	-19	-83	-4	-8	2	12	-37	-20	-25
E25	25	0.3	-109	-36	-19	-137	-36	-51	-2	23	-91	-13	-7
E26	25	0.3	-26	-9	-23	-111	-1	-6	2	18	-30	-16	-20
E27	25	0.3	-27	-15	-22	-95	-5	-9	3	15	-34	-18	-23

Table 3.11. Matrix induced errors calculated for ion lines for generating the multielement score plot

Error	Acid %	Salt %	Ca 317	Co 237	Ni 231	Rh 251	Mn 257	Cu 224	Fe 259	Cd 214	Zn 202
E1	0	0	0	0	0	0	0	0	0	0	0
E2	0	0	0	0	0	0	0	0	0	0	0
E3	0	0	0	0	0	0	0	0	0	0	0
E4	0	0.1	-367	-18	-10	35	-4	-10	-92	-32	-84
E5	0	0.1	-21	-15	-15	-8	-18	-23	-17	-63	-63
E6	0	0.1	-39	-25	-31	3	-28	-29	-29	-75	-91
E7	0	0.3	-182	-69	-49	7	-28	-29	-67	-101	-210
E8	0	0.3	-49	-31	-47	36	-26	-27	-24	-102	-160
E9	0	0.3	-62	-39	-53	-4	-28	-33	-26	-111	-167
E10	12	0	167	55	53	10	44	46	100	125	142
E11	12	0	-54	-38	-52	18	-43	-51	-38	-131	-175
E12	12	0	-59	-42	-56	12	-46	-48	-43	-129	-194
E13	12	0.1	-180	-48	-45	-26	-27	-31	-53	-110	-139
E14	12	0.1	-42	-27	-41	53	-26	-32	-23	-109	-165
E15	12	0.1	-39	-29	-41	20	-29	-34	-28	-115	-168
E16	12	0.3	-154	-25	-37	53	-24	-36	-53	-108	-190
E17	12	0.3	-30	-21	-34	49	-22	-27	-19	-105	-147
E18	12	0.3	-38	-23	-36	1	-24	-29	-23	-104	-165
E19	25	0	-172	-40	-68	51	-37	-38	-76	-116	-278
E20	25	0	-49	-31	-44	48	-38	-39	-34	-118	-162
E21	25	0	-52	-41	-51	1	-42	-45	-41	-127	-178
E22	25	0.1	-63	-31	-37	5	-26	-19	-53	-103	-105
E23	25	0.1	-30	-24	-36	48	-23	-29	-22	-105	-154
E24	25	0.1	-38	-25	-37	3	-24	-31	-24	-104	-159
E25	25	0.3	-91	-49	-54	61	-18	-19	-89	-94	-116
E26	25	0.3	-26	-19	-32	48	-18	-22	-16	-98	-144
E27	25	0.3	-34	-20	-31	6	-22	-25	-21	-95	-150

Next the principal component analysis was performed. The loading plot (showing relationships between the responses of matrix elements) and score plot (indicating the behaviors of the chosen analytical lines of the elements with regard to the matrices) were generated. By exploring the grouping of the lines in these plots, optimal internal standard reference line or lines can be chosen. Since a potential internal standard should have similar properties with the elements to be analyzed, the analyte and reference lines should have similar responses (or errors) in the considered matrix and the signal variation caused by matrix can be compensated for by using this possible reference line.

Figures 3.7 and 3.8 represent the loading plot and the score plot obtained by PCA. In Figure 3.7 acid content is shown as “A” and it has a percent acid value. In te same graph salt content also has a percent value and was labeled as “S”. When the loading plot is examined it can be seen that sample 4 (0.05 mg/L) which have a salt content of 0.1% but no acid content shows a very different behavior from the other matrices. Samples that do not contain any salt content but have an acid content of 12% (11 and 12) and which have an acid content of 25% (20 and 21) are grouped together at the upper right side of the graph. Samples that have the same matrices (10 and 19) are located very far from this group because of the lowest ME concentration which is 0.05 mg/L. In the same way, the other samples having same similar matrix contents in terms of acid, salt and multielement concentrations (such as 23 and 24; 14 and 15; 26 and 27; 17 and 18; 8 and 9) are located very close to each other showing the similar responses of these matrices. The other group which is distributed at the lower side of the graph (Figure 3.7) contains the samples at a concentration of 0.05 mg/L (7, 10, 13, 16, 22, and 25), except for samples 5 and 6.

In the score plot (Figure 3.8); the elements showing similar behaviors in the considered matrices are grouped in the middle of the graph. It can also be seen that the Cd II 214.438, Zn II 202.551, Li I 670.784 and both Ca lines at 317.933 nm and 422.673 nm are distributed at right side of the graph along the Principal Component 2. At the same time Rh I 343, Ni I 34 and Mn I 279 are located at the lower left side of the graph. Cu I 324 which is located at the upper right side of the graph, is also far from the other grouping. These elements are outside of the grouping occurred in the middle indicating the highest analytical errors were obtained by these elements when considering total error incurred for samples.

According to the score plot for the analyzed elements, Rh, Co, Ni and especially Rh II 251, Co I 345, Co II 237, Ni II 231 can potentially be used as internal standards for the other elements to correct for acid and salt matrix interferences. They were chosen as potential internal standards because they do not exist in the reference material (whale liver) and they are located closer to the other elements of interest indicating greater possible similarity in their behaviors under different matrix conditions.

Especially Co I 345 line is expected to correct significantly for the Cd I 228 and Cu I 324 lines while Co II 237 is expected to be useful for the Mn II 257 line due to the closeness of these lines in the score plots.

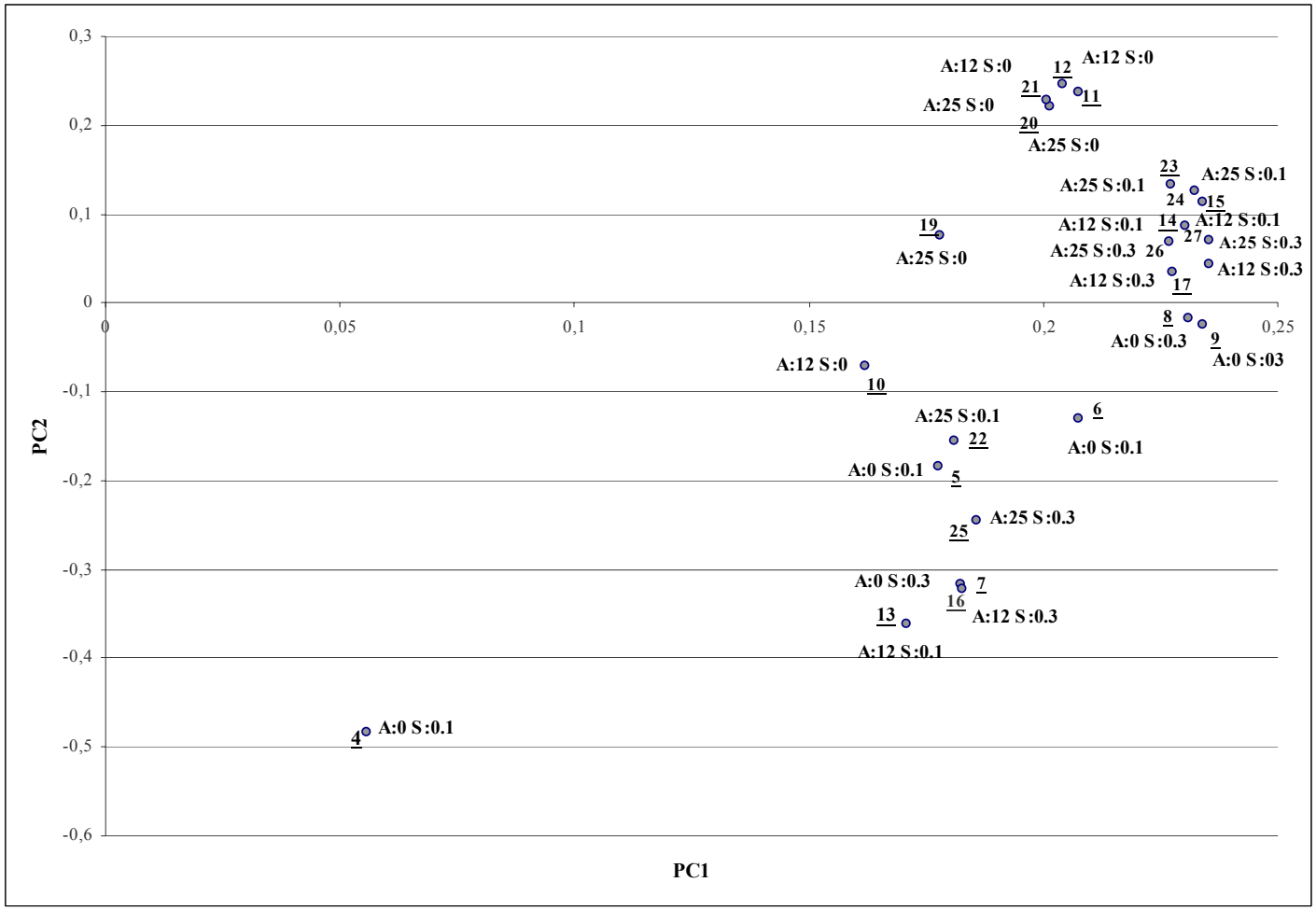

Figure 3.7. Loading plot obtained by the PCA (using multielement standard)

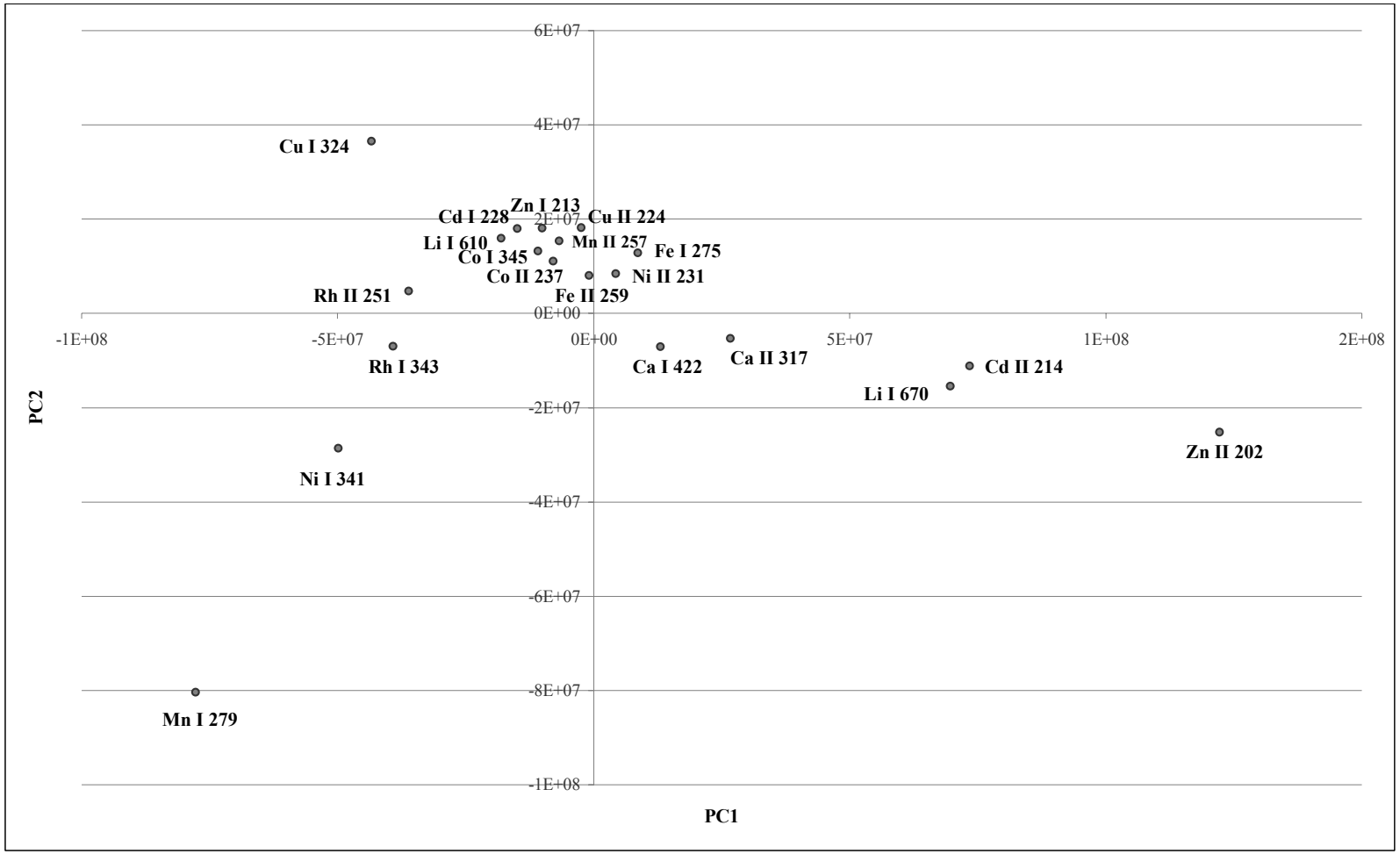

Figure 3.8. Score plot obtained by the PCA (using multielement standard)

3.3.3. Validation of Acid and Salt Effect Studies

In order to test the suitability of the proposed internal standards, a validation study was performed using the same experimental plan to have identical conditions. Cd, Mn, Zn were chosen as the analytes and Rh, Co, Ni were considered as internal standards.

Listed in the following Tables (3.12, 3.13, 3.14, 3.15, 3.16, and 3.17) are the calculated concentrations of the elements of interest (Cd, Mn and Zn) using both normal calibration and internal standard calibration (with Co, Ni and Rh as internal standards) at the 1 mg/L concentration level. The line graphs of these calculated concentrations can be seen in Appendix C.

In general, for all the lines of Cd, Mn and Zn negative errors in concentration measurement were obtained for sample 6 (no acid, 0.1% salt) when Rh was used as the internal standard. Since no anomalies were observed for the other chosen internal standards for the same sample, these errors appear to be due to experimental error. Actually for sample 6 the effect of the acid/salt matrix is minimal and no internal standardization correction was required. Any errors in determined concentrations were a reflection of normal experimental error and not due to acid/salt matrix effects.

Similarly the Zn 334 atom line was also problematic especially when acid and salt contents were increased. The calculated concentrations were even worse when internal standards were used for the correction.

Table 3.12. Normal Calibration and Internal Standard Calibration Results for Cd atom lines. All results are expressed as mg/L.

Emission Line : Cd I 326.106 nm												
		Internal standards										
#	**none**	**Co 340**	**Co 345**	**Co 237**	**Co 228.6**	**Ni 231**	**Ni 221**	**Ni 341**	**Ni 352**	**Rh 249**	**Rh 343**	**Rh 369**
3	0.98 ± 0.03	0.99 ± 0.03	0.98 ± 0.03	1.00 ± 0.03	0.98 ± 0.04	0.94 ± 0.03	0.96 ± 0.03	0.97 ± 0.02	0.97 ± 0.02	0.96 ± 0.0005	1.00 ± 0.07	0.98 ± 0.05
6	0.98 ± 0.12	0.91 ± 0.3	0.97 ± 0.05	1.02 ± 0.10	1.02 ± 0.10	1.02 ± 0.10	1.00 ± 0.10	1.00 ± 0.03	1.00 ± 0.04	0.61 ± 0.14	0.56 ± 0.20	0.53 ± 0.18
9	0.93 ± 0.07	0.75 ± 0.07	0.86 ± 0.05	0.95 ± 0.06	0.99 ± 0.04	0.89 ± 0.03	0.94 ± 0.04	0.94 ± 0.005	0.92 ± 0.02	0.89 ± 0.09	0.90 ± 0.07	0.89 ± 0.10
12	0.81 ± 0.20	0.66 ± 0.20	0.88 ± 0.21	0.84 ± 0.20	0.81 ± 0.20	0.74 ± 0.20	0.76 ± 0.20	0.87 ± 0.22	0.86 ± 0.23	0.68 ± 0.34	0.83 ± 0.44	0.80 ± 0.41
15	1.05 ± 0.13	0.97 ± 0.08	1.00 ± 0.02	1.06 ± 0.12	1.04 ± 0.13	0.96 ± 0.12	1.01 ± 0.12	1.02 ± 0.12	1.00 ± 0.12	0.91 ± 0.11	0.93 ± 0.09	0.92 ± 0.08
18	0.81 ± 0.08	0.62 ± 0.07	0.72 ± 0.04	0.91 ± 0.05	0.90 ± 0.03	0.80 ± 0.03	0.87 ± 0.03	0.81 ± 0.01	0.76 ± 0.08	0.74 ± 0.01	0.71 ± 0.06	0.69 ± 0.02
21	1.01 ± 0.14	0.87 ± 0.05	0.97 ± 0.14	1.00 ± 0.12	0.99 ± 0.13	1.02 ± 0.02	0.98 ± 0.14	0.98 ± 0.14	0.97 ± 0.12	0.81 ± 0.24	0.97 ± 0.31	0.92 ± 0.32
24	0.95 ± 0.16	0.73 ± 0.14	0.90 ± 0.12	1.00 ± 0.14	0.98 ± 0.14	0.96 ± 0.16	0.96 ± 0.15	0.96 ± 0.14	0.96 ± 0.16	0.90 ± 0.15	0.90 ± 0.16	0.86 ± 0.13
27	0.79 ± 0.03	0.59 ± 0.02	0.70 ± 0.04	0.87 ± 0.05	0.87 ± 0.06	0.78 ± 0.03	0.83 ± 0.04	0.74 ± 0.03	0.74 ± 0.04	0.77 ± 0.05	0.77 ± 0.07	0.73 ± 0.07
Emission Line : Cd I 228.802 nm												
		Internal standards										
#	**none**	**Co 340**	**Co 345**	**Co 237**	**Co 228.6**	**Ni 231**	**Ni 221**	**Ni 341**	**Ni 352**	**Rh 249**	**Rh 343**	**Rh 369**
3	1.00 ± 0.01	1.01 ± 0.01	0.99 ± 0.01	1.01 ± 0.02	1.00 ± 0.01	0.98 ± 0.03	0.99 ± 0.02	1.00 ± 0.02	1.00 ± 0.02	1.02 ± 0.05	1.01 ± 0.11	0.99 ± 0.09
6	0.98 ± 0.02	0.90 ± 0.04	0.91 ± 0.02	1.01 ± 0.01	1.00 ± 0.01	0.98 ± 0.01	0.99 ± 0.01	0.95 ± 0.04	0.95 ± 0.03	0.69 ± 0.03	0.62 ± 0.08	0.59 ± 0.07
9	0.99 ± 0.01	0.84 ± 0.07	0.90 ± 0.02	0.99 ± 0.02	0.99 ± 0.01	0.95 ± 0.02	0.96 ± 0.02	0.96 ± 0.02	0.97 ± 0.01	0.99 ± 0.03	0.96 ± 0.04	0.94 ± 0.01
12	0.99 ± 0.01	0.85 ± 0.03	0.96 ± 0.003	0.92 ±0.01	0.89 ± 0.01	0.89 ± 0.004	0.88 ± 0.01	0.97 ± 0.01	0.97 ± 0.01	0.83 ± 0.11	0.92 ± 0.18	0.90 ± 0.15
15	0.97 ± 0.003	0.86 ± 0.03	0.87 ± 0.01	0.97 ± 0.01	0.95 ± 0.01	0.92 ± 0.01	0.93 ± 0.01	0.95 ± 0.01	0.93 ± 0.01	0.90 ± 0.04	0.88 ± 0.05	0.87 ± 0.06
18	0.95 ± 0.01	0.78 ± 0.01	0.85 ± 0.03	0.98 ± 0.02	0.97 ± 0.01	0.94 ± 0.01	0.97 ± 0.01	0.91 ± 0.01	0.91 ± 0.002	0.88 ± 0.02	0.81 ± 0.02	0.79 ± 0.003
21	0.93 ± 0.01	0.78 ± 0.01	0.88 ± 0.02	0.92 ± 0.02	0.91 ± 0.01	0.90 ± 0.005	0.90 ± 0.01	0.91 ± 0.02	0.9 ± 0.01	0.81 ± 0.06	0.89 ± 0.10	0.86 ± 0.11
24	0.94 ± 0.003	0.76 ± 0.01	0.82 ± 0.01	0.96 ± 0.01	0.95 ± 0.005	0.92 ± 0.01	0.95 ± 0.01	0.90 ± 0.01	0.89 ± 0.01	0.87 ± 0.01	0.83 ± 0.02	0.80 ± 0.004
27	0.91 ± 0.02	0.74 ± 0.03	0.80 ± 0.02	0.97 ± 0.03	0.97 ± 0.04	0.93 ± 0.02	0.96 ± 0.02	0.87 ± 0.01	0.87 ± 0.02	0.94 ± 0.01	0.89 ± 0.03	0.85 ± 0.04

Table 3.13. Normal Calibration and Internal Standard Calibration Results for Cd ion lines. All results are expressed as mg/L.

Emission Line : Cd II 226.502 nm												
		Internal standards										
#	**none**	**Co 340**	**Co 345**	**Co 237**	**Co 228.6**	**Ni 231**	**Ni 221**	**Ni 341**	**Ni 352**	**Rh 249**	**Rh 343**	**Rh 369**
3	1.00 ± 0.02	1.01 ± 0.01	0.99 ± 0.02	1.00 ± 0.03	0.98 ± 0.02	1.00 ± 0.02	1.00 ± 0.003	0.99 ± 0.03	1.00 ± 0.03	1.01 ± 0.06	1.01 ± 0.12	0.99 ± 0.10
6	0.97 ± 0.03	0.89 ± 0.03	0.90 ± 0.03	1.00 ± 0.01	0.98 ± 0.01	0.97 ± 0.02	0.99 ± 0.01	0.93 ± 0.05	0.95 ± 0.04	0.68 ± 0.03	0.61 ± 0.08	0.59 ± 0.08
9	1.01 ± 0.02	0.86 ± 0.06	0.93 ± 0.02	1.02 ± 0.03	1.01 ± 0.01	0.97 ± 0.02	0.99 ± 0.01	0.99 ± 0.03	0.98 ± 0.05	1.01 ± 0.02	0.98 ± 0.04	0.96 ± 0.01
12	1.07 ± 0.01	0.92 ± 0.04	1.04 ± 0.001	1.00 ± 0.01	0.96 ± 0.01	0.96 ± 0.002	0.96 ± 0.01	1.06 ± 0.02	1.06 ± 0.01	0.91 ± 0.12	1.01 ± 0.19	0.99 ± 0.16
15	1.03 ± 0.01	0.91 ± 0.02	0.92 ± 0.01	1.03 ± 0.01	1.00 ± 0.003	0.98 ± 0.01	0.99 ± 0.02	1.00 ± 0.02	0.98 ± 0.01	0.96 ± 0.05	0.94 ± 0.07	0.92 ± 0.07
18	0.99 ± 0.02	0.81 ± 0.02	0.88 ± 0.05	1.02 ± 0.02	1.00 ± 0.002	0.98 ± 0.02	1.00 ± 0.01	0.95 ± 0.01	0.94 ± 0.01	0.90 ± 0.01	0.84 ± 0.03	0.81 ± 0.0002
21	1.00 ± 0.01	0.83 ± 0.02	0.94 ± 0.02	0.98 ± 0.02	0.96 ± 0.01	0.96 ± 0.01	0.97 ± 0.01	0.97 ± 0.02	0.96 ± 0.01	0.87 ± 0.07	0.96 ± 0.12	0.92 ± 0.12
24	1.00 ± 0.02	0.81 ± 0.02	0.87 ± 0.02	1.02 ± 0.02	1.00 ± 0.01	0.98 ± 0.02	1.01 ± 0.01	0.96 ± 0.01	0.95 ± 0.02	0.93 ± 0.02	0.89 ± 0.02	0.86 ± 0.01
27	0.95 ± 0.02	0.77 ± 0.04	0.83 ± 0.02	1.01 ± 0.03	1.00 ± 0.04	0.97 ± 0.02	0.99 ± 0.03	0.90 ± 0.01	0.90 ± 0.02	0.98 ± 0.01	0.93 ± 0.03	0.89 ± 0.03
Emission Line : Cd II 214.438 nm												
		Internal standards										
#	**none**	**Co 340**	**Co 345**	**Co 237**	**Co 228.6**	**Ni 231**	**Ni 221**	**Ni 341**	**Ni 352**	**Rh 249**	**Rh 343**	**Rh 369**
3	1.00 ± 0.01	1.00 ± 0.01	0.98 ± 0.01	1.00 ± 0.02	0.98 ± 0.01	0.97 ± 0.03	0.98 ± 0.02	0.99 ± 0.02	0.99 ± 0.03	1.01 ± 0.05	1.01 ± 0.11	0.99 ± 0.10
6	1.00 ± 0.04	0.92 ± 0.04	0.93 ± 0.04	1.03 ± 0.02	1.02 ± 0.02	1.01 ± 0.03	1.02 ± 0.02	0.99 ± 0.04	0.95 ± 0.07	0.70 ± 0.05	0.63 ± 0.10	0.60 ± 0.09
9	1.05 ± 0.01	0.90 ± 0.06	0.96 ± 0.01	1.06 ± 0.02	1.05 ± 0.004	1.01 ± 0.01	1.03 ± 0.01	1.03 ± 0.02	1.02 ± 0.04	1.05 ± 0.01	1.03 ± 0.03	1.01 ± 0.003
12	1.11 ± 0.005	0.95 ± 0.03	1.08 ± 0.005	1.04 ± 0.003	1.00± 0.01	1.00 ± 0.01	1.00 ± 0.01	1.10 ± 0.01	1.10 ± 0.02	0.94 ± 0.12	1.05 ± 0.20	1.03 ± 0.16
15	1.08 ± 0.004	0.96 ± 0.03	0.96 ± 0.01	1.08 ± 0.01	1.05 ± 0.01	1.03 ± 0.01	1.04 ± 0.02	1.05 ± 0.01	1.03 ± 0.01	1.01 ± 0.04	0.98 ± 0.06	0.97 ± 0.07
18	1.05 ± 0.02	0.86 ± 0.01	0.93 ± 0.05	1.08 ± 0.01	1.06 ± 0.01	1.03 ± 0.02	1.06 ± 0.01	1.00 ± 0.02	1.00 ± 0.01	0.96 ± 0.03	0.89 ± 0.02	0.86 ± 0.01
21	1.05 ± 0.01	0.87 ± 0.02	0.99 ± 0.02	1.03 ± 0.02	1.01 ± 0.01	1.01 ± 0.002	1.02 ± 0.003	1.02 ± 0.02	1.01 ± 0.01	0.92 ± 0.07	1.01 ± 0.12	0.97 ± 0.13
24	1.06 ± 0.02	0.87 ± 0.03	0.92 ± 0.03	1.09 ± 0.02	1.06 ± 0.01	1.04 ± 0.02	1.07 ± 0.01	1.02 ± 0.01	1.01 ± 0.02	0.99 ± 0.03	0.95 ± 0.03	0.91 ± 0.02
27	1.03 ± 0.01	0.83 ± 0.04	0.90 ± 0.03	1.09 ± 0.02	1.08 ± 0.03	1.04 ± 0.01	1.07 ± 0.01	0.97 ± 0.01	0.98 ± 0.01	1.06 ± 0.03	1.01 ± 0.05	0.97 ± 0.05

Table 3.14. Normal Calibration and Internal Standard Calibration Results for Mn atom lines. All results are expressed as mg/L.

Emission Line : Mn I 279.482 nm												
		Internal standards										
#	**none**	**Co 340**	**Co 345**	**Co 237**	**Co 228.6**	**Ni 231**	**Ni 221**	**Ni 341**	**Ni 352**	**Rh 249**	**Rh 343**	**Rh 369**
3	1.01± 0.01	1.02 ± 0.02	1.00 ± 0.01	1.01 ± 0.005	0.99 ± 0.002	0.98 ± 0.02	0.98 ± 0.01	0.99 ± 0.01	1.01 ± 0.02	1.06 ± 0.04	1.05 ± 0.10	1.03 ± 0.09
6	1.07 ± 0.02	0.98 ± 0.05	0.99 ± 0.02	1.09 ± 0.04	1.09 ± 0.04	1.07 ± 0.02	1.08 ± 0.04	1.01 ± 0.03	1.01 ± 0.03	0.78 ± 0.001	0.69 ± 0.06	0.67 ± 0.06
9	1.07 ± 0.02	0.92 ± 0.08	0.98 ± 0.02	1.07 ± 0.02	1.07 ± 0.03	1.03 ± 0.03	1.04 ± 0.04	1.03 ± 0.01	1.04 ± 0.01	1.12 ± 0.01	1.08 ± 0.004	1.06 ± 0.02
12	0.93 ± 0.003	0.80 ± 0.03	0.90 ± 0.003	0.87 ± 0.004	0.84 ± 0.01	0.83 ± 0.01	0.83 ± 0.01	0.91 ± 0.01	0.92 ± 0.01	0.81 ± 0.10	0.89 ± 0.17	0.88 ± 0.14
15	1.02 ± 0.01	0.91± 0.03	0.92 ± 0.01	1.02 ± 0.01	1.00 ± 0.01	0.97 ± 0.01	0.98 ± 0.01	0.99 ± 0.01	0.98 ± 0.01	0.99 ± 0.05	0.96 ± 0.07	0.94 ± 0.07
18	1.06 ± 0.01	0.88 ± 0.02	0.95 ± 0.04	1.09 ± 0.02	1.08 ± 0.01	1.05 ± 0.01	1.08 ± 0.01	1.01 ± 0.01	1.02 ± 0.003	1.01 ± 0.02	0.93 ± 0.03	0.90 ± 0.005
21	0.88 ± 0.003	0.74 ± 0.01	0.83 ± 0.01	0.86 ± 0.02	0.85 ± 0.01	0.85 ± 0.01	0.85 ± 0.01	0.85 ± 0.02	0.85 ± 0.01	0.79 ± 0.06	0.87 ± 0.10	0.83 ± 0.11
24	0.99 ± 0.02	0.81 ± 0.01	0.86 ± 0.02	1.01 ± 0.03	0.99 ± 0.02	0.97 ± 0.01	0.99 ± 0.02	0.93 ± 0.01	0.94 ± 0.01	0.95 ± 0.01	0.90 ± 0.001	0.86 ± 0.02
27	0.98 ± 0.01	0.79 ± 0.03	0.86 ± 0.03	1.03 ± 0.02	1.03 ± 0.03	1.00 ± 0.003	1.02 ± 0.01	0.92 ± 0.01	0.94 ± 0.003	1.05 ± 0.03	0.99 ± 0.05	0.94 ± 0.06
Emission Line : Mn I 403.076 nm												
		Internal standards										
#	**none**	**Co 340**	**Co 345**	**Co 237**	**Co 228.6**	**Ni 231**	**Ni 221**	**Ni 341**	**Ni 352**	**Rh 249**	**Rh 343**	**Rh 369**
3	0.98 ± 0.01	0.99 ± 0.02	0.99 ± 0.01	0.98 ± 0.003	0.96 ± 0.01	0.98 ± 0.01	0.96 ± 0.001	0.97 ± 0.01	0.98 ± 0.01	1.04 ± 0.03	1.01 ± 0.09	1.00 ± 0.07
6	1.16 ± 0.03	1.06 ± 0.07	1.10 ± 0.03	1.18 ± 0.05	1.18 ± 0.06	1.20 ± 0.05	1.17 ± 0.06	1.11 ± 0.03	1.10 ± 0.01	0.87 ± 0.002	0.76 ± 0.07	0.73 ± 0.06
9	1.08 ± 0.03	0.92 ± 0.08	1.01 ± 0.03	1.07 ± 0.02	1.07 ± 0.04	1.06 ± 0.03	1.05 ± 0.04	1.04 ± 0.02	1.04 ± 0.01	1.14 ± 0.02	1.08 ± 0.005	1.07 ± 0.03
12	0.88 ± 0.01	0.76 ± 0.04	0.88 ± 0.01	0.82 ± 0.01	0.79 ± 0.02	0.81 ± 0.01	0.79 ± 0.01	0.87 ± 0.02	0.87 ± 0.02	0.78 ± 0.11	0.85 ± 0.17	0.83 ± 0.15
15	1.09 ± 0.01	0.97 ± 0.03	1.00 ± 0.01	1.08 ± 0.01	1.07 ± 0.01	1.06 ± 0.01	1.05 ± 0.02	1.06 ± 0.02	1.05 ± 0.01	1.06 ± 0.04	1.01 ± 0.05	1.00 ± 0.06
18	1.08 ± 0.01	0.89 ± 0.03	0.98 ± 0.04	1.11 ± 0.03	1.10 ± 0.01	1.09 ± 0.02	1.09 ± 0.01	1.03 ± 0.003	1.03 ± 0.02	1.04 ± 0.0003	0.94 ± 0.05	0.91 ± 0.01
21	0.88 ± 0.01	0.73 ± 0.02	0.85 ± 0.03	0.86 ± 0.01	0.85 ± 0.01	0.87 ± 0.01	0.85 ± 0.01	0.85 ± 0.02	0.85 ± 0.001	0.80 ± 0.08	0.86 ± 0.12	0.83 ± 0.12
24	1.08 ± 0.02	0.89 ± 0.03	0.97 ± 0.03	1.11 ± 0.02	1.08 ± 0.02	1.09 ± 0.02	1.09 ± 0.01	1.03 ± 0.01	1.03 ± 0.02	1.06 ± 0.02	0.99 ± 0.02	0.96 ± 0.01
27	1.04 ± 0.01	0.84 ± 0.03	0.94 ± 0.04	1.10 ± 0.02	1.10 ± 0.03	1.09 ± 0.01	1.09 ± 0.01	0.99 ± 0.02	0.99 ± 0.01	1.13 ± 0.05	1.05 ± 0.07	1.01 ± 0.07

Table 3.15. Normal Calibration and Internal Standard Calibration Results for Mn ion lines. All results are expressed as mg/L.

Emission Line : Mn II 257.610 nm												
		Internal standards										
#	**none**	**Co 340**	**Co 345**	**Co 237**	**Co 228.6**	**Ni 231**	**Ni 221**	**Ni 341**	**Ni 352**	**Rh 249**	**Rh 343**	**Rh 369**
3	1.00 ± 0.01	1.01± 0.03	1.01 ± 0.01	1.00 ± 0.005	0.99 ± 0.01	1.00 ± 0.01	0.98 ± 0.01	0.99 ± 0.01	1.00 ± 0.01	1.06 ± 0.03	1.04 ± 0.09	1.02 ± 0.07
6	0.94 ± 0.02	0.87 ± 0.03	0.89 ± 0.02	0.96 ± 0.004	0.96 ± 0.004	0.97 ± 0.02	0.96 ± 0.002	0.90 ± 0.04	0.90 ± 0.05	0.69 ± 0.03	0.61 ± 0.08	0.59 ± 0.08
9	0.96 ± 0.01	0.82 ± 0.07	0.89 ± 0.02	0.96 ± 0.01	0.96 ± 0.02	0.94 ± 0.02	0.93 ± 0.03	0.93 ± 0.01	0.93 ± 0.03	1.01 ± 0.01	0.96 ± 0.02	0.95 ± 0.004
12	1.04 ± 0.01	0.90 ± 0.04	1.03 ± 0.01	0.97 ± 0.01	0.94 ± 0.01	0.96 ± 0.01	0.93 ± 0.01	1.03 ± 0.02	1.03 ± 0.02	0.92 ± 0.13	1.01 ± 0.20	0.99 ± 0.17
15	0.96 ± 0.01	0.86 ± 0.03	0.88 ± 0.01	0.96 ± 0.01	0.94 ± 0.01	0.94 ± 0.01	0.93 ± 0.004	0.94 ± 0.01	0.93 ± 0.004	0.94 ± 0.04	0.90 ± 0.05	0.89 ± 0.06
18	0.95 ± 0.02	0.79 ± 0.02	0.86 ± 0.04	0.97 ± 0.01	0.96 ± 0.004	0.96 ± 0.02	0.96 ± 0.003	0.91 ± 0.02	0.91 ± 0.01	0.91 ± 0.02	0.83 ± 0.02	0.80 ± 0.01
21	0.99 ± 0.01	0.83 ± 0.02	0.96 ± 0.02	0.97 ± 0.01	0.96 ± 0.003	0.98 ± 0.01	0.96 ± 0.01	0.96 ± 0.02	0.96 ± 0.01	0.90 ± 0.08	0.98 ± 0.12	0.94 ± 0.13
24	0.95 ± 0.01	0.78 ± 0.02	0.84 ± 0.02	0.97 ± 0.01	0.95 ± 0.01	0.95 ± 0.01	0.95 ± 0.003	0.90 ± 0.002	0.90 ± 0.01	0.92 ± 0.01	0.86 ± 0.02	0.83 ± 0.002
27	0.90 ± 0.005	0.73 ± 0.02	0.81 ± 0.03	0.95 ± 0.03	0.95 ± 0.03	0.94 ± 0.01	0.94 ± 0.01	0.86 ± 0.01	0.86 ± 0.01	0.97 ± 0.04	0.91 ± 0.06	0.87 ± 0.06
Emission Line : Mn II 259.373 nm												
		Internal standards										
#	**none**	**Co 340**	**Co 345**	**Co 237**	**Co 228.6**	**Ni 231**	**Ni 221**	**Ni 341**	**Ni 352**	**Rh 249**	**Rh 343**	**Rh 369**
3	1.01 ± 0.01	1.02 ± 0.03	1.00 ± 0.01	1.01 ± 0.003	0.99 ± 0.01	1.00 ± 0.01	0.98 ± 0.004	1.00 ± 0.01	1.01 ± 0.01	1.06 ± 0.03	1.05 ± 0.09	1.03 ± 0.07
6	0.95 ± 0.02	0.87 ± 0.03	0.88 ± 0.02	0.97 ± 0.05	0.96 ± 0.003	0.96 ± 0.02	0.96 ± 0.001	0.91 ± 0.04	0.90 ± 0.05	0.69 ± 0.03	0.61 ± 0.08	0.59 ± 0.08
9	0.96 ± 0.01	0.82 ± 0.07	0.88 ± 0.02	0.96 ± 0.005	0.96 ± 0.02	0.94 ± 0.02	0.94 ± 0.03	0.93 ± 0.01	0.93 ± 0.02	1.00 ± 0.002	0.96 ± 0.02	0.95 ± 0.01
12	1.05 ± 0.01	0.90 ± 0.04	1.02 ± 0.01	0.98 ± 0.02	0.95 ± 0.02	0.96 ± 0.01	0.94 ± 0.01	1.04 ± 0.02	1.04 ± 0.02	0.92 ± 0.13	1.01 ± 0.21	0.99 ± 0.18
15	0.97 ± 0.01	0.86 ± 0.04	0.87 ± 0.01	0.96 ± 0.01	0.94 ± 0.02	0.93 ± 0.01	0.93 ± 0.001	0.94 ± 0.005	0.93 ± 0.01	0.94 ± 0.04	0.91 ± 0.05	0.90 ± 0.06
18	0.96 ± 0.01	0.79 ± 0.02	0.85 ± 0.04	0.98 ± 0.02	0.97 ± 0.01	0.96 ± 0.02	0.97 ± 0.01	0.91 ± 0.01	0.92 ± 0.01	0.91 ± 0.01	0.83 ± 0.03	0.81 ± 0.004
21	1.00 ± 0.01	0.84 ± 0.02	0.95 ± 0.03	0.98 ± 0.01	0.97 ± 0.01	0.98 ± 0.01	0.97 ± 0.01	0.98 ± 0.02	0.97 ± 0.001	0.91 ± 0.08	0.99 ± 0.13	0.95 ± 0.14
24	0.95 ± 0.01	0.77 ± 0.02	0.83 ± 0.02	0.97 ± 0.01	0.95 ± 0.01	0.94 ± 0.02	0.95 ± 0.05	0.90 ± 0.01	0.90 ± 0.02	0.91 ± 0.02	0.86 ± 0.03	0.83 ± 0.01
27	0.91 ± 0.01	0.74 ± 0.03	0.80 ± 0.03	0.96 ± 0.02	0.96 ± 0.03	0.94 ± 0.01	0.95 ± 0.01	0.87 ± 0.01	0.87 ± 0.004	0.98 ± 0.04	0.92 ± 0.06	0.88 ± 0.06

Table 3.16. Normal Calibration and Internal Standard Calibration Results for Zn atom lines. All results are expressed as mg/L.

Emission Line : Zn I 213.856 nm												
		Internal standards										
#	**none**	**Co 340**	**Co 345**	**Co 237**	**Co 228.6**	**Ni 231**	**Ni 221**	**Ni 341**	**Ni 352**	**Rh 249**	**Rh 343**	**Rh 369**
3	1.00 ± 0.01	1.03 ± 0.01	1.01 ± 0.004	1.02 ± 0.01	1.01 ± 0.01	1.00 ± 0.03	1.00 ± 0.01	1.00 ± 0.02	1.02 ± 0.02	1.06 ± 0.05	1.05 ± 0.11	1.03 ± 0.09
6	0.95 ± 0.03	0.89 ± 0.02	0.90 ± 0.03	0.99 ± 0.02	0.99 ± 0.02	0.97 ± 0.01	0.98 ± 0.01	0.92 ± 0.05	0.92 ± 0.05	0.69 ± 0.02	0.61 ± 0.08	0.59 ± 0.07
9	0.96 ± 0.01	0.83 ± 0.07	0.89 ± 0.02	0.97 ± 0.01	0.97 ± 0.02	0.94 ± 0.02	0.95 ± 0.02	0.93 ± 0.01	0.94 ± 0.03	1.01 ± 0.01	0.97 ± 0.03	0.96 ± 0.003
12	0.96 ± 0.01	0.84 ± 0.02	0.95 ± 0.01	0.91 ± 0.004	0.88 ± 0.001	0.88 ± 0.01	0.87 ± 0.02	0.95 ± 0.004	0.96 ± 0.02	0.85 ± 0.10	0.94 ± 0.17	0.92 ± 0.14
15	0.96 ± 0.01	0.87 ± 0.03	0.88 ± 0.01	0.97 ± 0.01	0.96 ± 0.01	0.93 ± 0.01	0.94 ± 0.01	0.94 ± 0.01	0.94 ± 0.01	0.94 ± 0.05	0.92 ± 0.06	0.91 ± 0.07
18	0.93 ± 0.01	0.78 ± 0.01	0.84 ± 0.03	0.97 ± 0.02	0.97 ± 0.02	0.94 ± 0.01	0.96 ± 0.01	0.89 ± 0.02	0.91 ± 0.004	0.90 ± 0.02	0.83 ± 0.02	0.80 ± 0.01
21	0.91 ± 0.01	0.77 ± 0.02	0.87 ± 0.02	0.91 ± 0.01	0.90 ± 0.01	0.90 ± 0.01	0.90 ± 0.01	0.89 ± 0.02	0.89 ± 0.01	0.83 ± 0.07	0.91 ± 0.12	0.87 ± 0.12
24	0.92 ± 0.01	0.76 ± 0.02	0.81 ± 0.01	0.95 ± 0.004	0.93 ± 0.003	0.92 ± 0.02	0.93 ± 0.01	0.88 ± 0.01	0.89 ± 0.02	0.89 ± 0.02	0.84 ± 0.03	0.81 ± 0.01
27	0.89 ± 0.003	0.73 ± 0.02	0.79 ± 0.03	0.96 ± 0.03	0.96 ± 0.03	0.92 ± 0.01	0.94 ± 0.02	0.85 ± 0.01	0.86 ± 0.01	0.96 ± 0.04	0.91 ± 0.06	0.87 ± 0.06
Emission Line : Zn I 334.502 nm												
		Internal standards										
#	**none**	**Co 340**	**Co 345**	**Co 237**	**Co 228.6**	**Ni 231**	**Ni 221**	**Ni 341**	**Ni 352**	**Rh 249**	**Rh 343**	**Rh 369**
3	1.15 ± 0.18	1.13 ± 0.16	1.14 ± 0.18	1.18 ± 0.17	1.16 ± 0.17	1.17 ± 0.18	1.15 ± 0.16	1.16 ± 0.16	1.16 ± 0.18	1.04	1.14	1.10
6	0.99 ± 0.10	0.87 ± 0.14	0.91 ± 0.09	1.05 ± 0.10	1.05 ± 0.10	1.04 ± 0.11	1.04 ± 0.10	0.98 ± 0.07	0.92 ± 0.09	0.65 ± 0.07	0.61 ± 0.14	0.58 ± 0.13
9	1.17 ± 0.18	1.00 ± 0.17	1.07 ± 0.17	1.18 ± 0.16	1.20 ± 0.15	1.15 ± 0.16	1.17 ± 0.16	1.14 ± 0.16	1.11 ± 0.22	1.14 ± 0.19	1.16 ± 0.20	1.13 ± 0.16
12	1.07 ± 0.39	0.88 ± 0.38	1.04 ± 0.38	1.03 ± 0.33	0.99 ± 0.33	0.99 ± 0.31	0.98 ± 0.31	1.08 ± 0.36	1.05 ± 0.39	1.36	1.66	1.59
15	1.01 ± 0.16	0.95 ± 0.14	0.97 ± 0.08	1.04 ± 0.15	1.03 ± 0.15	1.00 ± 0.13	1.00 ± 0.14	1.02 ± 0.14	0.96 ± 0.15	0.89 ± 0.17	0.91 ± 0.15	0.89 ± 0.14
18	1.19 ± 0.32	1.12 ± 0.38	1.26 ± 0.46	1.45 ± 0.39	1.44 ± 0.40	1.40 ± 0.42	1.43 ± 0.40	1.35 ± 0.39	1.35 ± 0.44	1.05 ± 0.31	1.00 ± 0.24	0.97 ± 0.27
21	1.22 ± 0.07	1.05 ± 0.16	1.24 ± 0.19	1.29 ± 0.13	1.28 ± 0.14	1.28 ± 0.15	1.27 ± 0.15	1.28 ± 0.14	1.26 ± 0.15	1.12 ± 0.32	1.31 ± 0.41	1.25 ± 0.41
24	1.23 ± 0.16	1.02 ± 0.15	1.13 ± 0.18	1.34 ± 0.18	1.32 ± 0.17	1.30 ± 0.15	1.32 ± 0.16	1.25 ± 0.15	1.24 ± 0.16	1.26 ± 0.07	1.25 ± 0.06	1.19 ± 0.08
27	1.18 ± 0.03	0.95 ± 0.07	1.07 ± 0.14	1.32 ± 0.12	1.33 ± 0.12	1.28 ± 0.10	1.30 ± 0.10	1.19 ± 0.10	1.17 ± 0.11	1.28 ± 0.21	1.26 ± 0.23	1.20 ± 0.23

Table 3.17. Normal Calibration and Internal Standard Calibration Results for Zn ion lines. All results are expressed as mg/L.

Emission Line : Zn II 202.551 nm												
		Internal standards										
#	**none**	**Co 340**	**Co 345**	**Co 237**	**Co 228.6**	**Ni 231**	**Ni 221**	**Ni 341**	**Ni 352**	**Rh 249**	**Rh 343**	**Rh 369**
3	1.00 ± 0.01	1.03 ± 0.01	1.01 ± 0.01	1.02 ± 0.01	1.01 ± 0.01	1.00 ± 0.03	1.00 ± 0.01	0.99 ± 0.01	1.00 ± 0.02	1.06 ± 0.04	1.05 ± 0.10	1.03 ± 0.08
6	0.99 ± 0.06	0.92 ± 0.04	0.93 ± 0.06	1.03 ± 0.04	1.02 ± 0.04	1.01 ± 0.05	1.02 ± 0.04	0.95 ± 0.08	0.94 ± 0.08	0.71 ± 0.05	0.63 ± 0.10	0.61 ± 0.10
9	1.10 ± 0.05	0.95 ± 0.08	1.03 ± 0.05	1.12 ± 0.05	1.12 ± 0.04	1.08 ± 0.05	1.09 ± 0.05	1.07 ± 0.06	1.06 ± 0.08	1.15 ± 0.08	1.11 ± 0.09	1.10 ± 0.06
12	1.17 ± 0.03	1.02 ± 0.01	1.16 ± 0.03	1.11 ± 0.02	1.07 ± 0.02	1.07 ± 0.03	1.06 ± 0.03	1.16 ± 0.02	1.15 ± 0.03	1.03 ± 0.10	1.14 ± 0.18	1.11 ± 0.15
15	1.18 ± 0.01	1.06 ± 0.04	1.07 ± 0.01	1.19 ± 0.01	1.17 ± 0.02	1.14 ± 0.01	1.15 ± 0.0003	1.15 ± 0.005	1.12 ± 0.01	1.15 ± 0.05	1.12 ± 0.06	1.11 ± 0.07
18	1.11 ± 0.01	0.93 ± 0.01	1.01 ± 0.04	1.16 ± 0.02	1.15 ± 0.02	1.12 ± 0.01	1.14 ± 0.01	1.07 ± 0.02	1.06 ± 0.004	1.07 ± 0.03	0.99 ± 0.02	0.96 ± 0.01
21	1.14 ± 0.03	0.97 ± 0.04	1.09 ± 0.05	1.13 ± 0.03	1.12 ± 0.03	1.12 ± 0.04	1.12 ± 0.04	1.11 ± 0.04	1.09 ± 0.02	1.03 ± 0.12	1.13 ± 0.18	1.09 ± 0.19
24	1.16 ± 0.01	0.96 ± 0.003	1.03 ± 0.02	1.20 ± 0.03	1.18 ± 0.02	1.16 ± 0.02	1.18 ± 0.02	1.11 ± 0.02	1.10 ± 0.02	1.12 ± 0.001	1.06 ± 0.01	1.02 ± 0.01
27	1.11 ± 0.01	0.91 ± 0.02	0.99 ± 0.05	1.19 ± 0.04	1.19 ± 0.05	1.15 ± 0.02	1.17 ± 0.03	1.05 ± 0.02	1.05 ± 0.02	1.19 ± 0.06	1.13 ± 0.09	1.08 ± 0.09
Emission Line : Zn II 206.200 nm												
		Internal standards										
#	**none**	**Co 340**	**Co 345**	**Co 237**	**Co 228.6**	**Ni 231**	**Ni 221**	**Ni 341**	**Ni 352**	**Rh 249**	**Rh 343**	**Rh 369**
3	1.01 ± 0.002	1.02 ± 0.01	1.02 ± 0.002	1.01 ± 0.01	1.00 ± 0.01	0.99 ± 0.02	0.99 ± 0.01	1.00 ± 0.01	1.01 ± 0.02	1.07 ± 0.04	1.05 ± 0.10	1.03 ± 0.08
6	1.03 ± 0.06	0.94 ± 0.03	0.97 ± 0.06	1.05 ± 0.04	1.04 ± 0.04	1.04 ± 0.04	1.04 ± 0.04	0.99 ± 0.08	0.98 ± 0.09	0.74 ± 0.04	0.65 ± 0.10	0.62 ± 0.09
9	1.09 ± 0.03	0.93 ± 0.06	1.02 ± 0.03	1.09 ± 0.04	1.09 ± 0.02	1.05 ± 0.03	1.06 ± 0.03	1.06 ± 0.05	1.06 ± 0.06	1.13 ± 0.04	1.08 ± 0.06	1.06 ± 0.03
12	1.16 ± 0.02	1.00 ± 0.02	1.15 ± 0.01	1.08 ± 0.01	1.04 ± 0.01	1.04 ± 0.02	1.04 ± 0.02	1.14 ± 0.01	1.15 ± 0.02	1.02 ± 0.12	1.11 ± 0.20	1.09 ± 0.16
15	1.15 ± 0.02	1.02 ± 0.04	1.05 ± 0.02	1.14 ± 0.01	1.12 ± 0.02	1.09 ± 0.02	1.10 ± 0.01	1.12 ± 0.02	1.10 ± 0.02	1.12 ± 0.07	1.08 ± 0.08	1.06 ± 0.09
18	1.10 ± 0.02	0.91 ± 0.02	0.99 ± 0.05	1.13 ± 0.01	1.12 ± 0.01	1.09 ± 0.02	1.11 ± 0.01	1.05 ± 0.02	1.05 ± 0.01	1.05 ± 0.03	0.96 ± 0.02	0.93 ± 0.01
21	1.09 ± 0.01	0.91 ± 0.02	1.05 ± 0.03	1.07 ± 0.01	1.06 ± 0.01	1.06 ± 0.01	1.06 ± 0.01	1.06 ± 0.02	1.06 ± 0.001	0.99 ± 0.10	1.08 ± 0.14	1.03 ± 0.15
24	1.11 ± 0.01	0.90 ± 0.02	0.98 ± 0.02	1.13 ± 0.003	1.11 ± 0.004	1.09 ± 0.02	1.11 ± 0.01	1.06 ± 0.01	1.06 ± 0.02	1.07 ± 0.03	1.00 ± 0.03	0.97 ± 0.02
27	1.08 ± 0.02	0.87 ± 0.04	0.96 ± 0.04	1.13 ± 0.02	1.14 ± 0.02	1.10 ± 0.01	1.12 ± 0.005	1.02 ± 0.02	1.03 ± 0.01	1.17 ± 0.04	1.09 ± 0.07	1.04 ± 0.07

3.3.3.1. Test for Significance

Further data manipulation was warranted to determine the level of significant improvement for our results. In order to only consider data that was well above the limit of detection for our ICP-OES instrument, only data from solutions containing 1 mg/L were further considered in our assessments of whether or not significant improvements had indeed obtained. Furthermore, to make the data set more manageable, firstly for the normal calibration results the values that were outside of the 5% range of 1 mg/L (between the 0.95 and 1.05 mg/L) were sorted out and these were considered as the samples requiring improvement. Then the internal standard calibration results were checked only for the ones that had a problem with normal calibration. Concentration values within this 5% range were generally assumed to be reliable (within experimental error) and therefore did not warrant correction using internal standardization.

In order to determine whether these improvements were significant or not a test for comparison (Student's t test) of the two means obtained from the normal calibration and internal standard calibration was applied.

Standard equations for t-test in the comparison of two means are as follows:

$$t = \frac{\left|\bar{x}_1 - \bar{x}_2\right|}{s_{pooled}} \sqrt{\frac{n_1 n_2}{n_1 + n_2}} \tag{3.7}$$

$$s_{pooled} = \sqrt{\frac{s_1^2 (n_1 - 1) + s_2^2 (n_2 - 1)}{n_1 + n_2 - 2}} \tag{3.8}$$

Here x_1 and x_2 are defined as the averages for two sets of data consisting of n_1 and n_2 measurements with standard deviations s_1 and s_2. For our case x_1 values were taken as averages from the normal calibration values and x_2 values were taken as averages from the corrected values with internal standardization, s_1 and s_2 are taken as the standard deviations from normal calibration and corrected concentrations.

According to this test, if the calculated *t* is greater than the tabulated *t* at the considered confidence level (95% or 90%), the two results are considered to be different, i.e. a significant improvement thus observed with the use of internal

standardization. Comparison was done according to the tabulated t values for $n_1 + n_2 - 2$ (i.e. 4) degrees of freedom which is 2.132 at the 90% confidence level.

In the Tables through 3.16 and 3.27, these t-tests applied for the selected samples are illustrated. “NC” stands for the value obtained by the **n**ormal **c**alibration in mg/L and the values that fall in the range of 5% (0.95 – 1.05 mg/L) in some cases the values that are in the 2% range (0.98 – 1.02 mg/L) were also checked for the significance of improvement. “ND” is used to indicate that the results obtained by internal standardization are not different from the normal calibration values and hence no significant improvement was obtained so these values are represented as ND-NI (no difference-no improvement). Similarly, “D” indicates that the values obtained by normal calibration and internal standardization were significantly different and an improvement had been achieved with the proposed internal standards therefore “DI” sign is used for these values.

3.3.3.2. Internal Standardization for the Determination of Cd

Tables 3.18 - 3.21 show the t-test values for the Cd lines.

Table 3.18. t-test values for Cd line at 326.106 nm (all concentrations are in mg/L)

Emission line: Cd I 326.106 nm												
	NC	**Co 340**	**Co 345**	**Co 237**	**Co 228.6**	**Ni 231**	**Ni 221**	**Ni 341**	**Ni 352**	**Rh 249**	**Rh 343**	**Rh 369**
Sample 9	**0.93**			0.95	0.99							
t_{calc}				0.34	1.36							
$t_{tab\ (4)}$ 90%				2.13	2.13							
result				NDNI	NDNI							
Sample 12	**0.81**		0.88					0.87	0.86			
t_{calc}			0.40					0.39	0.29			
$t_{tab\ (4)}$ 90%			2.13					2.13	2.13			
result			NDNI					NDNI	NDNI			
Sample 18	**0.81**			0.91	0.90		0.87					
t_{calc}				1.96	2.06		1.42					
$t_{tab\ (4)}$ 90%				2.13	2.13		2.13					
result				NDNI	NDNI	NDNI	NDNI					
Sample 24	**0.95**			1.00	0.98	0.96	0.96	0.96	0.96			
t_{calc}				0.38	0.23	0.11	0.11	0.10	0.05			
$t_{tab\ (4)}$ 90%				2.13	2.13	2.13	2.13	2.13	2.13			
result				NDNI	NDNI	NDNI	NDNI	NDNI	NDNI			
Sample 27	**0.79**			**0.87**	0.87		0.83					
t_{calc}				**2.19**	2.12		1.53					
$t_{tab\ (4)}$ 90%				**2.13**	2.13	2.13	2.13					
result				**DI**								

Table 3.19. t-test values for Cd line at 228.802 nm (all concentrations are in mg/L)

Emission line: Cd I 228.802 nm												
	NC	**Co 340**	**Co 345**	**Co 237**	**Co 228.6**	**Ni 231**	**Ni 221**	**Ni 341**	**Ni 352**	**Rh 249**	**Rh 343**	**Rh 369**
Sample 24	**0.94**			**0.96**	0.95		0.95					
t_{calc}				**3.98**	2.02		1.70					
$t_{tab\ (4)}$ 90%				**2.13**	2.13		2.13					
result				**DI**	NDNI		NDNI					
Sample 27	**0.91**			**0.97**	**0.97**		**0.96**			**0.94**		
t_{calc}				**2.76**	**2.53**		**2.50**			**2.46**		
$t_{tab\ (4)}$ 90%				**2.13**	**2.13**		**2.13**			**2.13**		
result				**DI**	**DI**		**DI**			**DI**		

Table 3.20. t-test values for Cd line at 226.502 nm (all concentrations are in mg/L)

Emission line: Cd II 226.502 nm												
	NC	**Co 340**	**Co 345**	**Co 237**	**Co 228.6**	**Ni 231**	**Ni 221**	**Ni 341**	**Ni 352**	**Rh 249**	**Rh 343**	**Rh 369**
Sample 6	**0.97**			1.00	0.98		0.99					
t_{calc}				1.52	0.81		0.95					
$t_{tab\ (4)}$ 90%				2.13	2.13		2.13					
result				NDNI	NDNI		NDNI					
Sample 12	**1.07**		**1.04**	**1.00**	**0.96**	**0.96**	**0.96**	1.06	**1.06**		1.01	0.99
t_{calc}			**6.82**	**11.00**	**14.13**	**22.77**	**16.66**	1.38	**2.23**		0.58	0.93
$t_{tab\ (4)}$ 90%			**2.13**	**2.13**	**2.13**	**2.13**	**2.13**	2.13	**2.13**		2.13	2.13
result			**DI**	**DI**	**DI**	**DI**	**DI**	NDNI	**DI**		NDNI	NDNI
Sample 15	**1.03**				**1.00**	**0.98**	**0.99**	1.00	**0.98**	**0.96**		
t_{calc}					**5.55**	**5.94**	**3.42**	2.11	**4.55**	**2.24**		
$t_{tab\ (4)}$ 90%					**2.13**	**2.13**	**2.13**	2.13	**2.13**	**2.13**		
result					**DI**	**DI**	**DI**	NDNI	**DI**	**DI**		
Sample 27	**0.95**			**1.01**	1.00	0.97	**0.99**			**0.98**		
t_{calc}				**2.91**	2.12	1.25	**2.17**			**2.39**		
$t_{tab\ (4)}$ 90%				**2.13**	2.13	2.13	**2.13**			**2.13**		
result				**DI**	NDNI	NDNI	**DI**			**DI**		

Table 3.21. t-test values for Cd line at 214.438 nm (all concentrations are in mg/L)

Emission line: Cd II 214.438 nm												
	NC	**Co 340**	**Co 345**	**Co 237**	**Co 228.6**	**Ni 231**	**Ni 221**	**Ni 341**	**Ni 352**	**Rh 249**	**Rh 343**	**Rh 369**
Sample 9	**1.05**					**1.01**			1.02			**1.01**
t_{calc}						**5.85**			1.68			**11.51**
$t_{tab\ (4)}$ 90%						**2.13**			2.13			**2.13**
result						**DI**			NDNI			**DI**
Sample 12	**1.11**	**0.95**	**1.08**	**1.04**	**1.00**	**1.00**	**1.00**				1.05	1.03
t_{calc}		**8.30**	**8.92**	**21.64**	**25.18**	**22.69**	**13.37**				0.48	0.64
$t_{tab\ (4)}$ 90%		**2.13**	**2.13**	**2.13**	**2.13**	**2.13**	**2.13**				2.13	2.13
result		**DI**	**DI**	**DI**	**DI**	**DI**	**DI**				NDNI	NDNI
Sample 15	**1.08**	**0.96**	**0.96**		**1.05**	**1.03**	**1.04**	**1.05**	**1.03**	**1.01**	**0.98**	**0.97**
t_{calc}		**6.96**	**18.39**		**5.51**	**10.54**	**4.28**	**2.90**	**6.92**	**2.82**	**2.81**	**2.85**
$t_{tab\ (4)}$ 90%		**2.13**	**2.13**		**2.13**	**2.13**	**2.13**	**2.13**	**2.13**	**2.13**	**2.13**	**2.13**
result		**DI**	**DI**		**DI**	**DI**	**DI**	**DI**	**DI**	**DI**	**DI**	**DI**
Sample 18	**1.05**							**1.00**	**1.00**			
t_{calc}								**2.52**	**3.52**			
$t_{tab\ (4)}$ 90%								**2.13**	**2.13**			
result								**DI**	**DI**			
Sample 21	**1.05**		**0.99**		**1.01**	**1.01**	**1.02**	**1.02**	**1.01**		1.01	
t_{calc}			**4.77**		**5.23**	**5.67**	**4.83**	**2.56**	**3.63**		0.52	
$t_{tab\ (4)}$ 90%			**2.13**		**2.13**	**2.13**	**2.13**	**2.13**	**2.13**		2.13	
result			**DI**		**DI**	**DI**	**DI**	**DI**	**DI**		NDNI	
Sample 24	**1.06**					1.04		**1.02**	**1.01**	**0.99**	**0.95**	
t_{calc}						1.13		**3.28**	**3.00**	**3.54**	**5.12**	
$t_{tab\ (4)}$ 90%						2.13		**2.13**	**2.13**	**2.13**	**2.13**	
result						NDNI		**DI**	**DI**	**DI**	**DI**	
Sample 27	**1.03**								**0.98**	0.99		
t_{calc}									**4.00**	1.79		
$t_{tab\ (4)}$ 90%									**2.13**	2.13		
result									**DI**	NDNI		

When the normal and internal standard calibration Tables for the Cd lines were examined, it is observed that values closer to 1 mg/L are obtained when normal calibration except for the Cd 326 atom line. By considering the t-test results obtained it can be said that, internal standardization for the Cd 326 line did not work very well and only the Co 237 ion line was successful for correcting for the interference on sample 27 (25% acid, 0.3% salt). For the Cd I 228 line, the ion lines of Co at 237 nm and 228.6 nm, Ni at 221 nm and Rh at 249 nm showed significant improvements for samples 24

(25% acid, 0.1% salt) and 27 (25% acid, 0.3% salt) but the results for sample 21 (25% acid, no salt) couldn't be corrected. For the Cd II 226 line, all proposed internal standards except the atom lines of Co at 340 nm, Ni at 341 nm, and of Rh at both 343 nm and at 369 nm improved the measured concentration values for sample 12 (12% acid, no salt) significantly. The other concentrations which were in the 5% determined range but outside of 2% range (i.e., samples 15 (12% acid, 0.1% salt) and 27 (25% acid, 0.3% salt) with the concentrations of 1.03 and 0.95 mg/L respectively) were also improved by the Co II 237, Co II 228.6, Ni II 231, Ni II 221, Ni I 352 and Rh II 249 lines. For the Cd 214 ion line, normal calibration values were higher than the true value especially in the presence of salt and acid and all chosen lines helped to correct these positive errors for samples 12 (12% acid, no salt), 15 (12% acid, 0.1% salt) and 24 (25% acid, 0.1% salt). There were also some significant improvements for the concentration values that were within 5 and 2% determined range for samples 9 (no acid, 0.3% salt), 18 (12% acid, 0.3% salt), 21 (25% acid, no salt) and 27 (25% acid, 0.3% salt).

In summary, for Cd it can be seen that using the Co atom lines at 340 and 345 nm and Rh atom lines at 343 and 369 nm for internal standard correction did not show much improvement but the Co ion lines at 237 and 228.6 nm and Ni lines at 221, 231 and 352 nm and the Rh ion line at 249 nm were successful in correcting for acid/salt interferences when improvement was needed. The greatest improvements were seen for the Cd 226 and Cd 214 ion lines.

3.3.3.3. Internal Standardization for the Determination of Mn

Tables 3.22 - 3.25 show the t-test values to determine the significance of internal standard corrections for the Mn lines.

Table 3.22. t-test values for the Mn line at 279.482 nm (all concentrations are in mg/L)

Emission line: Mn I 279.482 nm												
	NC	**Co 340**	**Co 345**	**Co 237**	**Co 228.6**	**Ni 231**	**Ni 221**	**Ni 341**	**Ni 352**	**Rh 249**	**Rh 343**	**Rh 369**
Sample 6	**1.07**	**0.98**	**0.99**					**1.01**	**1.01**			
t_{calc}		**3.00**	**5.67**					**2.58**	**2.70**			
$t_{tab\ (4)}$ 90%		**2.13**	**2.13**					**2.13**	**2.13**			
result		**DI**	**DI**					**DI**	**DI**			
Sample 9	**1.07**		**0.98**			**1.03**	1.04	**1.03**	**1.04**			
t_{calc}			**4.50**			**2.15**	1.15	**2.77**	**2.21**			
$t_{tab\ (4)}$ 90%			**2.13**			**2.13**	2.13	**2.13**	**2.13**			
result			**DI**			**DI**	NDNI	**DI**	**DI**			
Sample 18	**1.06**		**0.95**			1.05		**1.01**	**1.02**	**1.01**		
t_{calc}			**4.96**			1.91		**5.70**	**7.52**	**4.16**		
$t_{tab\ (4)}$ 90%			**2.13**			2.13		**2.13**	**2.13**	**2.13**		
result			**DI**			NDNI		**DI**	**DI**	**DI**		

Table 3.23. t-test values for the Mn line at 403.076 nm (all concentrations are in mg/L)

Emission line: Mn I 403.076 nm												
	NC	**Co 340**	**Co 345**	**Co 237**	**Co 228.6**	**Ni 231**	**Ni 221**	**Ni 341**	**Ni 352**	**Rh 249**	**Rh 343**	**Rh 369**
Sample 9	**1.08**		**1.01**				1.05	1.04	**1.04**			
t_{calc}			**2.78**				1.01	1.71	**2.18**			
$t_{tab\ (4)}$ 90%			**2.13**				2.13	2.13	**2.13**			
result			**DI**				NDNI	NDNI	**DI**			
Sample15	**1.09**	**0.97**	**1.00**				**1.05**		**1.05**		**1.01**	**1.00**
t_{calc}		**6.04**	**11.95**				**3.97**		**5.48**		**2.51**	**2.53**
$t_{tab\ (4)}$ 90%		**2.13**	**2.13**				**2.13**		**2.13**		**2.13**	**2.13**
result		**DI**	**DI**				**DI**		**DI**		**DI**	**DI**
Sample 18	**1.08**		**0.98**					**1.03**	**1.03**	**1.04**		
t_{calc}			**3.60**					**6.12**	**4.12**	**5.49**		
$t_{tab\ (4)}$ 90%			**2.13**					**2.13**	**2.13**	**2.13**		
result			**DI**					**DI**	**DI**	**DI**		
Sample 24	**1.08**		**0.97**					**1.03**	**1.03**		**0.99**	**0.96**
t_{calc}			**5.01**					**3.39**	**3.18**		**5.06**	**9.53**
$t_{tab\ (4)}$ 90%			**2.13**					**2.13**	**2.13**		**2.13**	**2.13**
result			**DI**					**DI**	**DI**		**DI**	**DI**
Sample 27	**1.04**							**0.99**	**0.99**			1.01
t_{calc}								**4.15**	**5.31**			0.84
$t_{tab\ (4)}$ 90%								**2.13**	**2.13**			2.13
result								**DI**	**DI**			NDNI

Table 3.24. t-test values for the Mn line at 257.610 nm (all concentrations are in mg/L)

Emission line: Mn II 257.610 nm												
	NC	**Co 340**	**Co 345**	**Co 237**	**Co 228.6**	**Ni 231**	**Ni 221**	**Ni 341**	**Ni 352**	**Rh 249**	**Rh 343**	**Rh 369**
Sample 6	**0.94**			0.96	0.96	0.97	0.96					
t_{calc}				1.77	1.40	1.68	1.27					
$t_{tab\ (4)}$ 90%				2.13	2.13	2.13	2.13					
result				NDNI	NDNI	NDNI	NDNI					
Sample 9	**0.96**									**1.01**		
t_{calc}										**5.86**		
$t_{tab\ (4)}$ 90%										**2.13**		
result										**DI**		
Sample 12	**1.04**										1.01	0.99
t_{calc}											0.31	0.59
$t_{tab\ (4)}$ 90%											2.13	2.13
result											NDNI	NDNI
Sample 18	**0.95**			**0.97**								
t_{calc}				**2.18**								
$t_{tab\ (4)}$ 90%				**2.13**								
result				**DI**								
Sample 24	**0.95**			0.97								
t_{calc}				1.97								
$t_{tab\ (4)}$ 90%				2.13								
result				NDNI								
Sample 27	**0.90**			**0.95**	**0.95**	**0.94**	**0.94**			**0.97**		
t_{calc}				**3.19**	**2.76**	**7.48**	**5.57**			**2.85**		
$t_{tab\ (4)}$ 90%				**2.13**	**2.13**	**2.13**	**2.13**			**2.13**		
result				**DI**	**DI**	**DI**	**DI**			**DI**		

Table 3.25. t-test values for the Mn line at 259.373 nm (all concentrations are in mg/L)

Emission line: Mn II 259.373 nm												
	NC	**Co 340**	**Co 345**	**Co 237**	**Co 228.6**	**Ni 231**	**Ni 221**	**Ni 341**	**Ni 352**	**Rh 249**	**Rh 343**	**Rh 369**
Sample 6	**0.95**			0.97								
t_{calc}				1.60								
$t_{tab\ (4)}$ 90%				2.13								
result				NDNI								
Sample 9	**0.96**									**1.00**		
T calc										**5.66**		
T tab (..) 90%										**2.13**		
comment										**DI**		
Sample 12	**1.05**		**1.02**	**0.98**							1.01	0.99
t_{calc}			**2.89**	**5.99**							0.32	0.57
$t_{tab\ (4)}$ 90%			**2.13**	**2.13**							2.13	2.13
result			**DI**	**DI**							NDNI	NDNI
Sample 18	**0.96**			0.98	0.97		0.97					
t_{calc}				1.75	1.81		1.19					
$t_{tab\ (4)}$ 90%				2.13	2.13		2.13					
result				NDNI	NDNI		NDNI					
Sample 24	**0.95**			**0.97**								
t_{calc}				**2.22**								
$t_{tab\ (4)}$ 90%				**2.13**								
result				**DI**								
Sample 27	**0.91**			**0.96**	**0.96**		**0.95**			**0.98**		
t_{calc}				**3.63**	**3.07**		**6.36**			**2.85**		
$t_{tab\ (4)}$ 90%				**2.13**	**2.13**		**2.13**			**2.13**		
result				**DI**	**DI**		**DI**			**DI**		

For the Mn atom line at 279 nm, using the atom lines for Co at 340 and 345 nm and for Ni at 341 and at 352 nm were successful as expected from the closeness of these two lines in the PCA plots. Although they are located very far from each other in the score plot, the Ni II 231 line was also helpful for correcting the interferences for this line. The Rh II 249 line worked only for correction in the determination of Mn in sample 18 (12% acid, 0.3% salt). The inaccuracies for samples 12 (12% acid, no salt) and 21 (25% acid, no salt) could not be corrected by using any of these internal standards.

For the other selected Mn atom line at 403 nm, the values obtained by normal calibration were outside of the determined range and significant improvements were

obtained by using the Co I 340, Co I 345, Ni II 221, Ni I 341, Ni I 352, Rh II 249, Rh I 343, and Rh I 369 nm lines as the internal standards. The problematic samples 12 (12% acid, no salt) and 21 (25% acid, no salt) could not be corrected by using these proposed internal standards. The concentration values for sample 27 which was outside of the 2% accepted range was also corrected by the Ni atom lines at 341 nm and 352 nm. The normal calibration results for the Mn 257 and 259 ion lines were already within the 5% accepted range except for samples 6 (no acid, 0.1% salt) and 27 (25% acid, 0.3% salt) showing no need for internal standard correction. The Co ion lines (237 and 228.6 nm), the Ni ion line at 221 nm and the Rh ion line at 249 nm proved useful for correction of quantitative results for Mn ion lines analyses. For the Mn 257 nm line, the Ni 231 nm ion line (both showing similarity according to the score plot) also proved to be useful. In addition, the concentration results of samples between 9 and 24 were between the 5 and 2% determined range for Mn ion lines. Among these samples significant improvements were achieved for sample 9 (no acid, 0.3%salt) with the Rh II 249 line. For the Mn 257 line, the Co 237 ion line was successful in correcting the inaccuracy of sample 18 (12% acid, 0.3% salt). For the Mn 259 line, the Co II 237 and Co I 345 lines helped to improve the determined values for samples 12 (12% acid, no salt) and 24 (25% acid, 0.1% salt).

Among the selected internal standards, Co I 345 nm, Ni I 341 nm and Ni I 352 nm were successful in particular for the Mn atom lines, Co II 237 was successful only for Mn ion lines, and Rh II 249 showed significant improvements both for the Mn atom and ion lines.

3.3.3.4. Internal Standardization for the Determination of Zn

Tables 3.26 - 3.29 illustrate the t-tests applied for the Zn lines.

Table 3.26. t-test values for the Zn line at 213.856 nm (all concentrations are in mg/L)

Emission line: Zn I 213.856 nm												
	NC	**Co 340**	**Co 345**	**Co 237**	**Co 228.6**	**Ni 231**	**Ni 221**	**Ni 341**	**Ni 352**	**Rh 249**	**Rh 343**	**Rh 369**
Sample 6	**0.95**			0.99	0.99	0.97	0.98					
t_{calc}				2.03	1.93	1.32	1.56					
$t_{tab\ (4)}$ 90%				2.13	2.13	2.13	2.13					
result				NDNI	NDNI	NDNI	NDNI					
Sample 9	**0.96**			0.97	0.97					**1.01**	0.97	
t_{calc}				1.61	1.46					**4.82**	0.92	
$t_{tab\ (4)}$ 90%				2.13	2.13					**2.13**	2.13	
result				NDNI	NDNI					**DI**	NDNI	
Sample 15	**0.96**			0.97								
t_{calc}				2.10								
$t_{tab\ (4)}$ 90%				2.13								
result				NDNI								
Sample 18	**0.93**			**0.97**	**0.97**		**0.96**					
t_{calc}				**3.36**	**3.17**		**2.98**					
$t_{tab\ (4)}$ 90%				**2.13**	**2.13**		**2.13**					
result				**DI**	**DI**		**DI**					
Sample 24	**0.92**			**0.95**								
t_{calc}				**6.55**								
$t_{tab\ (4)}$ 90%				**2.13**								
result				**DI**								
Sample 27	**0.89**			**0.96**	**0.96**		**0.94**			**0.96**		
t_{calc}				**3.81**	**3.35**		**5.57**			**3.23**		
$t_{tab\ (4)}$ 90%				**2.13**	**2.13**		**2.13**			**2.13**		
result				**DI**	**DI**		**DI**			**DI**		

Table 3.27. t-test values for the Zn line at 334.502 nm (all concentrations are in mg/L)

Emission line: Zn I 334.502 nm												
	NC	**Co 340**	**Co 345**	**Co 237**	**Co 228.6**	**Ni 231**	**Ni 221**	**Ni 341**	**Ni 352**	**Rh 249**	**Rh 343**	**Rh 369**
Sample 9	**1.17**	1.00										
t_{calc}		1.20										
$t_{tab\ (4)}$ 90%		2.13										
result		NDNI										
Sample 12	**1.07**		1.04	1.03	0.99	0.99	0.98		1.05			
t_{calc}			0.09	0.15	0.27	0.28	0.33		0.06			
$t_{tab\ (4)}$ 90%			2.13	2.13	2.13	2.13	2.13		2.13			
result			NDNI	NDNI	NDNI	NDNI	NDNI	NDNI	NDNI			
Sample 18	**1.19**									1.05	1.00	0.97
t_{calc}										0.53	0.80	0.89
$t_{tab\ (4)}$ 90%										2.13	2.13	2.13
result										NDNI	NDNI	NDNI
Sample 21	**1.22**	1.05										
t_{calc}		1.62										
$t_{tab\ (4)}$ 90%		2.13										
result		NDNI										
Sample 24	**1.23**	1.02										
t_{calc}		1.62										
$t_{tab\ (4)}$ 90%		2.13										
result		NDNI										
Sample 27	**1.18**	**0.95**										
t_{calc}		**5.24**										
$t_{tab\ (4)}$ 90%		**2.13**										
result		**DI**										

Table 3.28. t-test values for the Zn line at 202.551 nm (all concentrations are in mg/L)

Emission line: Zn II 202.551 nm												
	NC	**Co 340**	**Co 345**	**Co 237**	**Co 228.6**	**Ni 231**	**Ni 221**	**Ni 341**	**Ni 352**	**Rh 249**	**Rh 343**	**Rh 369**
Sample 9	**1.10**	**0.95**	1.03									
t_{calc}		**2.71**	1.94									
$t_{tab\ (4)}$ 90%		**2.13**	2.13									
result		**DI**	NDNI									
Sample 12	**1.17**	**1.02**								**1.03**		
t_{calc}		**8.47**								**2.29**		
$t_{tab\ (4)}$ 90%		**2.13**								**2.13**		
result		**DI**								**DI**		
Sample 18	**1.11**		**1.01**								**0.99**	**0.96**
t_{calc}			**4.66**								**8.24**	**18.32**
$t_{tab\ (4)}$ 90%			**2.13**								**2.13**	**2.13**
result			**DI**								**DI**	**DI**
Sample 21	**1.14**	**0.97**								1.03		
t_{calc}		**5.84**								1.49		
$t_{tab\ (4)}$ 90%		**2.13**								2.13		
result		**DI**								NDNI		
Sample 24	**1.16**	**0.96**	**1.03**									**1.02**
t_{calc}		**27.30**	**11.21**									**13.06**
$t_{tab\ (4)}$ 90%		**2.13**	**2.13**									**2.13**
result		**DI**	**DI**									**DI**
Sample 27	**1.11**		**0.99**					**1.05**	**1.05**			
t_{calc}			**4.26**					**3.95**	**4.21**			
$t_{tab\ (4)}$ 90%			**2.13**					**2.13**	**2.13**			
result			**DI**					**DI**	**DI**			

Table 3.29. t-test values for the Zn line at 206.200 nm (all concentrations are in mg/L)

Emission line: Zn II 206.200 nm												
	NC	**Co 340**	**Co 345**	**Co 237**	**Co 228.6**	**Ni 231**	**Ni 221**	**Ni 341**	**Ni 352**	**Rh 249**	**Rh 343**	**Rh 369**
Sample 6	**1.03**							0.99	0.98			
t_{calc}								0.72	0.82			
$t_{tab\ (4)}$ 90%								2.13	2.13			
result								NDNI	NDNI			
Sample 9	**1.09**		**1.02**			1.05						
t_{calc}			**2.92**			1.55						
$t_{tab\ (4)}$ 90%			**2.13**			2.13						
result			**DI**			NDNI						
Sample 12	**1.16**	**1.00**			**1.04**	**1.04**	**1.04**			**1.02**		
t_{calc}		**9.67**			**11.78**	**8.72**	**8.06**			**2.09**		
$t_{tab\ (4)}$ 90%		**2.13**			**2.13**	**2.13**	**2.13**			**2.13**		
result		**DI**			**DI**	**DI**	**DI**			**NDNI**		
Sample 15	**1.15**	**1.02**	**1.05**									
t_{calc}		**5.60**	**7.17**									
$t_{tab\ (4)}$ 90%		**2.13**	**2.13**									
result		**DI**	**DI**									
Sample 18	**1.10**		**0.99**					**1.05**	**1.05**	**1.05**	**0.96**	
t_{calc}			**3.65**					**3.31**	**4.48**	**2.83**	**8.77**	
$t_{tab\ (4)}$ 90%			**2.13**					**2.13**	**2.13**	**2.13**	**2.13**	
result			**DI**					**DI**	**DI**	**DI**	**DI**	
Sample 21	**1.09**		**1.05**							0.99		1.03
t_{calc}			**2.14**							1.82		0.69
$t_{tab\ (4)}$ 90%			**2.13**							2.13		2.13
result			**DI**							NDNI		NDNI
Sample 24	**1.11**		**0.98**								**1.00**	**0.97**
t_{calc}			**10.02**								**5.10**	**12.46**
$t_{tab\ (4)}$ 90%			**2.13**								**2.13**	**2.13**
result			**DI**								**DI**	**DI**
Sample 27	**1.08**		**0.96**					**1.02**	**1.03**			1.04
t_{calc}			**4.82**					**3.92**	**4.80**			0.87
$t_{tab\ (4)}$ 90%			**2.13**					**2.13**	**2.13**			2.13
result			**DI**					**DI**	**DI**			NDNI

The values determined by normal calibration for all Zn lines generally showed inaccuracies of 5% or above thus requiring improvement. Even though the Ni 231 ion line is located very close to the Zn 213 line in the score plot, it didn't work well for the validation study. But another Ni ion line at 221 nm helped to correct the effect of the

acid/salt matrix interference on the Zn 213 line. The Co II 237 line located very close to the Zn I 213 in the score plot actually did show an improvement for this line as anticipated. The Co II 228 and Rh II 249 lines were helpful for the correction of samples 18 (12% acid, 0.3% salt) and 27 (25% acid, 0.3% salt), respectively but none of the selected internal standards could provide an improvement for sample 24 (25% acid, 0.1% salt). For sample 9 (which already had a concentration value within the 5% and 2% acceptable range in the normal calibration), a significant improvement was obtained with Rh ion line at 249 nm. For the problematic Zn 334 atom line some improvements were achieved but only the Co 340 atomic line showed a significant correction. Although the Zn 202 ion line is outside of the grouping in the score plot, the Co, Ni and Rh atom lines at 340, 345, 341, 352, 343 and 369 nm, respectively, provided significant improvements for this line. Only the Rh ion line helped to correct the inaccuracy of this line for sample 12 (12 acid, no salt). For the Zn II 206 line, all internal standard lines were successful in correcting the results from the normal calibration, the Co I 345 line being the best.

Atomic Co lines at 340 and 345 nm showed the most significant improvements when ratioed with the Zn ion lines for Zn determination. The Rh II 249 line also demonstrated good correction ability for Zn except for the Zn I 334 line.

3.3.4. Comparison of the Results with the Previous Experiments

The comparison of the concentration values obtained from the several trials for 1 mg/L analyte concentration level can be seen in Tables 3.30, 3.31 and 3.32 for Cd, Mn and Zn, respectively. The line graphs of these values can be seen in Appendix D.

In these tables and graphs “SE” stands for the trials in which **s**ingle **e**lement standards were used and “ME” stands for the trials performed with **m**ultielement **s**tandards. It should be noted here that solutions prepared using one single element standard also contains the other standards. For example, in the preparation of Cd synthetic samples, the other single element standards of Mn, Zn, Co, Ni and Rh were also added to these samples so they are not truly single element solutions but at least they do not contain any other interfering element that exists in the multielement standard solution.

Table 3.30. Comparison of the normal calibration results from the previous experiments for the Cd lines. All concentrations are expressed as mg/L.

Emission Line : Cd I 326.106 nm								
Sample	**Acid %**	**Salt %**	**Actual**	**SE3**	**SE2**	**SE1**	**ME2**	**ME1**
3	0	0	1.00	0.98	0.74	0.96		
6	0	0.1	1.00	0.98	1.09	0.88		
9	0	0.3	1.00	0.93	0.72	0.81		
12	12	0	1.00	0.81	0.41	0.87		
15	12	0.1	1.00	1.05	0.92	1.04		
18	12	0.3	1.00	0.81	0.84	0.87		
21	25	0	1.00	1.01	1.17	0.83		
24	25	0.1	1.00	0.95	0.88	0.78		
27	25	0.3	1.00	0.79	0.73	0.88		
Emission Line : Cd I 228.802 nm								
Sample	**Acid %**	**Salt %**	**Actual**	**SE3**	**SE2**	**SE1**	**ME2**	**ME1**
3	0	0	1.00	1.00	0.99	0.97	1.02	0.99
6	0	0.1	1.00	0.98	1.07	0.90	1.31	1.34
9	0	0.3	1.00	0.99	1.04	0.90	1.27	1.31
12	12	0	1.00	0.99	0.99	0.92	1.37	1.33
15	12	0.1	1.00	0.97	0.95	0.92	1.27	1.26
18	12	0.3	1.00	0.95	0.95	0.88	1.22	1.19
21	25	0	1.00	0.93	0.96	0.91	1.34	1.26
24	25	0.1	1.00	0.94	0.93	0.88	1.22	1.19
27	25	0.3	1.00	0.91	0.93	0.85	1.20	1.14
Emission Line : Cd II 226.502 nm								
Sample	**Acid %**	**Salt %**	**Actual**	**SE3**	**SE2**	**SE1**	**ME2**	**ME1**
3	0	0	1.00	1.00	0.99	0.97		
6	0	0.1	1.00	0.97	1.17	0.86		
9	0	0.3	1.00	1.01	1.11	0.84		
12	12	0	1.00	1.07	1.05	0.94		
15	12	0.1	1.00	1.03	0.99	0.90		
18	12	0.3	1.00	0.99	0.98	0.84		
21	25	0	1.00	1.00	1.02	0.92		
24	25	0.1	1.00	1.00	1.00	0.87		
27	25	0.3	1.00	0.95	0.95	0.81		
Emission Line : Cd II 214.438 nm								
Sample	**Acid %**	**Salt %**	**Actual**	**SE3**	**SE2**	**SE1**	**ME2**	**ME1**
3	0	0	1.00	1.00	0.99	0.96	1.06	0.98
6	0	0.1	1.00	1.00	1.24	0.85	1.85	1.83
9	0	0.3	1.00	1.05	1.17	0.82	2.23	2.10
12	12	0	1.00	1.11	1.07	0.92	2.42	2.15
15	12	0.1	1.00	1.08	1.01	0.89	2.27	1.99
18	12	0.3	1.00	1.05	1.00	0.82	2.16	1.88
21	25	0	1.00	1.05	1.06	0.92	2.40	2.03
24	25	0.1	1.00	1.06	1.03	0.87	2.15	1.90
27	25	0.3	1.00	1.03	0.98	0.82	2.06	1.84

Table 3.31. Comparison of the normal calibration results from the previous experiments for the Mn lines. All concentrations are expressed as mg/L.

Emission Line : Mn I 279.482 nm								
Sample	**Acid %**	**Salt %**	**Actual**	**SE3**	**SE2**	**SE1**	**ME2**	**ME1**
3	0	0	1.00	1.01	1.02	1.01	1.00	0.96
6	0	0.1	1.00	1.07	1.11	1.12	1.15	1.12
9	0	0.3	1.00	1.07	1.10	1.13	1.05	1.06
12	12	0	1.00	0.93	0.98	0.93	1.05	0.95
15	12	0.1	1.00	1.02	1.08	1.05	1.01	0.98
18	12	0.3	1.00	1.06	1.11	1.07	1.01	0.95
21	25	0	1.00	0.88	0.97	0.88	1.02	0.90
24	25	0.1	1.00	0.99	1.04	1.02	0.98	0.91
27	25	0.3	1.00	0.98	1.07	1.04	0.97	0.91
Emission Line : Mn I 403.076 nm								
Sample	**Acid %**	**Salt %**	**Actual**	**SE3**	**SE2**	**SE1**	**ME2**	**ME1**
3	0	0	1.00	0.98	1.03	0.98		
6	0	0.1	1.00	1.16	1.24	1.20		
9	0	0.3	1.00	1.08	1.20	1.17		
12	12	0	1.00	0.88	1.04	0.90		
15	12	0.1	1.00	1.09	1.24	1.14		
18	12	0.3	1.00	1.08	1.31	1.09		
21	25	0	1.00	0.88	1.03	0.87		
24	25	0.1	1.00	1.08	1.28	1.11		
27	25	0.3	1.00	1.04	1.26	1.08		
Emission Line : Mn II 257.610 nm								
Sample	**Acid %**	**Salt %**	**Actual**	**SE3**	**SE2**	**SE1**	**ME2**	**ME1**
3	0	0	1.00	1.00	1.01	1.01	1.03	0.99
6	0	0.1	1.00	0.94	1.01	0.90	1.32	1.29
9	0	0.3	1.00	0.96	0.96	0.86	1.32	1.31
12	12	0	1.00	1.04	1.01	0.95	1.51	1.40
15	12	0.1	1.00	0.96	0.90	0.88	1.33	1.28
18	12	0.3	1.00	0.95	0.91	0.83	1.27	1.21
21	25	0	1.00	0.99	0.99	0.93	1.47	1.33
24	25	0.1	1.00	0.95	0.92	0.87	1.28	1.21
27	25	0.3	1.00	0.90	0.87	0.83	1.25	1.16
Emission Line : Mn II 259.373 nm								
Sample	**Acid %**	**Salt %**	**Actual**	**SE3**	**SE2**	**SE1**	**ME2**	**ME1**
3	0	0	1.00	1.01	1.02	1.00		
6	0	0.1	1.00	0.95	1.00	0.90		
9	0	0.3	1.00	0.96	0.97	0.85		
12	12	0	1.00	1.05	1.01	0.95		
15	12	0.1	1.00	0.97	0.91	0.88		
18	12	0.3	1.00	0.96	0.93	0.83		
21	25	0	1.00	1.00	1.00	0.93		
24	25	0.1	1.00	0.95	0.92	0.86		
27	25	0.3	1.00	0.91	0.87	0.82		

Table 3.32. Comparison of the normal calibration results from the previous experiments for the Zn lines. All concentrations are expressed as mg/L.

Emission Line : Zn I 213.856 nm								
Sample	**Acid %**	**Salt %**	**Actual**	**SE3**	**SE2**	**SE1**	**ME2**	**ME1**
3	0	0	1.00	1.00	1.01	1.00	1.04	1.01
6	0	0.1	1.00	0.95	1.09	0.91	1.37	1.39
9	0	0.3	1.00	0.96	1.04	0.85	1.38	1.42
12	12	0	1.00	0.96	1.01	0.87	1.49	1.41
15	12	0.1	1.00	0.96	0.96	0.86	1.37	1.31
18	12	0.3	1.00	0.93	0.96	0.83	1.34	1.28
21	25	0	1.00	0.91	0.99	0.85	1.41	1.31
24	25	0.1	1.00	0.92	0.95	0.83	1.30	1.24
27	25	0.3	1.00	0.89	0.92	0.81	1.28	1.22
Emission Line : Zn I 334.502 nm								
Sample	**Acid %**	**Salt %**	**Actual**	**SE3**	**SE2**	**SE1**	**ME2**	**ME1**
3	0	0	1.00	0.78	0.98			
6	0	0.1	1.00	0.99	1.16			
9	0	0.3	1.00	0.83	0.99			
12	12	0	1.00	1.07	1.00			
15	12	0.1	1.00	1.01	1.02			
18	12	0.3	1.00	1.42	1.05			
21	25	0	1.00	1.32	0.78			
24	25	0.1	1.00	1.31	0.98			
27	25	0.3	1.00	1.24	0.90			
Emission Line : Zn II 202.551 nm								
Sample	**Acid %**	**Salt %**	**Actual**	**SE3**	**SE2**	**SE1**	**ME2**	**ME1**
3	0	0	1.00	1.00	1.01	0.96	1.08	1.02
6	0	0.1	1.00	0.99	1.07	0.85	2.06	2.03
9	0	0.3	1.00	1.10	1.17	0.78	2.88	2.70
12	12	0	1.00	1.17	1.11	0.86	3.16	2.84
15	12	0.1	1.00	1.18	1.05	0.85	2.89	2.59
18	12	0.3	1.00	1.11	1.04	0.79	2.85	2.51
21	25	0	1.00	1.14	1.13	0.86	2.99	2.68
24	25	0.1	1.00	1.16	1.09	0.84	2.79	2.51
27	25	0.3	1.00	1.11	1.03	0.81	2.70	2.44
Emission Line : Zn II 206.200 nm								
Sample	**Acid %**	**Salt %**	**Actual**	**SE3**	**SE2**	**SE1**	**ME2**	**ME1**
3	0	0	1.00	1.01	0.99	1.00		
6	0	0.1	1.00	1.03	1.29	0.89		
9	0	0.3	1.00	1.09	1.23	0.81		
12	12	0	1.00	1.16	1.09	0.91		
15	12	0.1	1.00	1.15	1.04	0.89		
18	12	0.3	1.00	1.10	1.03	0.84		
21	25	0	1.00	1.09	1.09	0.91		
24	25	0.1	1.00	1.11	1.05	0.88		
27	25	0.3	1.00	1.08	1.02	0.84		

If the normal calibration values obtained from all trials for sample 3 that did not have the any salt or acid content were examined, it could be seen that the values were

very close the true value (1 mg/L). For the other samples there were some inaccuracies that indicate the presence of the acid and salt matrix interferences on analyte signals. For all Cd, Mn and Zn lines, the calculated concentrations for the last three samples 21 (25% acid, no salt), 24 (25% acid, 0.1% salt) and 27 (25% acid, 0.3% salt) were generally more than 5% inaccurate and compensation by internal standardization was achieved with the selected Co, Ni and Rh lines in the validation study. These samples have the highest acid and salt contents and also show the effect of acid and salt matrix.

Although there were different observations for the values obtained for all elements (Cd, Mn and Zn) it appears that there is a general trend for all elements concerning the presence of only acid and only salt contents in the samples. When the acid content of the samples were increased, there were an enhancement of the analyte signal with respect to the salt-only case. This seems to show that acid has a higher influence on the analyte signal as compared to the "salt-only case". When salt was added to the samples, the measured concentrations showed a decrease (negative error).

The most striking observation achieved when the results from previous experiments were compared with the latest ones was the difference that occurred in the results regarding the standards used for the trials. The concentrations calculated from the first two trials (ME1 and ME2) were much higher than those obtained from the subsequent experiments (SE1, SE2 and SE3). The effect was even worse for the ion lines. The only difference between the preparations of these trials was the use of ICP multielement standard solution in the former trial which contains not only the elements of interest (Cd, Mn, Zn, Co, Ni), but also a complex array of other elements including Ca and Li. For the latter trials which investigated the use of Co, Ni and Rh as internal standards, the solutions only contained the elements under study (Cd, Mn, Zn, Co, Ni, and Rh).

Similar observations have been reported in previous studies and it has been shown by the other researchers that calcium causes a stronger matrix effect than sodium and depending on the elements considered when several interferent elements are present in the sample, the matrix effect is either enhanced or reduced with respect to a single concomitant solution (Todoli and Mermet 2002).

In order to illustrate the relationship between the elements (Cd, Mn Zn, Co, Ni and Zn) when the concentrations were obtained using single element standard solutions, PCA was applied again. Tables 3.33 and 3.34 demonstrate the calculated errors used as the data matrix for the PCA by using previously mentioned formulae. It should be noted

again that (-) and (+) signs indicate the difference from the sample 1 and not the true value. Three dimensional graphs of these matrix induced errors can also be seen in Appendix B.

Table 3.33. Matrix induced errors obtained for atom lines when generating the single element score plot

Error	Acid %	Salt %	Cd 326	Cd 228	Co 340	Co 345	Mn 279	Mn 403	Ni 352	Ni 351	Zn 213	Rh 343	Rh 369
E1	0	0	0	0	0	0	0	0	0	0	0	0	0
E2	0	0.1	9	7	-6	-10	-10	-23	-4	-6	9	-46	-49
E3	0	0.3	16	7	-7	-10	-11	-20	-5	-6	15	-16	-21
E4	12	0	10	6	2	-3	8	7	1	0	13	-23	-26
E5	12	0.1	-8	6	-7	-9	-3	-17	-3	-1	14	-10	-16
E6	12	0.3	10	10	-5	-7	-6	-12	-1	-4	17	-20	-27
E7	25	0	14	6	-1	-3	13	11	-3	-1	15	-25	-29
E8	25	0.1	19	10	-10	-12	-1	-13	-4	-5	17	-16	-21
E9	25	0.3	9	12	-11	-13	-3	-11	-3	-6	19	-12	-19

Table 3.34. Matrix induced errors obtained for ion lines when generating the single element score plot

Error	Acid %	Salt %	Cd 226	Cd 214	Co 258	Co 228	Mn 257	Mn 259	Ni 231	Ni 221	Zn 202	Zn 206	Rh 249
E1	0	0	0	0	0	0	0	0	0	0	0	0	0
E2	0	0.1	11	11	9	11	11	11	10	12	11	11	-33
E3	0	0.3	14	15	12	17	15	16	14	17	19	19	7
E4	12	0	3	4	5	5	5	5	6	5	11	10	-31
E5	12	0.1	7	8	10	11	12	12	10	11	12	11	4
E6	12	0.3	14	14	15	19	17	17	17	19	17	16	9
E7	25	0	5	4	6	6	7	7	9	6	10	9	-12
E8	25	0.1	11	10	13	15	14	15	13	15	13	12	6
E9	25	0.3	17	15	17	21	18	18	19	20	15	17	10

Figure 3.9 shows a score plot obtained from PCA using the results from previous experiments that used the single element standards.

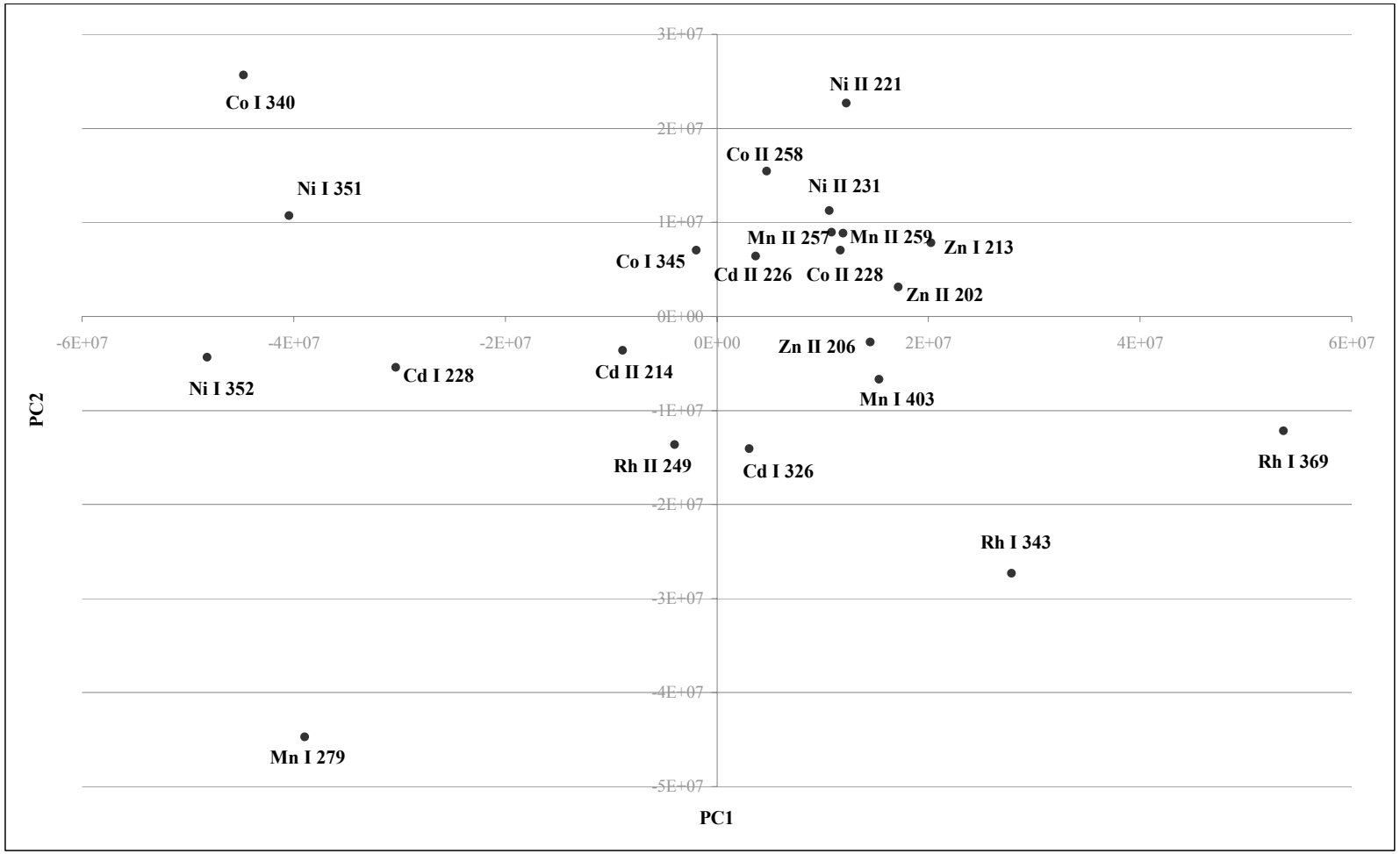

Figure 3.9. The score plot obtained by the PCA (using single element standards)

It should be noted that the elements used generating this plots are different from the elements used for the construction of the previous score plot (i.e., the plot obtained with the multielement standard Figure 3.8). In spite of this difference, if we compare these two plots it can be seem that Mn I 279 line and Rh I 343 line are located far from the other groupings. In the same way Ni II 231, Co I 345, Mn II 257 and Zn I 213 lines are distributed in the same grouping cluster.

3.3.5. Modified Analysis of Whale Liver Samples

After the validation study applicability of the selected internal standards was tested using the Beluga whale liver homogenates supplied from NIST.

Samples S1-1 and S1-2 (replicate of S1) were digested using 0.4 g liver homogenates, whereas S2-1 and its replicates S2-2 and S2-3 were digested using 0.3 g liver homogenates. These samples were not spiked with the chosen internal standards and normal calibration was used for the calculation of Cd, Mn, and Zn concentrations. The other samples S6-1 and S6-2 (which contain 0.4 g liver homogenates) and S7-1 and S7-2 (which contain 0.3 g liver homogenates) were spiked with the determined internal standards (Co, Ni and Rh) and both normal calibration and internal standardization were applied to calculate the concentrations in order to see the effect of using spiked standards.

In Table 3.35 the calculated concentration values using normal calibration both for spiked and unspiked samples are shown. The Cd 326 atom line and Mn 403 atom line were not included in these tables due to erroneous results obtained by these lines. In order to determine whether the concentrations were different from the certified values for Cd, Mn and Zn, a t-test was applied. Table 3.36 shows these results. “D” sign indicates that the calculated concentrations are different from the certified value. “ND” sign is used to point out that the calculated concentrations are not very different from the certified value therefore these concentrations can be accepted.

Table 3.35. The concentration values for Beluga whale liver homogenates (in ug/g, wet mass) obtained by normal calibration

samples			Cd 228.802	Cd 226.502	Cd 214.438	Mn 279.482	Mn 257.610	Mn 259.373	Zn 213.856	Zn 206.200	Zn 202.551
no internal std spike	0.4 g	S1	2.50	2.51	2.36	1.05	2.52	3.32	41.24	42.14	41.77
		S1-2	2.47	2.55	2.40	1.28	2.39	3.26	29.94	30.27	30.52
	0.3 g	S2	2.55	2.55	2.39	1.28	2.68	3.53	29.23	29.31	29.67
		S2-2	2.40	2.44	2.31	0.33	2.32	3.18	29.64	29.55	30.22
		S2-3	2.51	2.53	2.31	0.22	2.46	3.34	29.57	30.20	30.15
		average	**2.49 ± 0.06**	**2.52 ± 0.04**	**2.35 ± 0.04**	**0.83 ± 0.52**	**2.47 ± 0.14**	**3.33 ± 0.13**	**31.93 ± 5.21**	**32.29 ± 5.52**	**32.47 ± 5.21**
with internal std spike	0.4 g	S6	2.52	2.54	2.39	2.84	4.46	5.22	28.49	28.77	29.46
		S6-2	2.75	2.78	2.58	2.88	4.25	5.04	30.16	30.78	30.98
	0.3 g	S7	2.55	2.56	2.34	1.00	2.35	3.21	30.58	30.73	31.33
		S7-2	2.56	2.54	2.33	1.84	2.67	3.55	30.61	30.68	30.96
		average	**2.59 ± 0.11**	**2.61 ± 0.12**	**2.41 ± 0.12**	**2.14 ± 0.90**	**3.43 ± 1.08**	**4.25 ± 1.02**	**29.96 ± 1.00**	**30.24 ± 0.98**	**30.68 ± 0.83**

Table 3.36. The results obtained by the *t*-test. (Certified values for Cd is 2.35 ± 0.06, for Mn is 2.37 ± 0.08 and for Zn is 26.31± 0.66 ug/g, wet mass)

	Cd 228.802	Cd 226.502	Cd 214.438	Mn 279.482	Mn 257.610	Mn 259.373	Zn 213.856	Zn 206.200	Zn 202.551
For unspiked samples									
calc. conc	**2.49 ± 0.06**	**2.52 ± 0.04**	**2.35 ± 0.04**	**0.83 ± 0.52**	**2.47 ± 0.14**	**3.33 ± 0.13**	**31.93 ± 5.21**	**32.29 ± 5.52**	**32.47 ± 5.21**
$t_{calculated}$	3.712	4.969	0.120	6.541	1.485	14.018	2.389	2.407	2.621
$t_{tab\ (8)}$ **CL: 95%**	2.306	2.306	2.306	2.306	2.306	2.306	2.306	2.306	2.306
result	D	D	**ND**	D	**ND**	D	D	D	D
For spiked samples									
calc. conc	**2.59 ± 0.11**	**2.61 ± 0.12**	**2.41 ± 0.12**	**2.14 ± 0.90**	**3.43 ± 1.08**	**4.25 ± 1.02**	**29.96 ± 1.00**	**30.24 ± 0.98**	**30.68 ± 0.83**
$t_{calculated}$	4.365	4.290	1.013	0.584	2.233	4.174	6.607	7.208	8.816
$t_{tab\ (7)}$ **CL: 95 %**	2.365	2.365	2.365	2.365	2.365	2.365	2.365	2.365	2.365
result	D	D	**ND**	**ND**	**ND**	D	D	D	D

It can be seen that for all Cd lines there is no considerable difference between the samples digested with 0.4 g and 0.3 g liver homogenates both for spiked and unspiked samples. The calculated concentrations for Cd were different from the certified value except for the Cd 214 ion line. According to the *t*-test for the Cd II 214 line, there is no significant difference between the certified values; therefore, the value can be accepted.

For the Mn 279 atom line there was a considerable difference between the samples containing 0.4 g and 0.3 g whale liver homogenates both for spiked and unspiked samples. Furthermore, concentrations for unspiked samples were very different from the certified value but for spiked samples these differences were not significant. For the other Mn lines at 257 and 259 nm, for unspiked samples concentrations were not changing much regarding the digested samples using 0.4 g and 0.3 g whale livers but on the other hand it seems that spiked samples were affected by changing the actual whale liver amount. For Mn 257 line, according to the *t*-test, results for both spiked and unspiked samples are not different from the certified value.

For all lines of Zn, only S1-1 differs from the other samples for both spiked and unspiked samples and according to the *t*-test applied; there is a significant difference between the calculated values and certified values.

To summarize, for Cd atom lines at 326 and 228 nm and the ion line at 226 nm an improvement is needed. In the same way, concentrations obtained by Mn I 279 and Mn II 259 should be corrected and finally all Zn lines need to be improved by using internal standard calibration.

Corrected concentrations obtained by internal standardization were listed in Tables 3.37 – 3.39 for Cd, Mn and Zn respectively. In these tables t-test values can also be seen. It should be noted again that "DNI" indicates that the calculated concentrations are different from the certified value so there is no improvement after the application of internal standardization. On the other hand "ND" sign is used to indicate the corrected concentrations by internal standardization are significantly different from the certified values and the improvement by the selected internal standards are represented with the "NDI" sign

Table 3.37. The calculated concentrations for Cd lines by using Co, Ni and Rh as the internal standards and test for significance values

	Internal standards									
Emission line: Cd I 326.106 nm										
	Co I 340	**Co I 345**	**Co II 237**	**Co II 228**	**Ni II 231**	**Ni II 221**	**Ni I 341**	**Ni I 352**	**Rh II 249**	**Rh I 369**
sample	9.69 ± 2.34	13.87 ± 4.20	13.60 ±5.13	8.44 ± 5.44	12.43 ± 4.21	11.75 ± 3.85	7.48 ± 5.64	7.98 ± 5.81	3.07 ± 2.40	18.28 ± 8.96
$t_{calculated}$	7.141	6.251	4.992	2.547	5.447	5.561	2.071	2.210	0.684	4.048
$t_{tab\ (7)}$ CL: 95	2.365	2.365	2.365	2.365	2.365	2.365	2.365	2.365	2.365	2.365
result	DNI	DNI	DNI	DNI	DNI	DNI	**NDI**	**NDI**	**NDI**	DNI
Emission line: Cd I 228.802 nm										
	Co I 340	**Co I 345**	**Co II 237**	**Co II 228**	**Ni II 231**	**Ni II 221**	**Ni I 341**	**Ni I 352**	**Rh II 249**	**Rh I 369**
sample	0.25 ± 0.02	2.69 ± 0.10	2.54 ± 0.13	2.53 ± 0.02	2.40 ± 0.25	2.19 ± 0.17	2.48 ± 0.19	2.30 ± 0.09	0.92 ± 0.14	2.71 ± 0.04
$t_{calculated}$	66.440	6.406	3.066	5.546	0.432	1.999	1.481	0.997	21.169	10.035
$t_{tab\ (7)}$ CL: 95	2.365	2.365	2.365	2.365	2.365	2.365	2.365	2.365	2.365	2.365
result	DNI	DNI	DNI	DNI	**NDI**	**NDI**	**NDI**	**NDI**	DNI	DNI
Emission line: Cd II 226.502 nm										
	Co I 340	**Co I 345**	**Co II 237**	**Co II 228**	**Ni II 231**	**Ni II 221**	**Ni I 341**	**Ni I 352**	**Rh II 249**	**Rh I 369**
sample	2.46 ± 0.17	2.75 ± 0.12	2.63 ± 0.13	2.64 ± 0.03	2.39 ± 0.26	2.12 ± 0.17	2.15 ± 0.19	2.67 ± 0.04	0.99 ± 0.15	2.55 ± 0.04
$t_{calculated}$	1.380	6.388	4.315	8.860	0.354	2.784	2.258	9.120	19.305	5.645
$t_{tab\ (7)}$ CL: 95	2.365	2.365	2.365	2.365	2.365	2.365	2.365	2.365	2.365	2.365
result	**NDI**	DNI	DNI	DNI	**NDI**	DNI	**NDI**	DNI	DNI	DNI
Emission line: Cd II 214.438 nm										
	Co I 340	**Co I 345**	**Co II 237**	**Co II 228**	**Ni II 231**	**Ni II 221**	**Ni I 341**	**Ni I 352**	**Rh II 249**	**Rh I 369**
sample	2.66 ± 0.13	2.79 ± 0.20	2.59 ± 0.10	2.48 ± 0.08	2.20 ± 0.30	2.20 ± 0.17	2.44 ± 0.09	2.23 ± 0.14	0.93 ± 0.11	2.36 ± 0.10
$t_{calculated}$	4.629	4.665	4.674	2.724	1.129	1.884	1.753	1.841	25.057	0.231
$t_{tab\ (7)}$ CL: 95	2.365	2.365	2.365	2.365	2.365	2.365	2.365	2.365	2.365	2.365
result	DNI	DNI	DNI	DNI	**NDI**	**NDI**	**NDI**	**NDI**	DNI	**NDI**

Table 3.38. The calculated concentrations for Mn lines by using Co, Ni and Rh as the internal standards and test for significance values

	Internal standards									
Emission line: Mn I 279.482 nm										
	Co I 340	**Co I 345**	**Co II 237**	**Co II 228**	**Ni II 231**	**Ni II 221**	**Ni I 341**	**Ni I 352**	**Rh II 249**	**Rh I 369**
sample	2.69 ± 0.40	2.80 ± 0.06	2.55 ± 0.39	2.67 ± 0.19	1.87 ± 0.37	2.08 ± 0.34	2.53 ± 0.40	2.32 ± 0.23	1.31 ± 0.09	2.64 ± 0.26
$t_{calculated}$	2.005	6.831	1.138	3.222	3.336	2.037	0.987	0.509	18.453	2.331
$t_{tab\ (5)}$ CL: 95	2.571	2.571	2.571	2.571	2.571	2.571	2.571	2.571	2.365	2.571
result	**NDI**	DNI	**NDI**	DNI	DNI	**NDI**	**NDI**	**NDI**	DNI	**NDI**
Emission line: Mn I 403. nm										
	Co I 340	**Co I 345**	**Co II 237**	**Co II 228**	**Ni II 231**	**Ni II 221**	**Ni I 341**	**Ni I 352**	**Rh II 249**	**Rh I 369**
sample	2.02 ± 0.22	1.83 ± 0.09	1.90 ± 0.20	1.90 ± 0.04	1.55 ± 0.21	1.50 ± 0.19	1.82 ± 0.23	2.02 ± 0.09	0.98 ± 0.19	2.08 ± 0.10
$t_{calculated}$	3.460	7.857	4.848	7.683	8.286	9.448	5.315	5.073	15.046	4.152
$t_{tab\ (5)}$ CL: 95	2.571	2.571	2.571	2.571	2.571	2.571	2.571	2.571	2.365	2.571
result	DNI	DNI	DNI	DNI	DNI	DNI	DNI	DNI	DNI	DNI
Emission line: Mn II 257.610 nm										
	Co I 340	**Co I 345**	**Co II 237**	**Co II 228**	**Ni II 231**	**Ni II 221**	**Ni I 341**	**Ni I 352**	**Rh II 249**	**Rh I 369**
sample	3.66 ± 0.46	3.72 ± 0.01	3.44 ± 0.44	3.55 ± 0.17	2.72 ± 0.43	2.80 ± 0.39	3.31 ± 0.46	2.79 ± 0.23	1.53 ± 0.07	3.68 ± 0.27
$t_{calculated}$	7.152	22.505	6.138	13.525	2.032	2.752	5.182	3.956	16.727	11.136
$t_{tab\ (5)}$ CL: 95	2.571	2.571	2.571	2.571	2.571	2.571	2.571	2.571	2.365	2.571
result	DNI	DNI	DNI	DNI	**NDI**	DNI	DNI	DNI	DNI	DNI
Emission line: Mn II 259.373 nm										
	Co I 340	**Co I 345**	**Co II 237**	**Co II 228**	**Ni II 231**	**Ni II 221**	**Ni I 341**	**Ni I 352**	**Rh II 249**	**Rh I 369**
sample	2.43 ± 0.68	2.71 ± 0.72	2.36 ± 0.98	2.34 ± 0.61	1.98 ± 0.86	1.88 ± 0.70	2.17 ± 0.67	2.01 ± 0.79	0.46 ± 0.11	2.59 ± 0.79
$t_{calculated}$	0.238	1.227	0.025	0.148	1.206	1.798	0.784	1.190	30.035	0.730
$t_{tab\ (5)}$ CL: 95	2.571	2.571	2.571	2.571	2.571	2.571	2.571	2.571	2.365	2.571
result	**NDI**	**NDI**	**NDI**	**NDI**	**NDI**	**NDI**	**NDI**	**NDI**	DNI	**NDI**

Table 3.39. The calculated concentrations for Zn lines by using Co, Ni and Rh as the internal standards and test for significance values

	Internal standards									
Emission line: Zn I 213.856 nm										
	Co I 340	**Co I 345**	**Co II 237**	**Co II 228**	**Ni II 231**	**Ni II 221**	**Ni I 341**	**Ni I 352**	**Rh II 249**	**Rh I 369**
sample	32.22 ± 1.41	30.98 ± 1.35	30.38 ± 1.24	30.91 ± 0.85	26.66 ± 2.60	25.84 ± 1.27	26.65 ± 1.70	27.19 ± 0.54	7.53 ± 1.13	34.79 ± 1.34
$t_{calculated}$	8.378	6.862	6.376	9.167	0.293	0.722	0.415	2.134	31.425	12.562
$t_{tab\,(7)}$ CL: 95	2.365	2.365	2.365	2.365	2.365	2.365	2.365	2.365	2.365	2.365
result	DNI	DNI	DNI	DNI	**NDI**	**NDI**	**NDI**	**NDI**	DNI	DNI
Emission line: Zn II 206.200 nm										
	Co I 340	**Co I 345**	**Co II 237**	**Co II 228**	**Ni II 231**	**Ni II 221**	**Ni I 341**	**Ni I 352**	**Rh II 249**	**Rh I 369**
sample	30.21 ± 2.35	29.78 ± 0.91	29.90 ± 1.09	30.26 ± 0.94	25.22 ± 1.73	25.31 ± 1.02	26.96 ± 1.54	27.04 ± 0.36	7.49 ± 1.17	34.35 ± 1.39
$t_{calculated}$	3.588	6.641	6.145	7.427	1.314	1.796	0.859	1.969	30.749	11.554
$t_{tab\,(7)}$ CL: 95	2.365	2.365	2.365	2.365	2.365	2.365	2.365	2.365	2.365	2.365
result	DNI	DNI	DNI	DNI	**NDI**	**NDI**	**NDI**	**NDI**	DNI	DNI
Emission line: Zn II 202.551 nm										
	Co I 340	**Co I 345**	**Co II 237**	**Co II 228**	**Ni II 231**	**Ni II 221**	**Ni I 341**	**Ni I 352**	**Rh II 249**	**Rh I 369**
sample	30.84 ± 2.35	30.85 ± 1.31	30.58 ± 1.22	30.85 ± 0.67	25.47 ± 2.03	25.79 ± 1.26	26.92 ± 1.65	27.34 ± 0.71	6.96 ± 1.00	33.89 ± 1.09
$t_{calculated}$	4.169	6.832	6.778	10.181	0.879	0.810	0.768	2.253	35.040	12.985
$t_{tab\,(7)}$ CL: 95	2.365	2.365	2.365	2.365	2.365	2.365	2.365	2.365	2.365	2.365
result	DNI	DNI	DNI	DNI	**NDI**	**NDI**	**NDI**	**NDI**	DNI	DNI

When these tables are explored it is seen that for Cd, significant improvements were obtained especially by using selected Ni lines. Rh II 249 and Rh I 369 lines were also useful for Cd I 326 and Cd II 214 lines respectively. On the other hand Co lines were not successful for correcting the results for Cd. The concentrations for Mn I 403 line could not be corrected with internal standardization. For Mn 279 all proposed internal standards except Co II 228, Ni II 231 and Rh II 249 were helpful to obtain concentrations which were not different from the certified value. For Mn 259 line, significant improvements were achieved by using all proposed internal standards except Rh II 249 nm. By using all the Ni lines, concentrations that were not very different from the certified value were obtained for all Zn lines.

3.4. Conclusion

ICP-OES is still one of the most appropriate techniques for elemental analysis with some important features. However, its potentially excellent analytical characteristics are degraded in the presence of matrix effects. When robust plasma conditions are used, these effects are reduced but not totally eliminated; therefore, generally different methods such as internal standardization may be applied to compensate for these effects.

The choice of appropriate internal standard is very important since the success of internal standardization highly depends on the similarity between the analyte and internal standard.

In these studies the applicability of the PCA method for choosing the proper internal standards to compensate for the matrix effects caused by acid and salt was examined.

Although it has been reported by other researchers that the energies of the analyte and internal standard lines should be similar, in this study no simple relationships between the energies of analytes and internal standards were observed.

It was found that elements having the highest energies such as Cd and Zn were more affected in the presence of acid and salt matrices. Moreover, it is known that the lines with close excitation energies are expected to behave similarly in the presence of acid and salt matrices. Unlike the observations of other authors, the results obtained in this study showed that the lines with close excitation energies like the Cd II 226 nm line

(14.47 eV) and the Cd II 214 nm line (14.77 eV) as well as the Zn II 206 nm (15.40 eV) and Zn II 202 nm lines (15.51 eV) had similar responses in the presence of matrix effects.

For all Cd, Mn and Zn lines, the calculated concentrations for the samples having high acid and salt content indicating the matrix effects were generally more than 5% inaccurate and compensation by internal standardization was achieved with the selected Co, Ni and Rh lines in the validation study.

Significant difference was observed between the analysis of samples and standards which were prepared from multielement solutions versus single element solutions. These results confirmed that calcium causes a stronger matrix effect than sodium and when several interferent elements are present in the sample (Ca, Na and Li in our case), the matrix effect is either enhanced or reduced with respect to a single concomitant solution.

In the analysis for real samples all proposed Ni lines (Ni II 231, Ni II 221, Ni I 341 and Ni I 352 lines) proved to be useful for use as internal standards.

REFERENCES

Agusa, T., Kunito, T., Tanabe, S., Pourkazemi, M., Aubrey, D.G. 2004. "Concentrations of Trace Elements in Muscle of Sturgeons in the Caspian Sea", *Marine Pollution Bulletin*. No.49, pp. 789–800.

Al-Ammar and A.S., Barnes, R.M. 1998. "Correction for Non-Spectroscopic Matrix Effects in Inductively Coupled Plasma Atomic Emission Spectroscopy by Internal Standardization Using Spectral Lines of the Same Analyte", *Spectrochimicaica. Acta B*. No. 53, pp. 1583-1593.

Anan, Y., Kunito, T., Sakai, H., Tanabe, S. 2002a. "Subcellular Distribution of Trace Elements in the Liver of Sea Turtles", *Marine Pollution Bulletin*. No. 45, pp. 224–229.

Anan, Y., Kunito, T., Ikemoto, T., Kubota, R., Watanabe, I., Tanabe, S., Miyazaki, N., Petrov, E.A. 2002b. "Elevated Concentrations of Trace Elements in Caspian Seals (*Phoca Caspica*) Found Stranded During the Mass Mortality Events in 2000", *Archives of Environmental Contamination and Toxicology*. No.42, pp. 354–362.

Ancora, S., Volpi, V., Olmastroni, S., Focardi, S., Leonzio, C. 2002. "Assumption and Elimination of Trace Elements in Adélie Penguins from Antarctica: a Preliminary Study", *Marine Environmental Research*. No.54, pp.341–344.

Becker, P.R., Wise, S.A., Thorsteinsot, L., Koster, B.J., Rowles, T. 1997a. "Specimen Banking of Marine Organisms in the United States: Current Status and Long-Term Prospective", *Chemosphere*. No.34, pp.1889-1906.

Becker, P.R., Mackey E.A., Demiralp, R., Schantz, M.M., Koster, B. J., Wise, S.A. 1997b. "Concentrations of Chlorinated Hydrocarbons and Trace Elements in Marine Mammal Tissues Archived in the U.S. National Biomonitoring Specimen Bank", *Chemosphere*. No.34, pp.2067-2098.

Becker, P.R., Porter B.J., Mackey E.A., Schantz M.M., Demiralp R., Wise , S.A. 1999. "National Marine Mammal Tissue Bank and Quality Assurance Program: Protocols, Inventory, and Analytical Results", NISTIR 6279, National Institute of Standards and Technology.

Becker, P.R. 2000. "Concentration of Chlorinated Hydrocarbons and Heavy Metals in Alaska Arctic Marine Mammals", *Marine Pollution Bulletin*. No.40, pp. 819-829.

Bennett, P.M., Jepson, P.D., Law, R.J., Jones, B.R., Kuiken, T., Baker, J.R., Rogan, E., Kirkwood, J.K. 2001. "Exposure to Heavy Metals and Infectious Disease Mortality in Harbour Porpoises from England and Wales", *Environmental Pollution*. No.112, pp.33-40.

Brenner, I. B., Segal, I., Mermet, M., Mermet, J. M., 1995. “Study of the Depressive Effects of Nitric Acid on the Line Intensities of Rare Earth Elements in Inductively Coupled Plasma Atomic Emission Spectrometry”, *Spectrochimica Acta B.* No. 50, pp. 333–340.

Brenner, I.B., Zander, A., Cole, M., Wiseman, A., 1997. “Comparison of Axially and Radially Viewed Inductively Coupled Plasmas for Multielement Analysis: Effect of Sodium and Calcium”, *Journal of Analytical Atomic Spectrometry,,* No. 12, pp. 897-906.

Brenner, I.B., Zischka, M., Maichin, B., Knapp, G., 1998. “Ca and Na Interference Effects in Axially Viewed ICP Using Low and High Aerosol Loadings”, *Journal of Analytical Atomic Spectrometry,* No. 13, pp. 1257-1264.

Brenner, I.B., Le Marchand, A., Daraed, C., Chauvet, L., 1999. “Compensation of Ca And Na Interference Effects in Axially and Radially Viewed Inductively Coupled Plasmas”, *Microchemical Journal*. No. 63, pp. 344-355.

Brenner, I.B. and Zander, A.T., 2000. “Axially and Radially Viewed Inductively Coupled Plasmas – A Critical Review”, *Spectrochimica Acta B*. No. 55, pp. 1195 - 1240.

Botto, R.I., 1985. “Method for Correcting for Acid and Salt Matrix Interferences in ICP-OES”, *Spectrochimica Acta B*. No. 40, pp. 397-412.

Bustamante, P., Garrigue, C., Breau, L., Caurant F., Dabin, W., Greaves, J., Dodemont, R. 2003. “Trace Elements in Two Odontocete Species (*Kogia Breviceps* And *Globicephala Macrorhynchus*) Stranded in New Caledonia (South Pacific)”, *Environmental Pollution*. No.124, pp.263–271.

Capelli, R., Drava, G., De Pellegrini, R., Minganti, V., Poggi, R. 2000. “Study of Trace Elements in Organs and Tissues of Striped Dolphins (*Stenella Coeruleoalba)* Found Dead Along the Ligurian Coasts Italy”, *Advances in Environmental Research*. No.4, pp.31-43.

Cardellicchio, N. Decataldo, A., Di Leo, A., Giandomenico, S. 2002. “Trace Elements in Organs and Tissues of Striped Dolphins (*Stenella Coeruleoalba*) from the Mediterranean Sea (Southern Italy)”, *Chemosphere*. No.49, pp.85–90.

Carre, M., Lebas, K., Marichy, M., Mermet, M., Poussel, E., Mermet, J.M., 1995. “Influence of the Sample Introduction System on Acid Effects in Inductively Coupled Plasma Atomic Emission Spectrometry”, *Spectrochimica Acta B.* No. 50, pp. 271-283.

Cave, M., 1998. “Improvement of Short-Term Precision in Inductively Coupled Plasma Atomic Emission Spectrometry by Principal Component Analysis Modeling”, *Journal of Analytical Atomic Spectrometry,* No. 13, pp. 125-129.

Chang, C.C. and Jiang, S.J. 1997. “Determination of Copper, Cadmium and Lead in Biological Samples by Electrothermal Vaporization Isotope Dilution Inductively Coupled Plasma Mass Spectrometry”, *Journal of Analytical Atomic Spectrometry,* No.12, pp. 75–80.

Chan, G.C.Y., Chan, W.T., Mao, X., Russo, R. E., 2000. “Investigation of Matrix Effects in Inductively Coupled Plasma-Atomic Emission Spectroscopy Using Laser Ablation and Solution Nebulization - Effect of Second Ionization Potential”, *Spectrochimica. Acta B*, No. 56, pp. 77-92.

Chausseau, M., Poussel, E., Mermet, J.M., 2000. “Effect of the Operating Parameters on Second Scale Time Correlation between Lines of the Same Element Using Axially Viewed Inductively Coupled Plasma-Multichannel-Based Emission Spectrometry”, *Spectrochimica Acta B*, No. 55, pp. 1431-1450.

Chen, W., Wee, P., Brindle, I.D. 2000. “Elimination of the Memory Effects of Gold, Mercury and Silver in Inductively Coupled Plasma Atomic Emission Spectroscopy”, *Journal of Analytical Atomic Spectrometry,* No.15, pp. 409-413.

Christopher, S.J. 2001. “NIST Results For The 2000 Interlaboratory Comparison Exercise for Trace Elements in Marine Mammals, Report of Analysis 839.01-01-015, National Institute of Standards and Technology.

Dennaud, J., Howes, A., Poussel, E., Mermet, J.M., 2001. “Study of Ionic-to-Atomic Line Intensity Ratios for Two Axial Viewing-Based Inductively Coupled Plasma Atomic Emission Spectrometers”, *Spectrochimica Acta B*. No. 56, pp. 101-112.

Dubuisson, C., Poussel, E., Mermet, J.-M., 1997. “Comparison of Axially and Radially Viewed Inductively Coupled Plasma Atomic Emission Spectrometry in Terms of Signal-to-Background Ratio and Matrix Effects”, *Journal of Analytical Atomic Spectrometry,* No. 12, pp. 281-286.

Dubuisson, C., Poussel, E., Todoli, J.L., Mermet, J.-M., 1998a. “Effect of Sodium during the Aerosol Transport and Filtering in Inductively Coupled Plasma Atomic Emission Spectrometry”, *Spectrochimica Acta B*. No. 53, pp. 593-600.

Dubuisson, C., Poussel, E., Mermet, J.-M., Todoli, J.L., 1998b. “Comparison of the Effect of Acetic Acid with Axially and Radially Viewed Inductively Coupled Plasma Atomic Emission Spectrometry: Influence of the Operating Conditions”, *Journal of Analytical Atomic Spectrometry,* No. 13, pp. 63-67.

Dubuisson, C., Poussel, E., Mermet, J.-M., 1998c. “Comparison of Ionic Line-Based Internal Standardization with Axially and Radially Viewed Inductively Coupled Plasma Atomic Emission Spectrometry to Compensate for Sodium Effects on Accuracy”, *Journal of Analytical Atomic Spectrometry,* No. 13, pp. 1265-1269.

Epstein, M.S. and Buehler, B., 1998. Analysis of Whale Tissue, Report of Analysis 839.01-98-026, National Institute of Standards and Technology.

Epstein, M.S., 2000. Analysis Of Rough Toothed Dolphin Kidney And Liver Tissue, Report of Analysis 839.01-00-043, National Institute of Standards and Technology.

Fernandez, A., Murillo, M., Carrion, N., Mermet, J.M., 1994. "Influence of Operating Conditions on the Effects of Acids in Inductively Coupled Plasma Atomic Emission Spectrometry", *Journal of Analytical Atomic Spectrometry,* No. 9, pp. 217-221.

Galley, P.J., Glick, M., Hieftje, G.M., 1993. "Easily Ionizable Element Interferences in Inductively Coupled Plasma Atomic Emission Spectroscopy – I.Effect on Radial Analyte Emission Patterns", *Spectrochimica Acta B.* No. 48, pp. 769-788.

Galley, P.J., Hieftje, G.M., 1994. "Easily Ionizable Element Interferences in Inductively Coupled Plasma Atomic Emission Spectrometry – II.Minimization of EIE Effects by Choice of Observation Volume", *Spectrochimica Acta B.* No. 49, pp. 703-724.

Garavaglia, R.N., Rebagliati, R.J., Roberti, M.J., Batistoni, D.A., 2002. "Matrix Effects in the Analysis of Biological Matrices by Axial View Inductively Coupled Plasma Optical Emission Spectrometry", *Spectrochimica Acta B.* No. 57, pp. 1925-1938.

Griffiths, M.L., Svozil, D., Worsfold, P.J., Denham, S., Evans, E.H., 2000. "Comparison of Traditional and Multivariate Calibration Techniques Applied to Complex Matrices Using Inductively Coupled Plasma Atomic Emission Spectroscopy", *Journal of Analytical Atomic Spectrometry,* No. 15, pp. 967-972.

Grotti, M., Magi, E., Frache, R., 2000. "Multivariate Investigation of Matrix Effects in Inductively Coupled Plasma Atomic Emission Spectrometry Using Pneumatic or Ultrasonic Nebulization", *Journal of Analytical Atomic Spectrometry,* No. 15, pp. 89-95.

Grotti, M., Magi, E., Leardi, R., 2003a. "Selection of Internal Standards in Inductively Coupled Plasma Atomic Emission Spectrometry by Principal Component Analysis", *Journal of Analytical Atomic Spectrometry,* No. 18, pp. 274-281.

Grotti, M. and Frache, R., 2003b. "Reduction of Acid Effects in Inductively Coupled Plasma Optical Emission Spectrometry Using Internal Standards Selected by Principal Component Analysis", *Journal of Analytical Atomic Spectrometry,* No. 18, pp. 1192-1197.

Harrington, C.F., Merson, S.A., D' Silva, T.M. 2004. "Method to Reduce the Memory Effect of Mercury in the Analysis of Fish Tissue Using Inductively Coupled Plasma Mass Spectrometry", *Analytica Chimica Acta*. No. 505, pp.247–254.

Harvell, C.D., Kim, K., Burkholder, J.M., Colwell, R.R., Epstein, P.R., Grimes, D.J., Hofmann, E.E., Lipp, E.K., Osterhaus, A.D.M.E., Overstreet, R.M., Porter, J.W., Smith, G.W., Vasta, G.R. 1999. "Emerging Marine Diseases - Climate Links and Anthropogenic Factors", *Science*. No. 285, pp.1505–1510.

Hobbs, S. E. and Olesik, J. W., 1997. "The Influence of Incompletely Desolvated Droplets and Vaporizing Particles on Chemical Matrix Effects in Inductively Coupled Plasma Spectrometry: Time-Gated Optical Emission And Laser-Induced Fluorescence Measurements", *Spectrochimica Acta B*. No. 52, p. 353

Hoekstra, P.F., Braune, B.M., Elkin, B., Armstrong, F.A.J., Muir, D.C.G. 2003. "Concentrations of Selected Essential and Non-Essential Elements in Arctic Fox (*Alopex Lagopus*) and Wolverines (*Gulo gulo*) from the Canadian Arctic", *The Science of the Total Environment*. No. 309, pp.81–92.

Hoenig, M., Dočekalová, Baeten, H., 1998. "Study of Matrix Interferences in Trace Element Analysis of Environmental Samples by Inductively Coupled Plasma Atomic Emission Spectrometry with Ultrasonic Nebulization", *Journal of Analytical Atomic Spectrometry,* No. 13, pp. 195-199.

Iglesias, M., Vaculovic, T., Studynkova, J., Poussel, E., Mermet, J.M., 2004. "Influence of the Operating Conditions and of the Optical Transition on Non-Spectral Matrix Effects in Inductively Coupled Plasma Atomic Emission Spectrometry", *Spectrochimica Acta B*. No. 59, pp. 1841-1850.

Ikemoto, T., Kunito, T., Watanabe, I., Yasunaga, G., Baba, N., Miyazaki, N., Petrov, E. A., Tanabe, S. 2004. "Comparison of Trace Element Accumulation in Baikal Seals (*Pusa Sibirica*), Caspian Seals (*Pusa Caspica*) and Northern Fur Seals (*Callorhinus ursinus*)", *Environmental Pollution*. No.127, pp.83–97.

Ivaldi, J.C. and Tyson, J.F., 1995. "Performance Evaluation of an Axially Viewed Horizontal Inductively Coupled Plasma for Optical Emission Spectrometry", *Spectrochimica Acta B.* No. 50, pp. 1207– 1226.

Ivaldi, J.C. and Tyson, J.F., 1996. "Real-Time Internal Standardization with an Axially-Viewed Inductively Coupled Plasma for Atomic Emission Spectrometry", *Spectrochimica Acta B*. No. 51, pp. 1443-1450.

Johnson, D., 1996. "Determination of Metals in A 3% Sodium Chloride (NaCl) Matrix by Axially-Viewed ICP-AES", *ICP-AES Varian instruments at work*, ICP-19, pp.1-7.

Johnson, M.D., Kenney, N., Stoica, A., Hilakivi-Clarke, L., Singh, B., Chepko, G., Clarke, R., Sholler, P.F., Lirio, A.A., Foss, C., Reiter, R., Trock, B., Paik, S., Martin, M.B. 2003. "Cadmium Mimics the in Vivo Effects of Estrogen in the Uterus and Mammary Gland", *Nature Medicine*. No. 9, pp.1081–1084.

Kola, H. and Perämäki, P., 2004. "The Study of the Selection of Emission Lines and Plasma Operating Conditions for Efficient Internal Standardization in Inductively Coupled Plasma Optical Emission Spectrometry", *Spectrochimica Acta B*. No. 59, pp. 231-242.

Kunito, T., Watanabe, I., Yasunaga G., Fujise, Y., Tanabe, S. 2002. "Using Trace Elements in Skin to Discriminate the Populations of Minke Whales in Southern Hemisphere", *Marine Environmental Research*. No. 53, pp.175–197.

Kunito, T., Nakamura, S., Ikemoto, T., Anan, Y., Kubota, R., Tanabe, S., Rosas, F.C.W., Fillmann, G., Readman, J.W. 2004. "Concentration and Subcellular Distribution of Trace Elements in Liver of Small Cetaceans Incidentally Caught Along the Brazilian Coast", *Marine Pollution Bulletin*. No. 49, pp.574–587.

Law, R.J., Morris, R.J., Allchin, C.R., Jones, B.R., Nicholson, M.D. 2003. "Metals and Organochlorines in Small Cetaceans Stranded on the East Coast of Australia", *Marine Pollution Bulletin*. No.46, pp.1200–1211.

Lehn, S.A., Warner, K.A., Huang, M., Hieftje, G.M., 2003. "Effect of Sample Matrix on the Fundamental Properties of the Inductively Coupled Plasma", *Spectrochimica Acta B*. No. 58, pp. 1785-1806.

Lopez-Molinero, A., Caballero, A.V., Castillo, J.R., 1994. "Classification of Emission Spectral Lines in Inductively Coupled Plasma Atomic Emission Spectroscopy Using Principal Component Analysis", *Spectrochimica Acta B*. No. 49, pp. 677-682.

Maestre, S., Mora, J., Todoli, J.L., Canals, A., "Evaluation of Several Commercially Available Spray Chambers for Use in Inductively Coupled Plasma Optical Emission Spectrometry", Journal of Analytical Atomic Spectrometry,, 1999, 14, 61-67.

Martin, M.B., Voeller, H.J., Gelmann, E.P., Lu, J., Stoica, E-G., Hebert, E.J., Reiter, R., Singh, B., Danielsen, M., Pentecost, E., Stoica, A. 2002. "Role of Cadmium in the Regulation of AR Gene Expression and Activity", *Endocrinology*. No. 143, pp 263-275.

Masson, P., 1999. "Matrix Effect during Trace Element Analysis in Plant Samples by Inductively Coupled Plasma Atomic Emission Spectrometry with Axial View Configuration and Pneumatic Nebulizer", *Spectrochimica Acta B*. No. 54, pp.603-612.

Masson, P., Vives, A., Orignac, D., Prunet, T., 2000. "Influence of Aerosol Desolvation from the Ultrasonic Nebulizer on the Matrix Effect in Axial View Inductively Coupled Plasma Atomic Emission Spectrometry", *Journal of Analytical Atomic Spectrometry,* No.15, pp. 543-547.

Méndez, L., Alvarez-Castañeda, S.T., Acosta, B., Sierra-Beltrán, A.P. 2002. "Trace Metals in Tissues of Gray Whale (*Eschrichtius Robustus*) Carcasses from the Northern Pacific Mexican Coast", *Marine Pollution Bulletin*. No. 44, pp.217–221.

Mermet, J.-M., 1991. "Use of Magnesium as a Test Element for Inductively Coupled Plasma Atomic Emission Spectrometry Diagnostics", *Analytica. Chimica Acta*. No. 250, pp. 85-94.

Mermet, J.-M., 1998. "Revisitation of the Matrix Effects in Inductively Coupled Plasma Atomic Emission Spectrometry: The Key Role of the Spray Chamber", *Journal of Analytical Atomic Spectrometry,* No. 13, 419-422.

Mermet, J.-M., 2002. "Trends in Instrumentation and Data Processing in ICP-OES", *Journal of Analytical Atomic Spectrometry,* No. 17, pp. 1065 - 1071.

Mermet, J.-M., 2005. “Is It Still Possible, Necessary and Beneficial to Peform Research in ICP-Atomic Emission Spectrometry?”, *Journal of Analytical Atomic Spectrometry,* No. 20, pp. 11-16.

Mermet, J.M. and Ivaldi, J.C., 1993. “Real-Time Internal Standardization for Inductively Coupled Plasma Atomic Emission Spectrometry Using a Custom Segmented-Array Charge Coupled Device Detector”, *Journal of Analytical Atomic Spectrometry,* No. 8, pp. 795-801.

Miller, J.N. and Miller J.C., 2000 (4^{th} edn). *Statistics and Chemometrics for Analytical Chemistry*, (Pearson Education Limited, England), pp. 217 – 218.

Monaci, F., Borrel, A., Leonzio, C., Marsili, L., Calzada, N. 1998. “Trace Elements in Striped Dolphins *(Stenella Coeruleoalba)* from the Western Mediterranean”, *Environmental Pollution*. No. 99, pp. 61-68.

Mora, J., Maestre, S., Hernandis, V., Todoli, J.L., 2003. “Liquid-Sample Introduction in Plasma Spectrometry”, *Trends Anal. Chem.*, No. 22, 123-132.

Moreda-Piñeiro, A., Marcos, A., Fisher, A., Hill, S.J., 2001. “Chemometrics Approaches for the Study of Systematic Error in Inductively Coupled Plasma Atomic Emission Spectrometry and Mass Spectrometry”, *Journal of Analytical Atomic Spectrometry,* No. 16, pp. 350-359.

Mössner, S. and Ballschmiter, K. 1997. “Marine Mammals as Global Pollution Indicators for Organochlorines”, *Chemosphere*. No. 34, pp.1285-1296.

Myers, S.A. and Tracy, D.H., 1983. “Improved Performance Using Internal Standardization in Inductively-Coupled Plasma Emission Spectroscopy”, *Spectrochimica Acta B.* No. 38, pp. 1227-1253.

NIST/NOAA, 2004. National Marine Analytical Quality Assurance Program - Description and Results of the 2003 Interlaboratory Comparison Exercise for the Determination of Trace Elements in Marine Mammals, First draft to participants, National Institute of Standards and Technology, USA.

Nixon, D.E., Burritt, M.F., Moyer, T.P. 1999. “The Determination of Mercury in Whole Blood and Urine by Inductively Coupled Plasma Mass Spectrometry”, *Spectrochimica Acta B.* No. 54, pp.1141-1153

Novotny, I., Farinas, J.C., Jia-liang, W., Poussel, E., Mermet, J.M., 1996. “Effect of Power and Carrier Gas Flow Rate on the Tolerance to Water Loading in Inductively Coupled Plasma Atomic Emission Spectrometry”, *Spectrochimica Acta B.* No. 51, pp. 1517-1526.

Nölte, J., 2003. ICP Emission Spectrometry, A Practical Guide. (Wiley-VCH, Germany), pp. 1-123

Otto, M., 1998. *Chemometrics. Statistics and Computer Application in Analytical Chemistry*, (Wiley-WCH, New York), pp. 124 – 126.

Paul, M.C., and Toia, R.F. 2003. "E.I.A Novel Method for the Determination of Mercury And Selenium in Shark Tissue Using High-Resolution Inductively Coupled Plasma-Mass Spectrometry" Spectrochimica Acta B. No. 58, pp.1687–1697

Ponce, R.A., Egeland, G.M., Middaugh, J.P., Becker, P.R. 1997. "Twenty Years of Trace Metal Analyses of Marine Mammals: Evaluation and Summation of Data from Alaska and Other Arctic Regions", *Section of Epidemiology*. No. 1

Pugh, R.S., Kucklick, J.R., Christopher, S.J., Vander Pol, S.S., Becker, P.R., Porter, B.J., Mackey, E.A., Schantz, M.M., Demiralp, R., Wise, S.A. 2003. National Marine Mammal Tissue Bank CY 2002 Report, National Institute of Standards and Technology, USA.

Romero, X., Poussel, E., Mermet, J.-M., 1997a. "Influence of the Operating Conditions on the Efficiency of Internal Standardization in Inductively Coupled Plasma Atomic Emission Spectrometry", *Spectrochimica Acta B*. No. 52, pp. 487-493.

Romero, X., Poussel, E., Mermet, J.-M., 1997b. "The Effect of Sodium on Analyte Ionic Line Intensities in Inductively Coupled Plasma Atomic Emission Spectrometry: Influence of the Operating Conditions", *Spectrochimica Acta B*. No. 52, pp. 495-502.

Ruelas-Inzunza, J. and Páez-Osuna, F. 2002. "Distribution of Cd, Cu, Fe, Mn, Pb and Zn in Selected Tissues of Juvenile Whales Stranded in the SE Gulf of California (Mexico)", *Environment International*. No. 28, pp.325–329.

Ryan, A. 1998. "Analysis of Blood Serum on the Liberty Series II ICP-OES with the axially-viewed plasma", *ICP-OES Varian instruments at work*, ICP-24, pp.1-9.

Sedcole, J.R., Lee, J., Pritchard, M.W., 1986. "Internal Standard Selection in the Presence of Matrix Interactions in an Inductively Coupled Argon Plasma Optimized for Simultaneous Multielement Analysis by Atomic Emission Spectrometry", *Spectrochimica Acta B.* No. 41, pp. 227-235.

Sesi, N.N., Hieftje, G.M., 1996. "Studies Into The Interelement Matrix Effect in Inductively Coupled Plasma Spectrometry", *Spectrochimica Acta B.* No. 51, pp. 1601-1628.

Skoog, A.D., Holler, F.J., Nieman, T.A., 1998 (5^{th} Edn). Principles of Instrumental Analysis. Saunders College Publishing, U.S.), pp. 231

Stepan, M., Musil, P., Poussel, E., Mermet, J.M., 2001. "Matrix-Induced Shift Effects in Axially Viewed Inductively Coupled Plasma Atomic Emission Spectrometry", *Spectrochimica Acta B*. No. 56, pp. 443-453.

Stewart, I.I. and Olesik, J.W., 1998a. "The Effect of Nitric Acid Concentration and Nebulizer Gas Flow Rates on Aerosol Properties and Transport Rates in Inductively Coupled Plasma Sample Introduction", *Journal of Analytical Atomic Spectrometry,* No.13, pp. 1249-1256.

Stewart, I.I. and Olesik, J.W., 1998b. "Steady-State Acid Effects in ICP-MS", *Journal of Analytical Atomic Spectrometry,* No. 13, pp. 1313-1320.

Sun, Y.-C, Wu, S.-H, Lee, C.-C., 2003. "Investigation of Non-Spectroscopic Interference and Internal Standardization Method in Axially and Radially Viewed Inductively Coupled Plasma Optical Emission Spectrometry Using Cross-Flow and Ultrasonic Nebulization", *Journal of Analytical Atomic Spectrometry,* No. 18, pp. 1163 – 1170.

Tilbury, K.L., Stein, J.E., Krone, C.A., Brownell Jr., R.L., Blokhin, S.A., Bolton, J.L., Ernest, D.W. 2002. "Chemical Contaminants in Juvenile Gray Whales (*Eschrichtius Robustus*) from a Subsistence Harvest in Arctic Feeding Grounds", *Chemosphere*. No. 47, pp.555–564.

Todoli, J.L. and Mermet, J.M., 1998. "Minimization of Acid Effects at Low Consumption Rates in an Axially Viewed Inductively Coupled Plasma Atomic Emission Spectrometer by Using Micronebulizer-Based Sample Introduction Systems", *Journal of Analytical Atomic Spectrometry,* No. 13, pp. 727-734.

Todoli, J.-L. and Mermet, J.-M., 1999. "Acid Interferences in Atomic Spectrometry,: Analyte Signal Effects and Subsequent Reduction", *Spectrochimica Acta B*. No. 54, pp. 895-929.

Todoli, J.-L. and Mermet, J.-M., 2000. "Effect of the Spray Chamber Design on Steady and Transient Acid Interferences in Inductively Coupled Plasma Atomic Emission Spectrometry", *Journal of Analytical Atomic Spectrometry,* No. 15, pp. 863-867.

Todoli, J.-L., Mermet, J.-M., Canals, A., Hernandis, V., 1998. "Acid Effects in Inductively Coupled Plasma Atomic Emission Spectrometry with Different Nebulizers Operated at Very Low Sample Consumption Rates", *Journal of Analytical Atomic Spectrometry,* No.13, pp. 55-62.

Todoli, J.-L., Gras, L., Hernandis, V., Mora, J., 2002. "Elemental Matrix Effects", *Journal of Analytical Atomic Spectrometry,* No.17, pp. 142-169.

Tyler, G., 1994. "ICP-MS, or ICP-OES and AAS?-A Comparison", *Varian ICP-MS Instruments At Work*, ICP-MS-1, pp.1-7.

Villaneuva, M., Catasus, M., Salin, E.D., Pomares, M., 2000. "Study of Mixed-Matrix Effects Induced by Ca and Mg in ICP-OES", *Journal of Analytical Atomic Spectrometry,* No. 15, pp. 877-881.

Van Den Broeck, K., Vandecasteele, C., Geuns, J.M.C., 1997. "Determination of Arsenic by Inductively Coupled Plasma Mass Spectrometry in Mung Bean Seedlings for Use as a Bio-indicator of Arsenic Contamination", *Journal of Analytical Atomic Spectrometry,* No.12, pp. 987-991.

Van Veen, E.H. and de Loos-Vollebregt, M.T.C., 1999. "On the Use of Line Intensity Ratios and Power Adjustments to Control Matrix Effects in Inductively Coupled Plasma Optical Emission Spectrometry", *Journal of Analytical Atomic Spectrometry,* No. 14, pp. 831-838.

WEB_1, 2003. Site for the cetaceans (15/01/2003). http://www.cetecean.org

Yılmaz, A.B. 2003. "Levels of Heavy Metals (Fe, Cu, Ni, Cr, Pb, and Zn) in Tissue of Mugil Cephalus and Trachurus Mediterraneus from Iskenderun Bay, Turkey", *Environmental Research*. No. 92, pp.277–281.

Zhou, J.L., Salvador, S.M., Liu, Y.P., Sequeira, M. 2001. "Heavy Metals in the Tissues of Common Dolphins (*Delphinus Delphis)* Stranded on the Portuguese Coast", *The Science of the Total Environment*. No. 273, pp.61-76.

APPENDIX A

CORRECTED CONCENTRATIONS BY USING ARGON AND HIDROJEN AS THE INTERNAL STANDARDS

Table A.1.The calculated concentrations for Cd I 228 and Cd II 214 in the validation study by using argon and hydrogen as the internal standards

Sample	Cd 228/Ar 750	Cd 228/Ar 751	Cd 228/H 656	Cd 228/H 486	Cd 214/Ar 750	Cd 214/Ar 751	Cd 214/H 656	Cd 214/H 486
3	1.03 ± 0.02	1.03 ± 0.01	1.03 ± 0.02	0.90 ± 0.03	1.02 ± 0.02	1.02 ± 0.01	1.02 ± 0.02	0.89 ± 0.03
6	0.82 ± 0.02	0.82 ± 0.03	0.99 ± 0.02	0.96 ± 0.03	0.84 ± 0.003	0.84 ± 0.01	1.01 ± 0.03	0.98 ± 0.02
9	0.70 ± 0.01	0.71 ± 0.01	1.00 ± 0.04	2.96 ± 3.23	0.75 ± 0.01	0.76 ± 0.01	1.07 ± 0.03	3.14 ± 3.40
12	0.73 ± 0.01	0.75 ± 0.01	1.10 ± 0.06	2.08 ± 1.46	0.83 ± 0.004	0.84 ± 0.003	1.24 ± 0.06	2.36 ± 1.66
15	0.72 ± 0.01	0.73 ± 0.01	1.09 ± 0.05	2.97 ± 3.20	0.8 ± 0.01	0.82 ± 0.01	1.21 ± 0.06	3.31 ± 3.56
18	0.7 ± 0.01	0.71 ± 0.01	1.11 ± 0.05	1.26 ± 0.13	0.77 ± 0.01	0.78 ± 0.02	1.22 ± 0.05	1.38 ± 0.15
21	0.7 ± 0.01	0.71 ± 0.003	1.29 ± 0.01	7.48 ± 10.52	0.79 ± 0.01	0.8 ± 0.01	1.45 ± 0.02	8.36 ± 11.73
24	0.65 ± 0.01	0.67 ± 0.005	1.26 ± 0.05	3.55 ± 3.43	0.74 ± 0.01	0.75 ± 0.01	1.42 ± 0.04	3.98 ± 3.78
27	0.61 ± 0.01	0.62 ± 0.01	1.40 ± 0.23	6.00 ± 7.99	0.69 ± 0.01	0.7 ± 0.01	1.57 ± 0.28	6.64 ± 8.78

Table A.2. The values calculated for Cd I 228 and Cd II 214 lines in the analysis of beluga whale liver samples by using argon and hydrogen as the internal standards

Sample	Cd 228/Ar 751	Cd 228/H 656	Cd 214/Ar 751	Cd 214/H 656
S6	2.57	2.43	2.58	2.48
S7	2.63	2.48	2.52	2.45

APPENDIX B

3-D GRAPHS FOR THE MATRIX INDUCED ERRORS

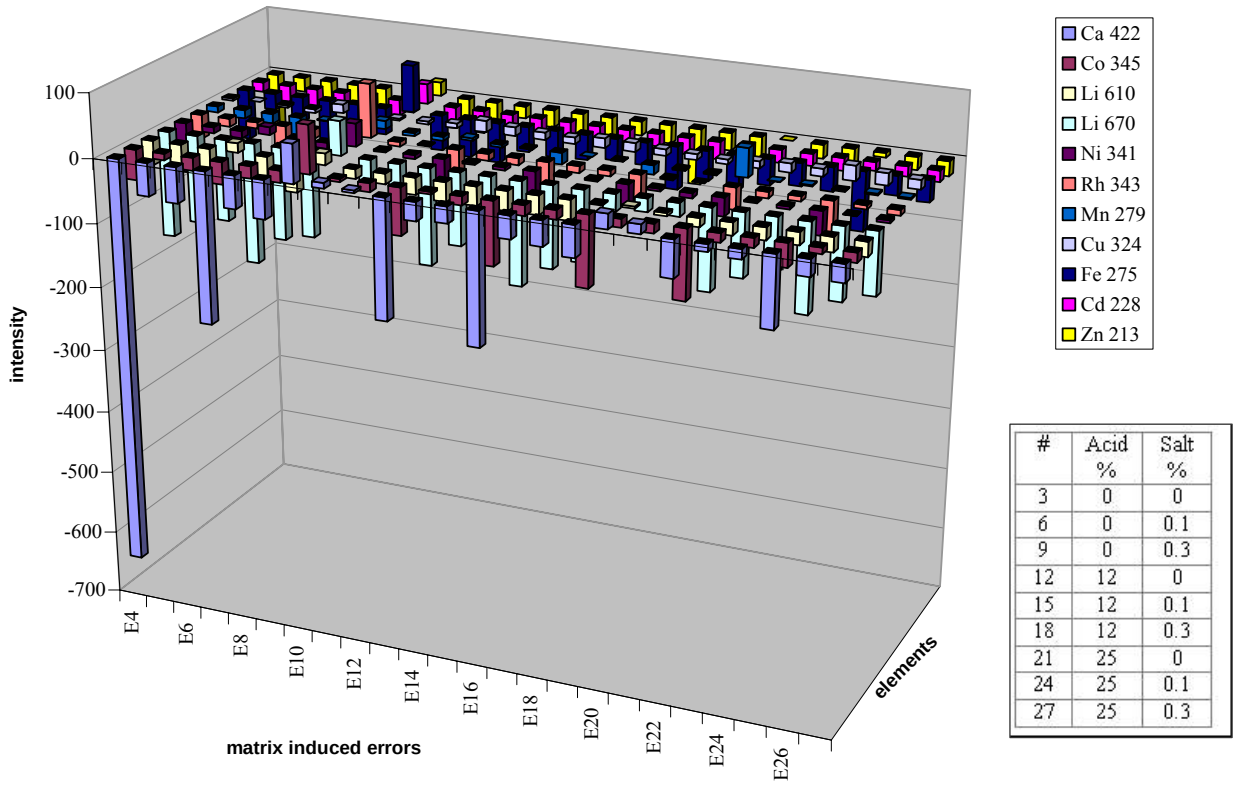

#	Acid %	Salt %
3	0	0
6	0	0.1
9	0	0.3
12	12	0
15	12	0.1
18	12	0.3
21	25	0
24	25	0.1
27	25	0.3

Figure B.1. 3-D graph for the matrix induced errors calculated for atom lines for generating the multielement score plot

APPENDIX B-1

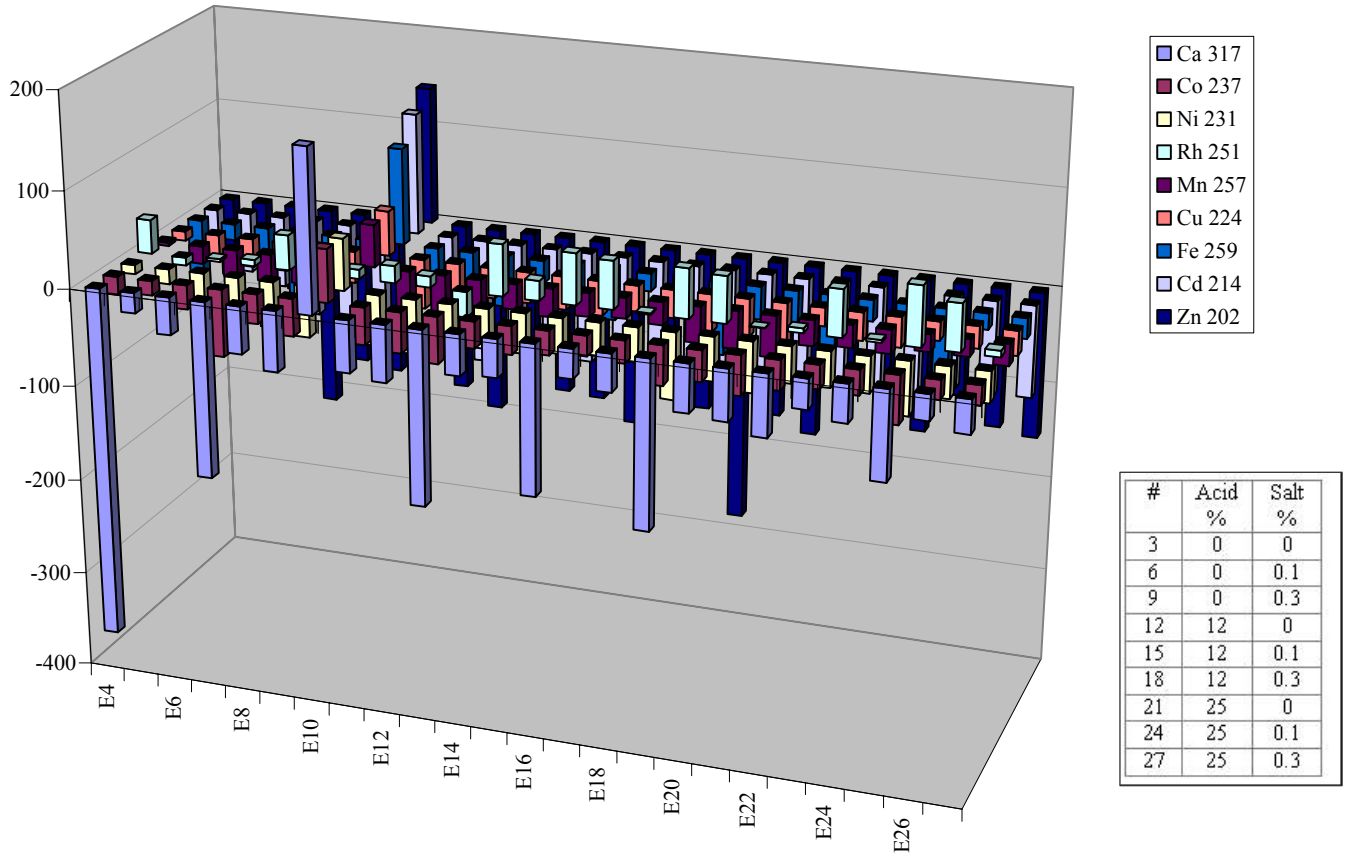

#	Acid %	Salt %
3	0	0
6	0	0.1
9	0	0.3
12	12	0
15	12	0.1
18	12	0.3
21	25	0
24	25	0.1
27	25	0.3

Figure B.2. 3-D graph for the matrix induced errors calculated for ion lines for generating the multielement score plot

APPENDIX B-2

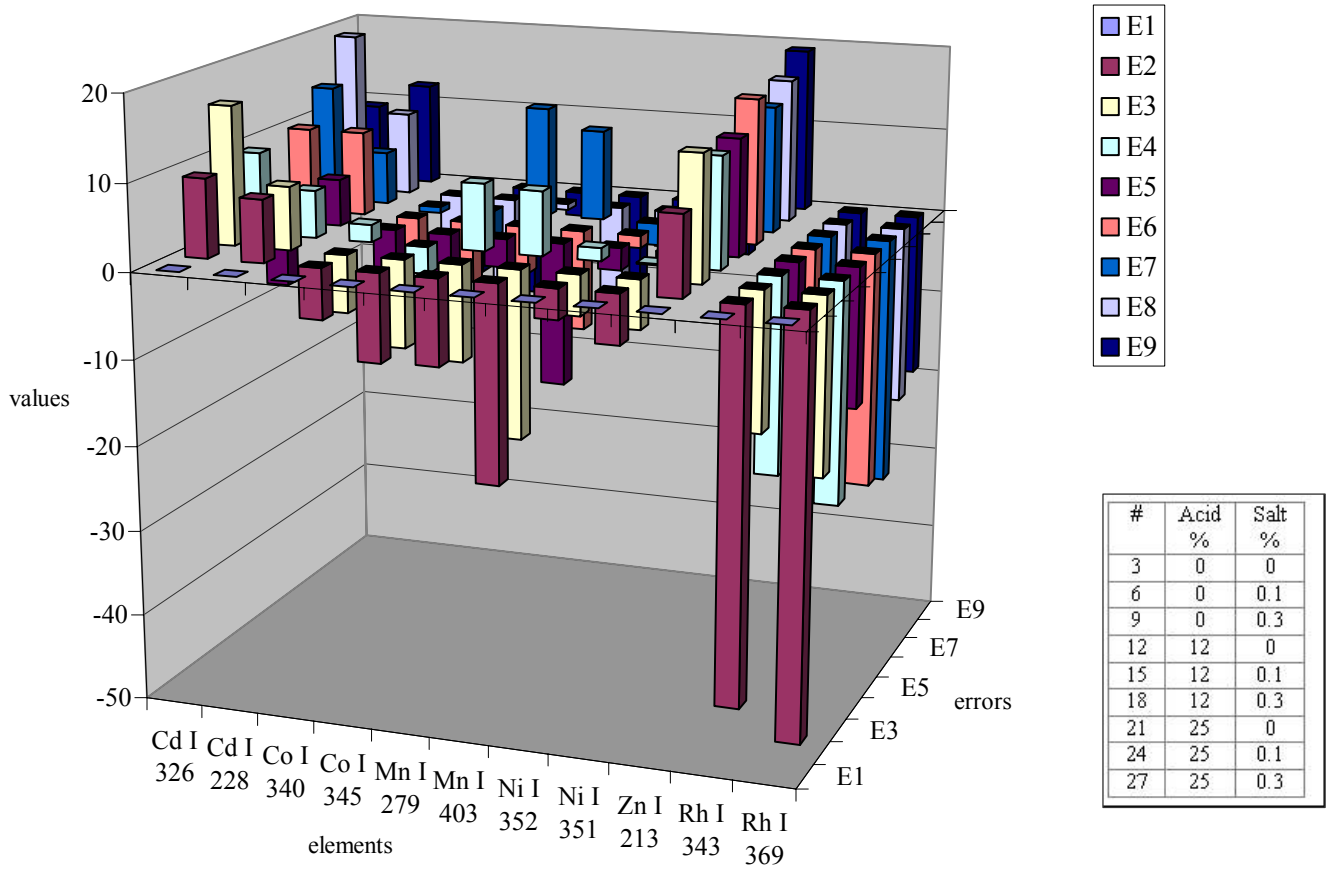

#	Acid %	Salt %
3	0	0
6	0	0.1
9	0	0.3
12	12	0
15	12	0.1
18	12	0.3
21	25	0
24	25	0.1
27	25	0.3

Figure B.3. 3-D graph for the matrix induced errors calculated for atom lines for generating the single element score plot

APPENDIX B-3

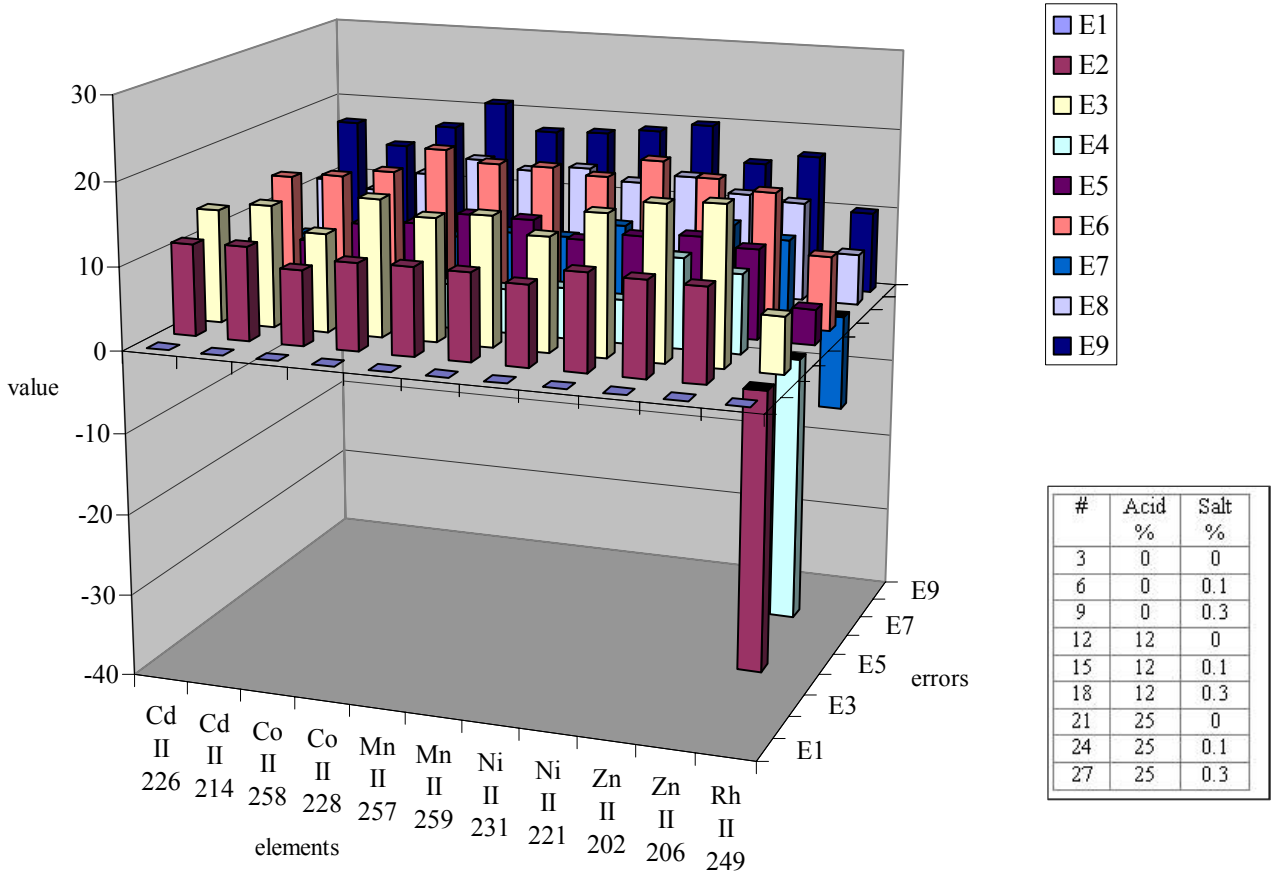

#	Acid %	Salt %
3	0	0
6	0	0.1
9	0	0.3
12	12	0
15	12	0.1
18	12	0.3
21	25	0
24	25	0.1
27	25	0.3

Figure B.4. 3-D graph for the matrix induced errors calculated for ion lines for generating the single element score plot

APPENDIX C

LINE GRAPHS FOR THE VALIDATION STUDY

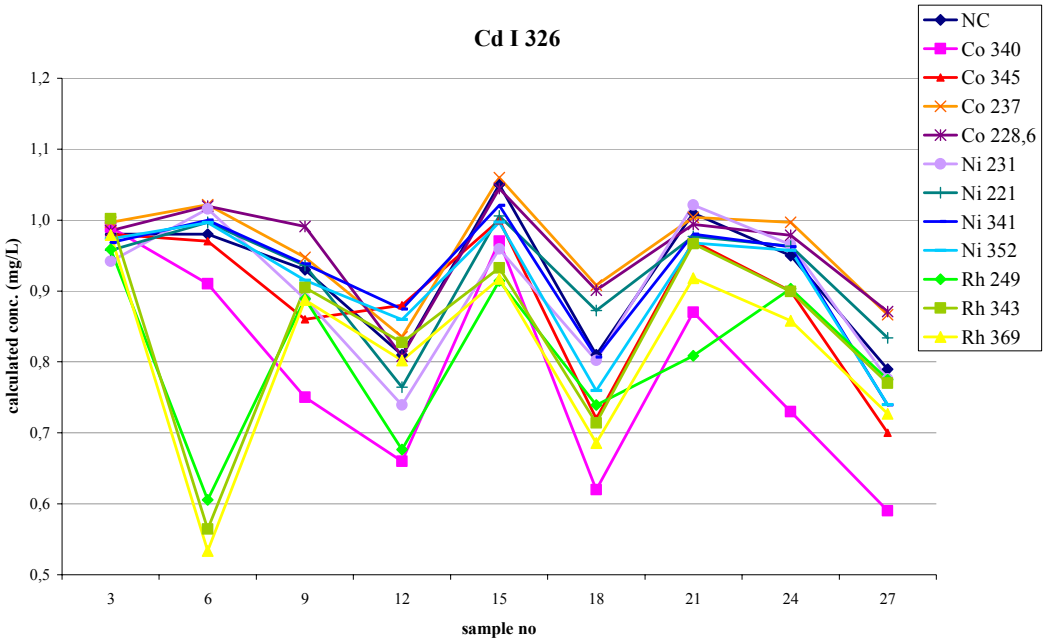

(a)

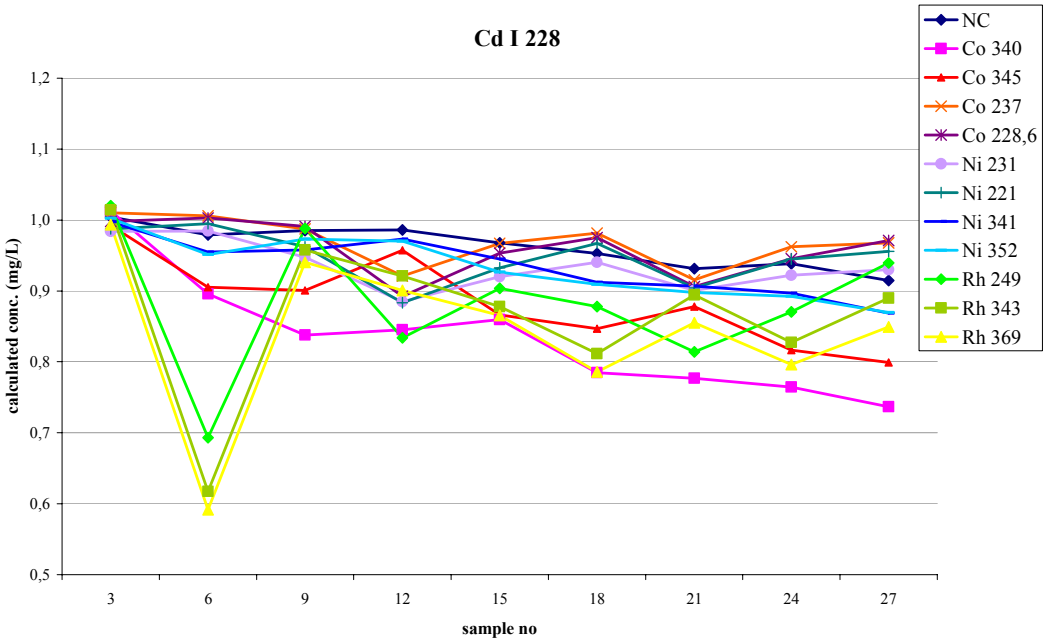

(b)

sample	3	6	9	12	15	18	21	24	27
Acid %	0	0	0	12	12	12	25	25	25
Salt %	0	0.1	0.3	0	0.1	0.3	0	0.1	0.3

Figure C.1. Line graphs for the Cd atom lines for the values obtained in the validation study: (a) for Cd I 326, (b) for Cd I 228

APPENDIX C-1

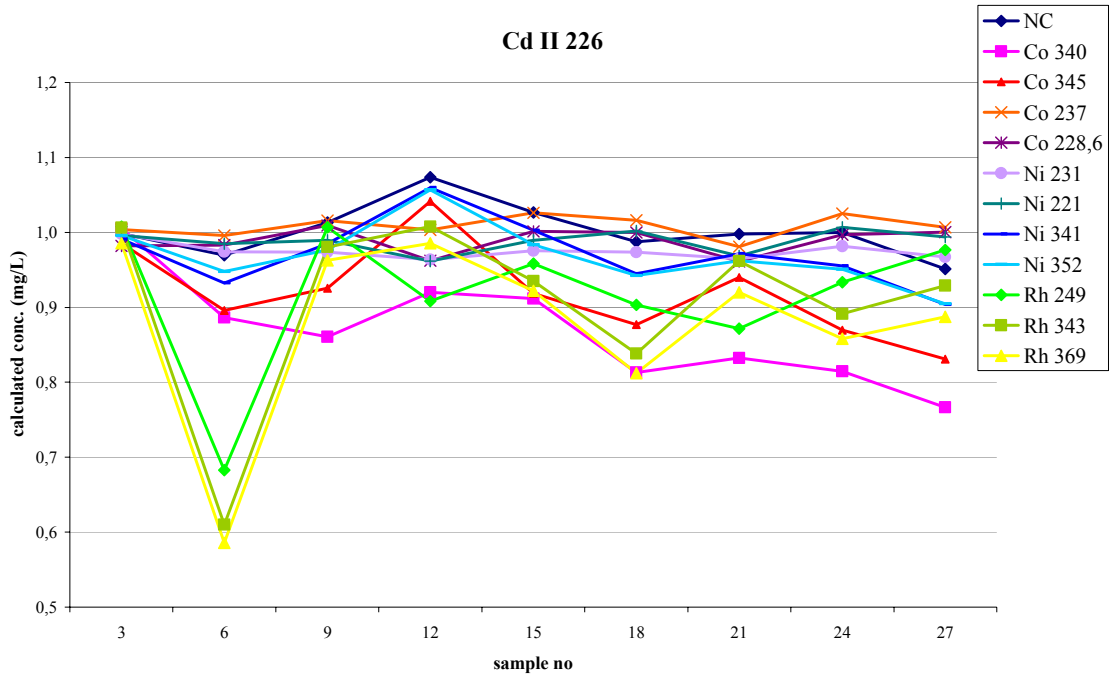

(a)

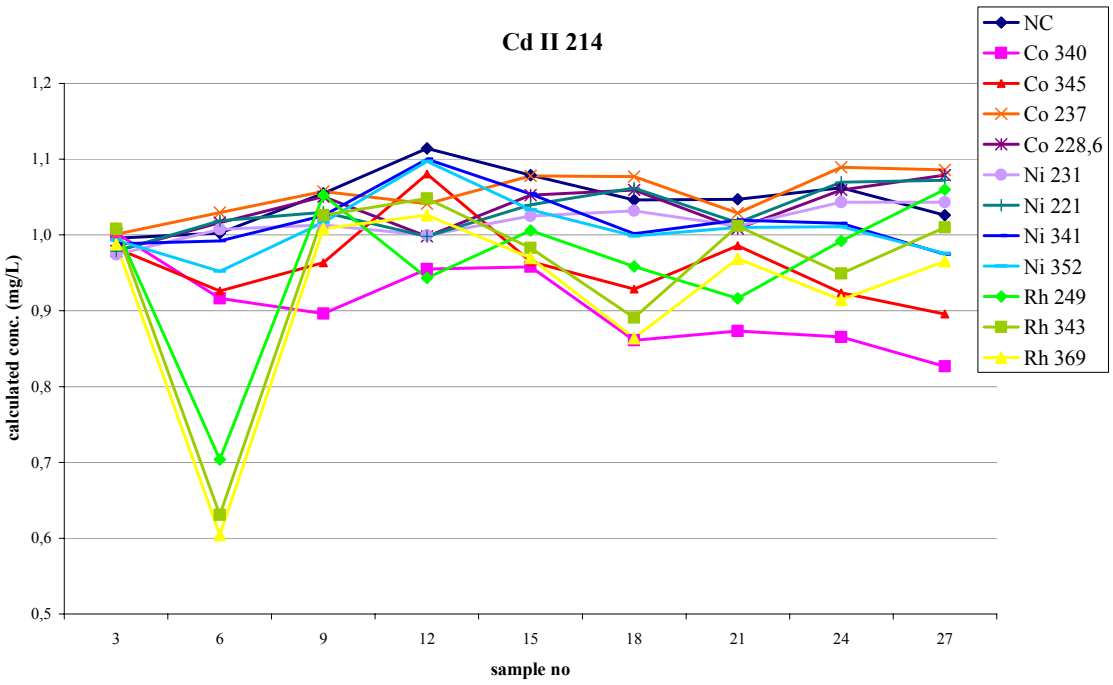

(b)

sample	3	6	9	12	15	18	21	24	27
Acid %	0	0	0	12	12	12	25	25	25
Salt %	0	0.1	0.3	0	0.1	0.3	0	0.1	0.3

Figure C.2. Line graphs for the Cd ion lines for the values obtained in the validation study: (a) for Cd II 226, (b) for Cd II 214

APPENDIX C-2

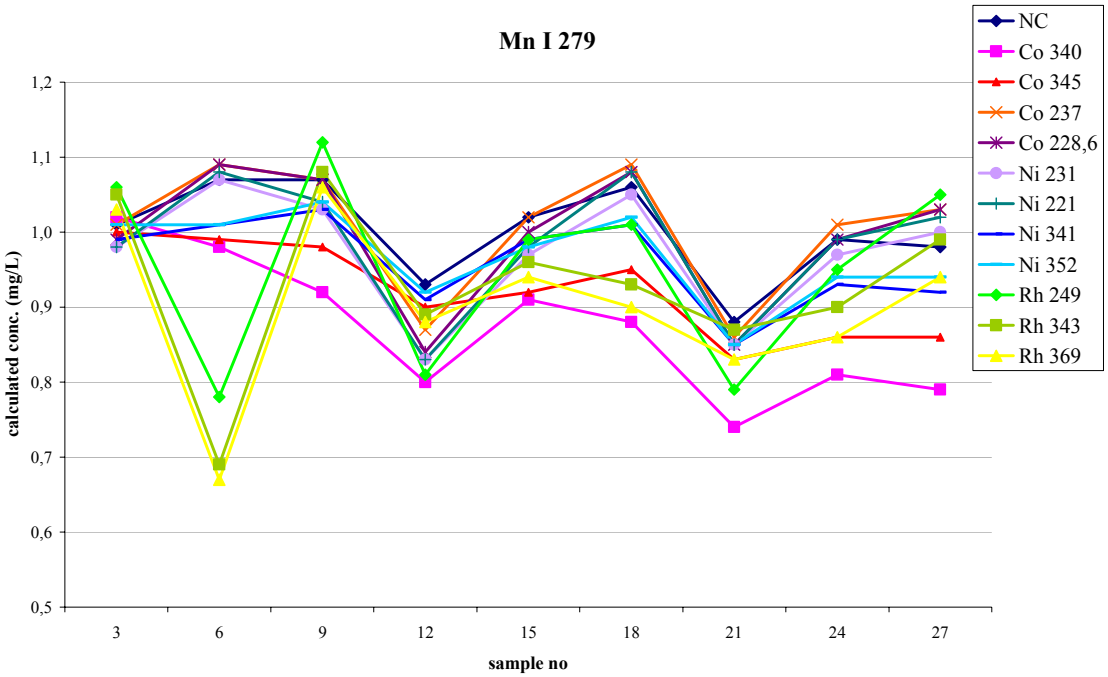

(a)

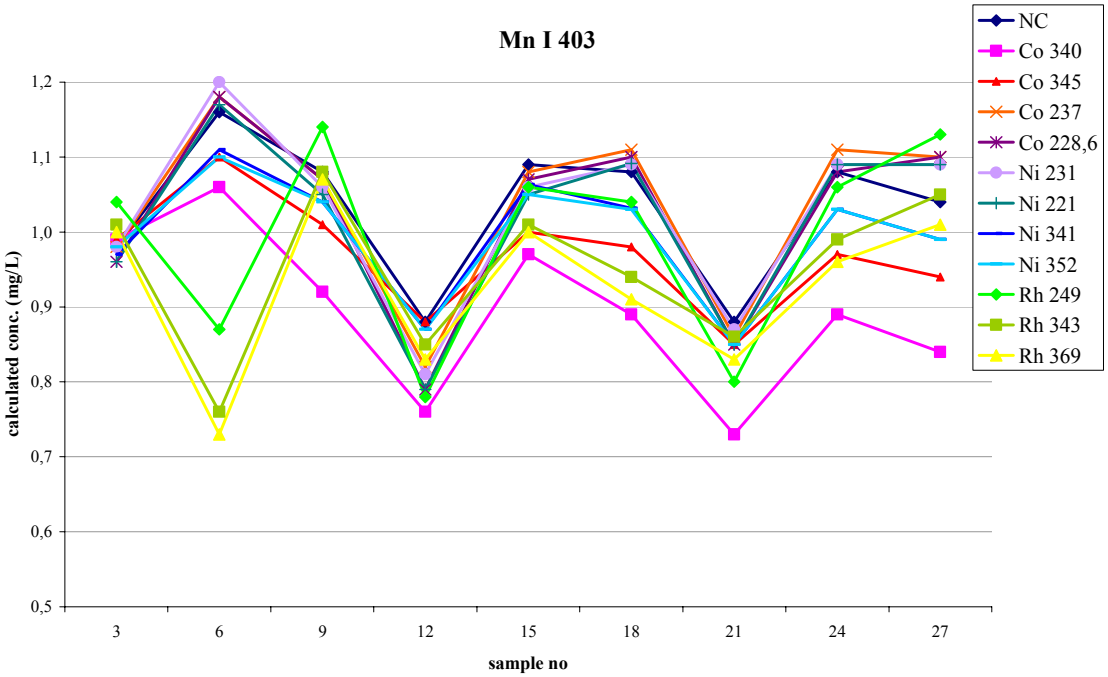

(b)

sample	3	6	9	12	15	18	21	24	27
Acid %	0	0	0	12	12	12	25	25	25
Salt %	0	0.1	0.3	0	0.1	0.3	0	0.1	0.3

Figure C.3. Line graphs for the Mn atom lines for the values obtained in the validation study: (a) for Mn I 279, (b) for Mn I 403

APPENDIX C-3

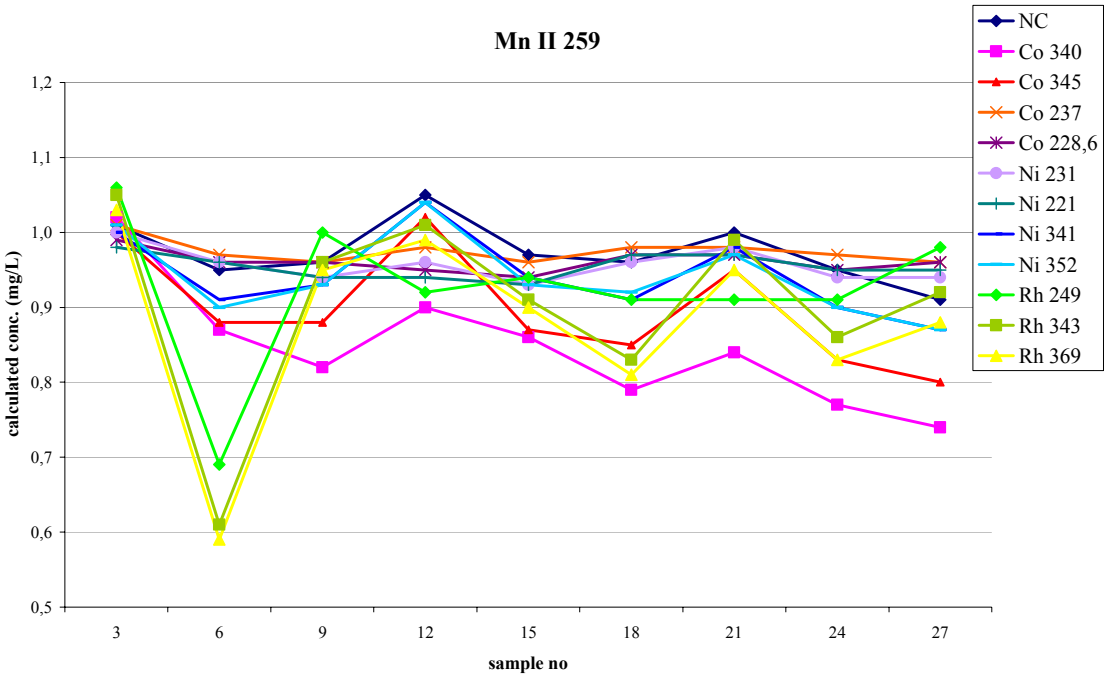

(a)

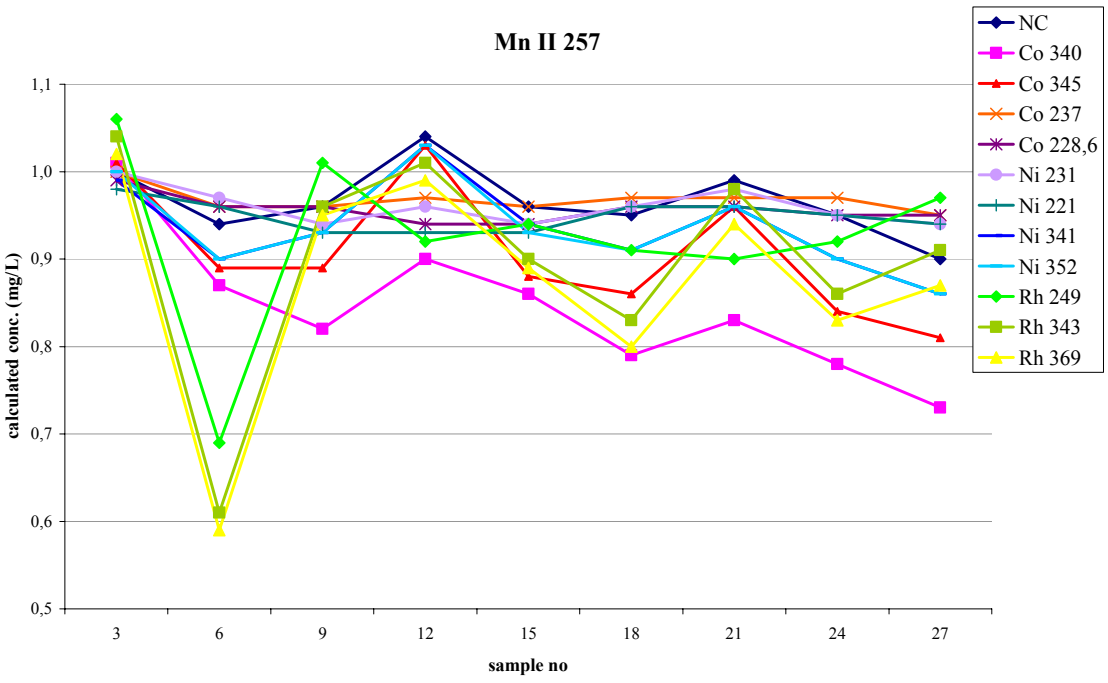

(b)

sample	3	6	9	12	15	18	21	24	27
Acid %	0	0	0	12	12	12	25	25	25
Salt %	0	0.1	0.3	0	0.1	0.3	0	0.1	0.3

Figure C.4. Line graphs for the Mn ion lines for the values obtained in the validation study: (a) for Mn II 259, (b) for Mn II 257

APPENDIX C-4

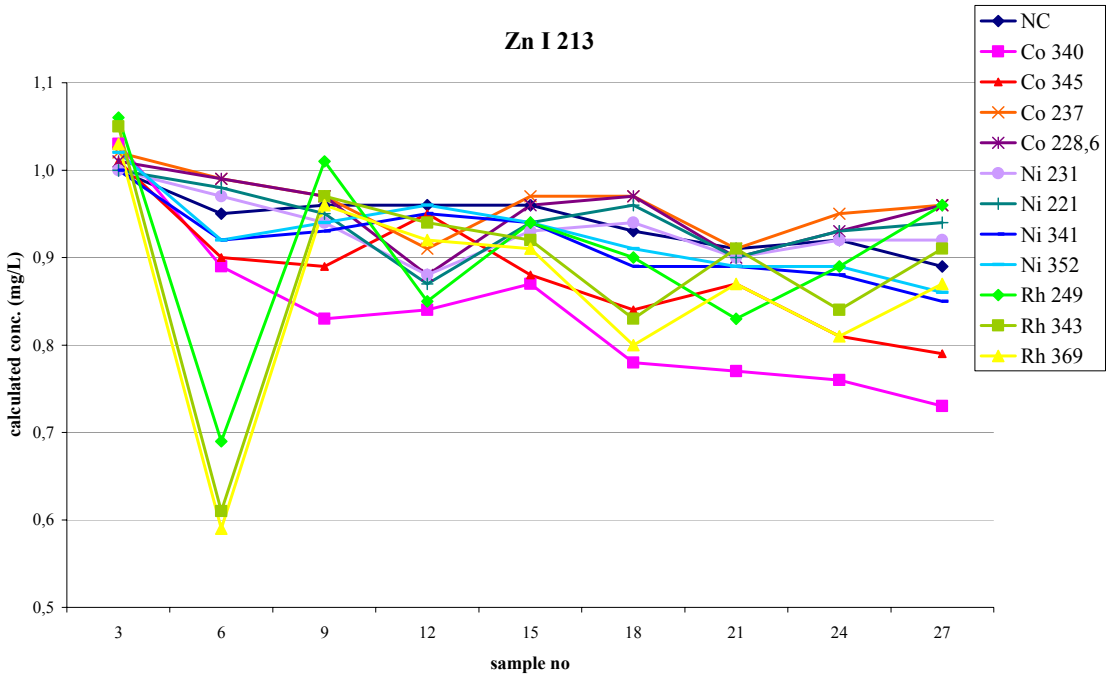

(a)

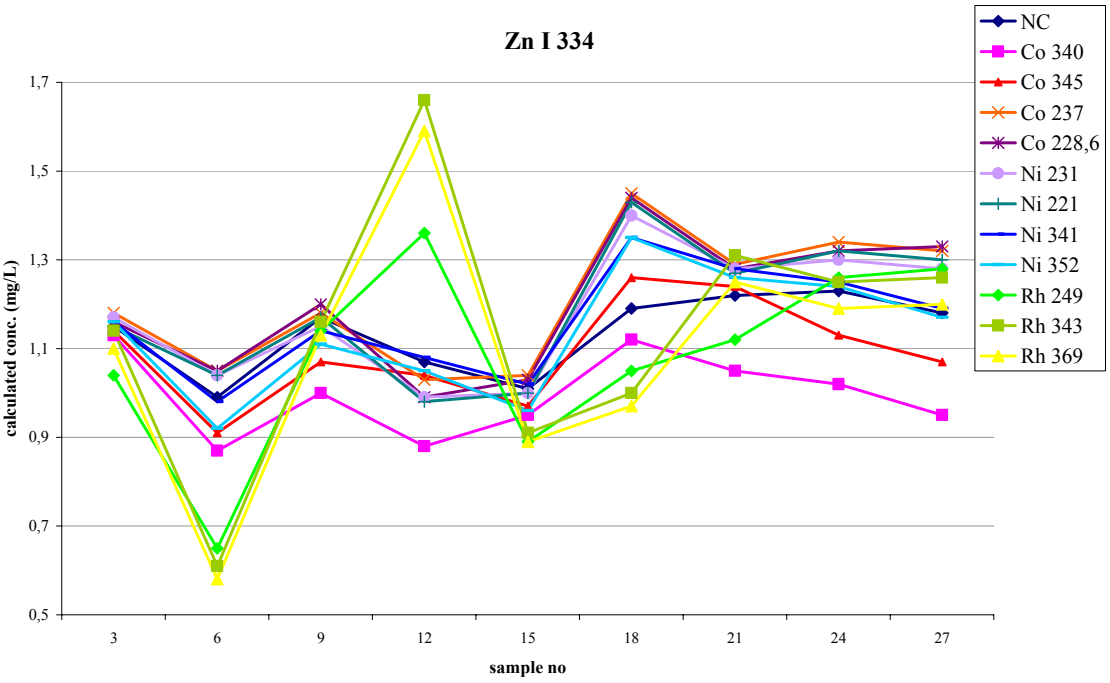

(b)

sample	3	6	9	12	15	18	21	24	27
Acid %	0	0	0	12	12	12	25	25	25
Salt %	0	0.1	0.3	0	0.1	0.3	0	0.1	0.3

Figure C.5. Line graphs for the Zn atom lines for the values obtained in the validation study: (a) for Zn I 213, (b) for Zn I 334

APPENDIX C-5

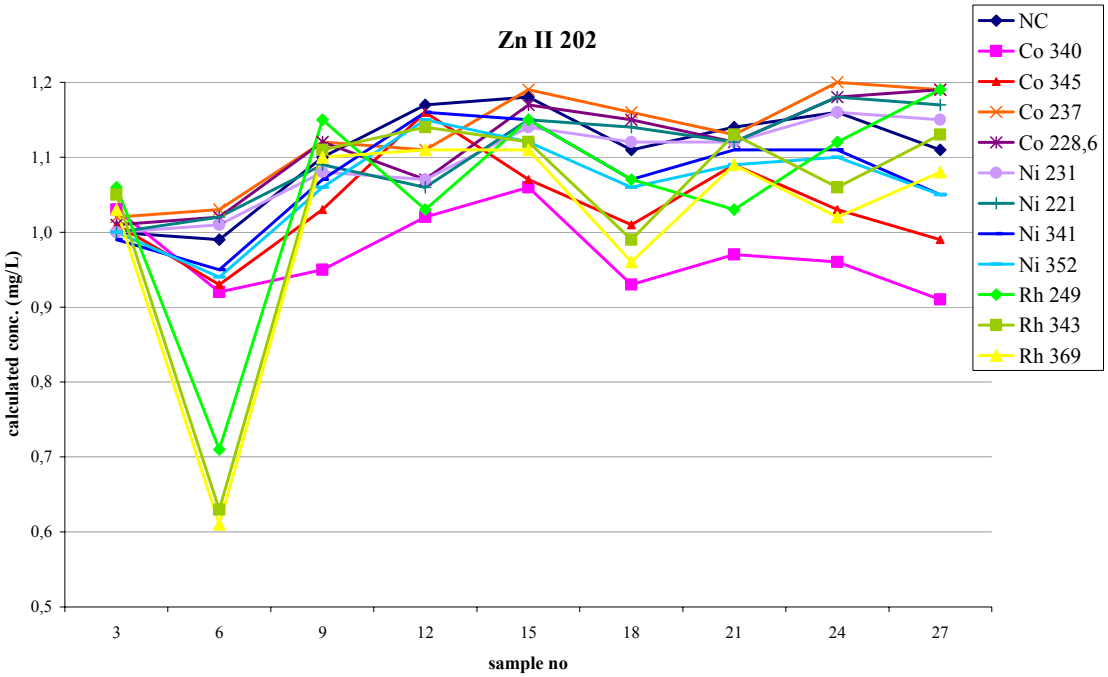

(a)

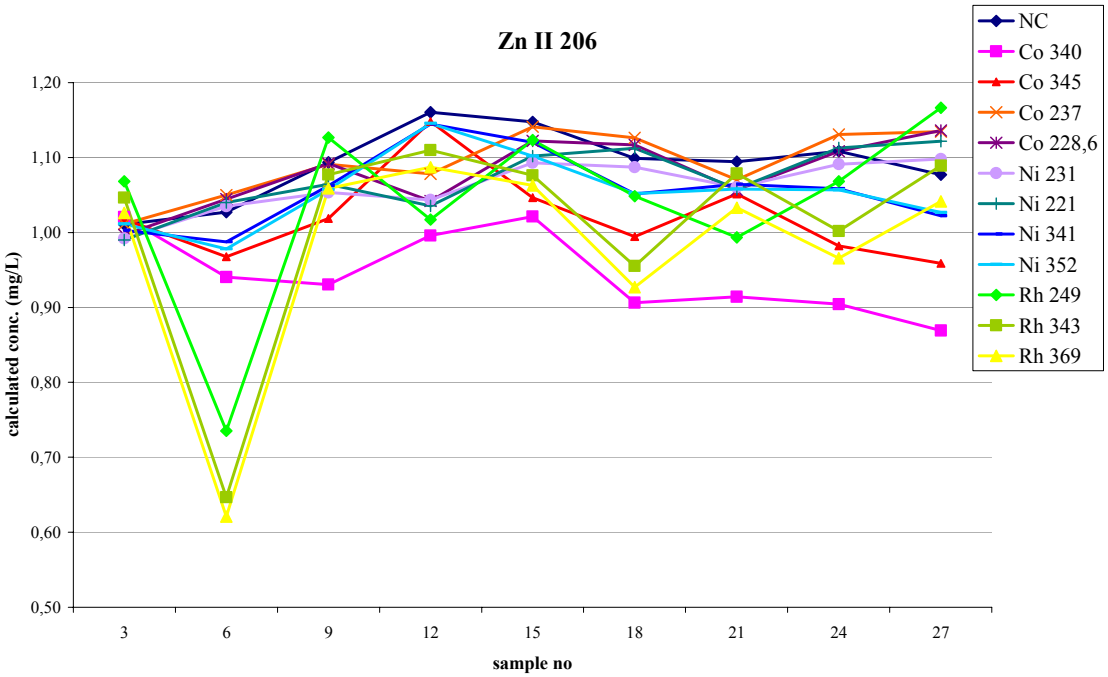

(b)

sample	3	6	9	12	15	18	21	24	27
Acid %	0	0	0	12	12	12	25	25	25
Salt %	0	0.1	0.3	0	0.1	0.3	0	0.1	0.3

Figure C.6. Line graphs for the Zn ion lines for the values obtained in the validation study: (a) for Zn II 202, (b) for Zn II 206

APPENDIX D

LINE GRAPHS FOR COMPARISON OF RESULTS

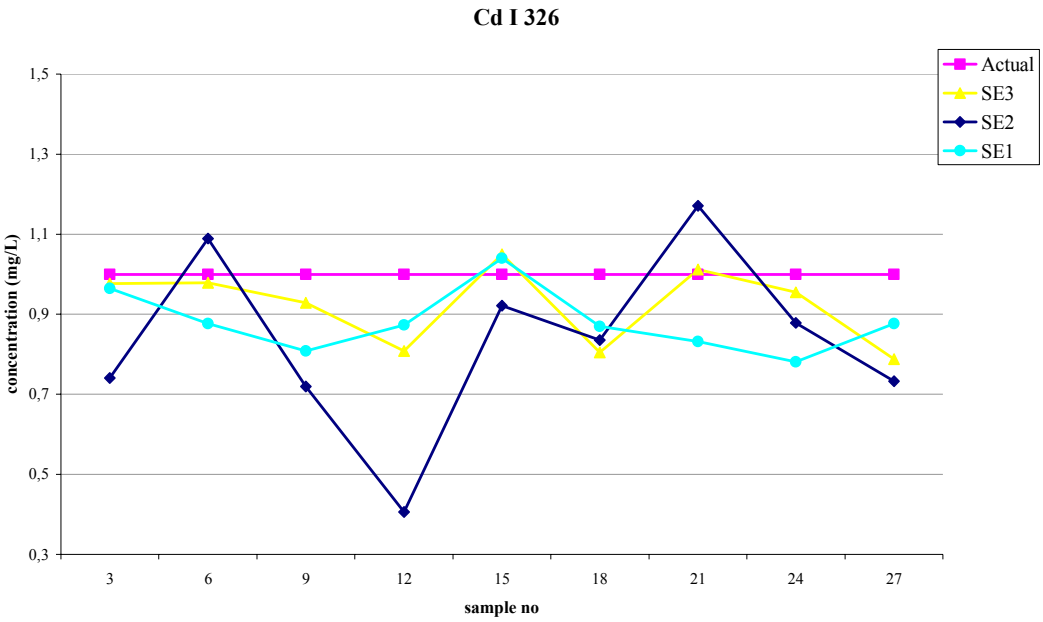

(a)

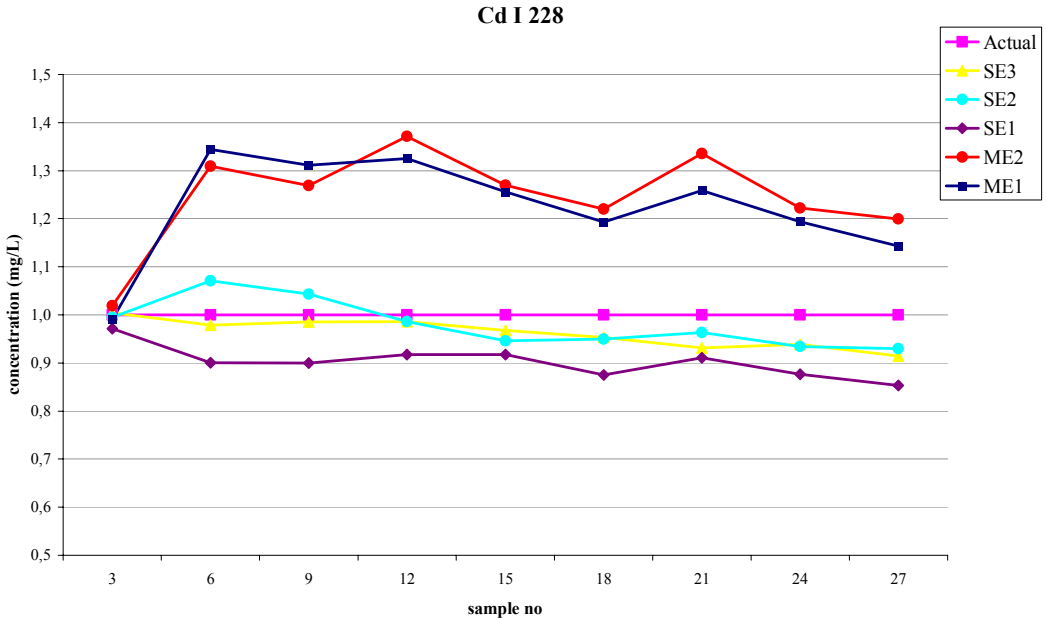

(b)

sample	3	6	9	12	15	18	21	24	27
Acid %	0	0	0	12	12	12	25	25	25
Salt %	0	0.1	0.3	0	0.1	0.3	0	0.1	0.3

Figure D.1. Line graphs for the Cd atom lines for comparison of the results from different experiments: (a) for Cd I 326, (b) for Cd I 228

APPENDIX D-1

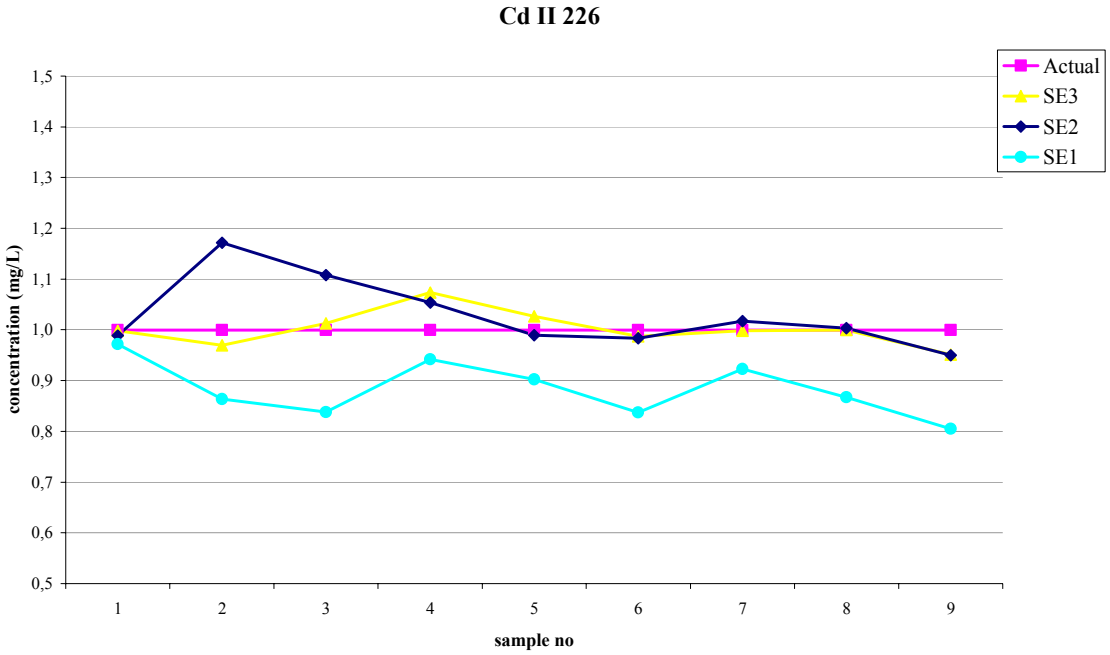

(a)

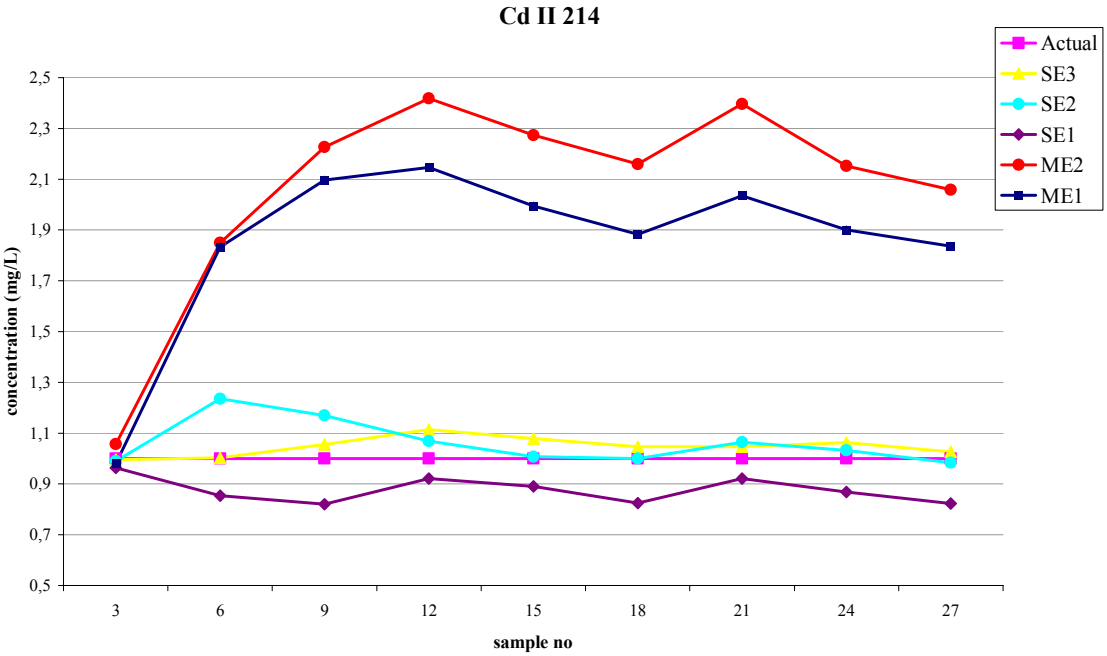

(b)

sample	3	6	9	12	15	18	21	24	27
Acid %	0	0	0	12	12	12	25	25	25
Salt %	0	0.1	0.3	0	0.1	0.3	0	0.1	0.3

Figure D.2. Line graphs for the Cd ion lines for comparison of the results from different experiments: (a) for Cd II 226, (b) for Cd II 214

APPENDIX D-2

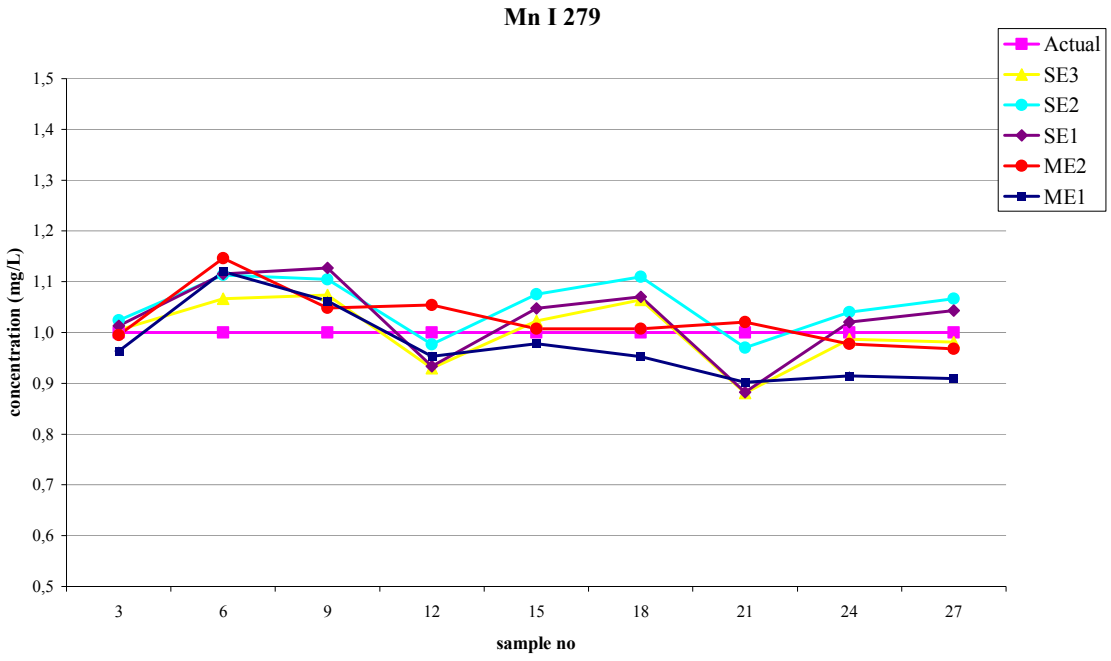

(a)

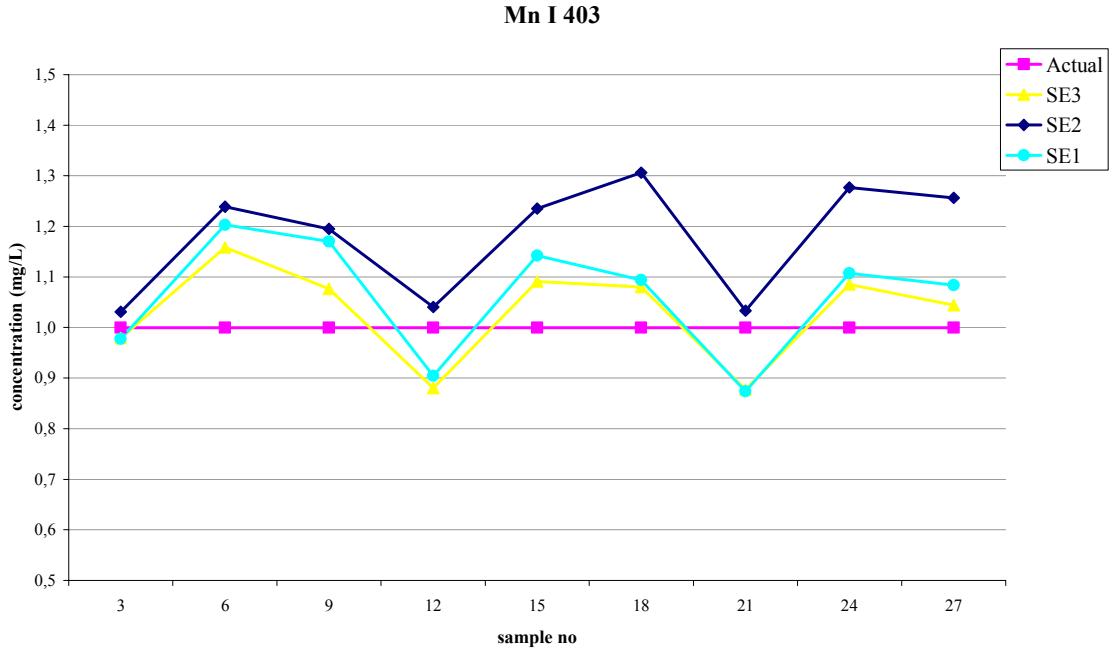

(b)

sample	3	6	9	12	15	18	21	24	27
Acid %	0	0	0	12	12	12	25	25	25
Salt %	0	0.1	0.3	0	0.1	0.3	0	0.1	0.3

Figure D.3. Line graphs for the Mn atom lines for the values obtained in the validation study: (a) for Mn I 279, (b) for Mn I 403

APPENDIX D-3

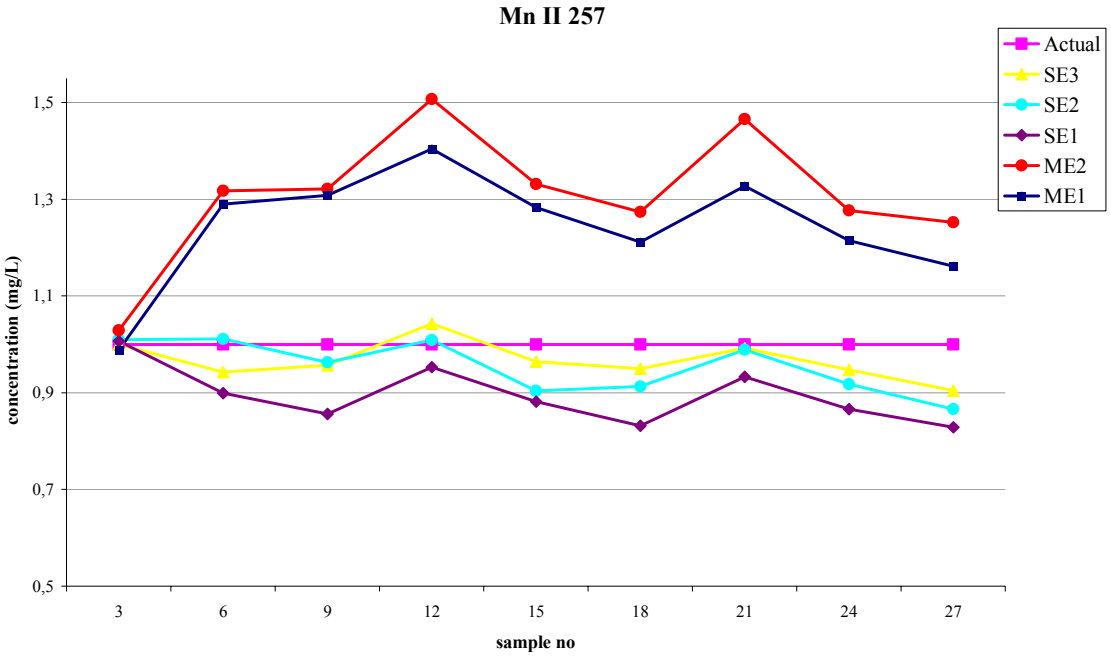

(a)

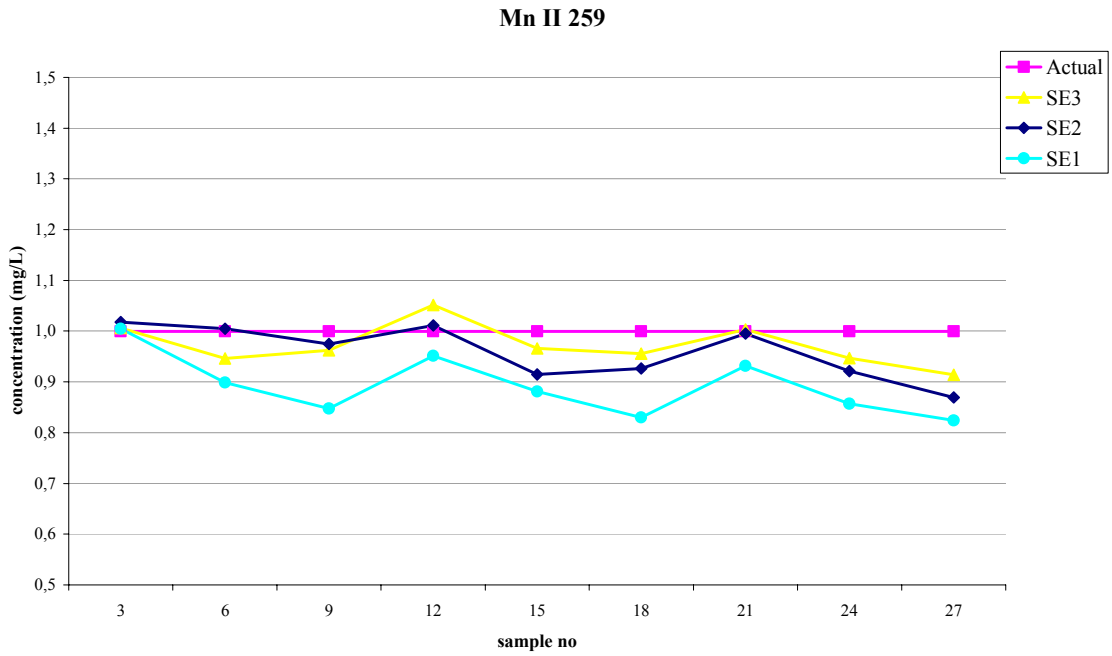

(b)

sample	3	6	9	12	15	18	21	24	27
Acid %	0	0	0	12	12	12	25	25	25
Salt %	0	0.1	0.3	0	0.1	0.3	0	0.1	0.3

Figure D.4. Line graphs for the Mn ion lines for the values obtained in the validation study: (a) for Mn II 259, (b) for Mn II 259

APPENDIX D-4

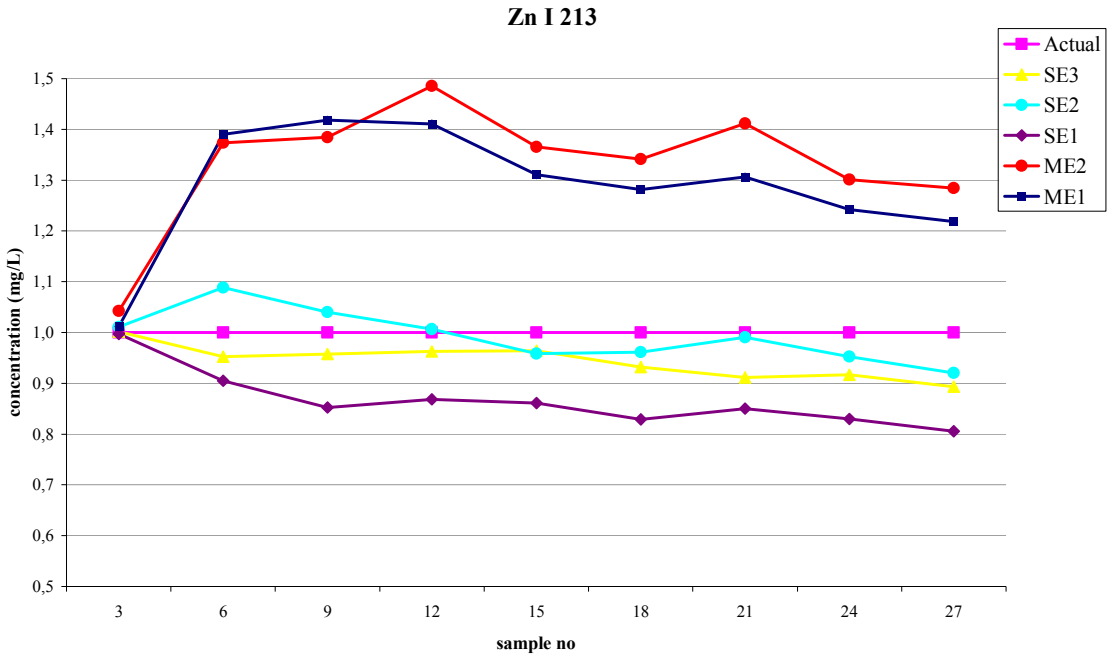

(a)

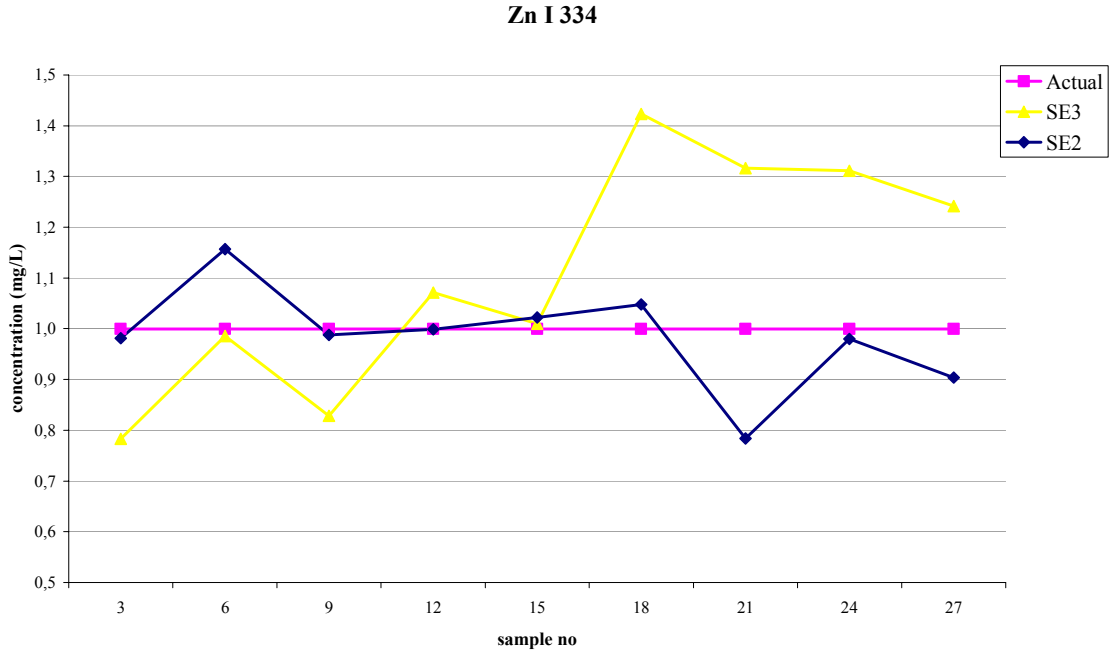

(b)

sample	3	6	9	12	15	18	21	24	27
Acid %	0	0	0	12	12	12	25	25	25
Salt %	0	0.1	0.3	0	0.1	0.3	0	0.1	0.3

Figure D.5. Line graphs for the Zn atom lines for the values obtained in the validation study: (a) for Zn I 213, (b) for Zn I 334

APPENDIX D-5

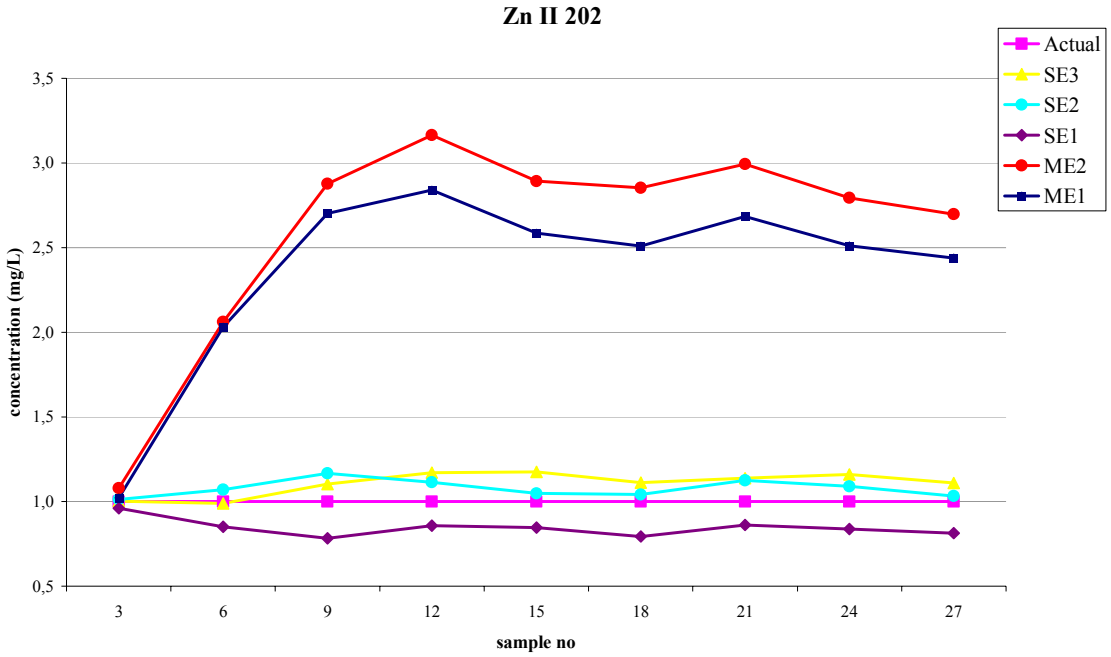

(a)

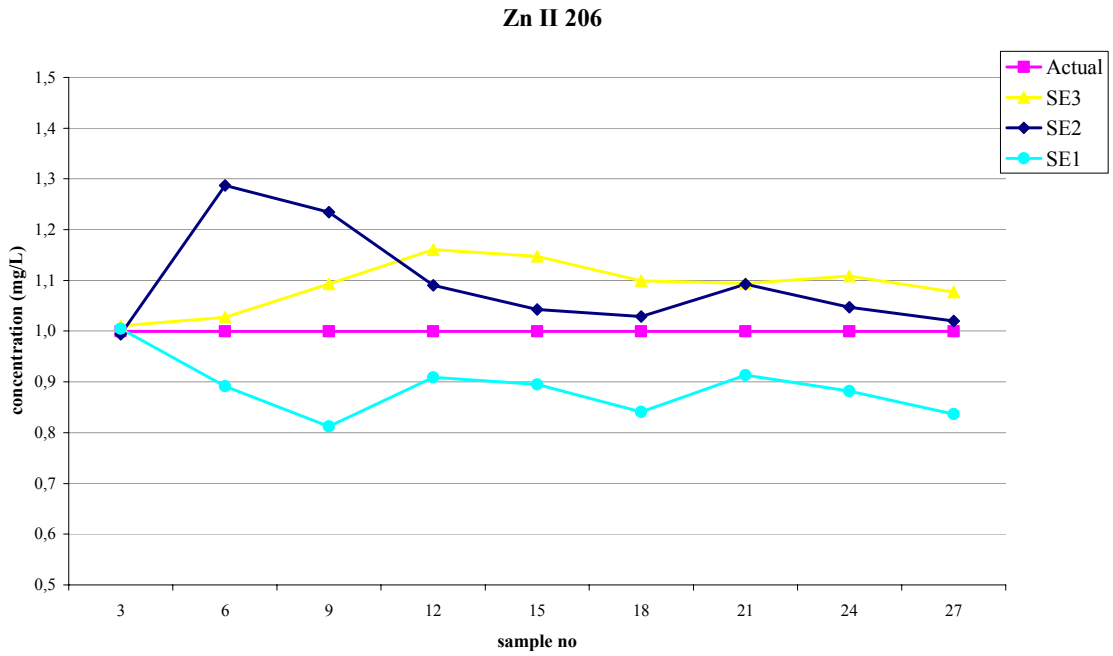

(b)

sample	3	6	9	12	15	18	21	24	27
Acid %	0	0	0	12	12	12	25	25	25
Salt %	0	0.1	0.3	0	0.1	0.3	0	0.1	0.3

Figure D.6. Line graphs for the Zn ion lines for the values obtained in the validation study: (a) for Zn II 202, (b) for Zn II 206